CHEMICAL REVIEWS

REVIEW

pubs.acs.org/CR

# Pyrene-Based Materials for Organic Electronics

Teresa M. Figueira-Duarte[†] and Klaus Müllen[*,‡]

[†]BASF SE, Carl-Bosch-Strasse 38, 67056 Ludwigshafen, Germany

[‡]Max Planck Institute for Polymer Research, Ackermannweg 10, P.O. Box 3148, Mainz, Germany

## CONTENTS

1. Introduction 7260
2. Electronic and Optoelectronic Organic Devices 7262
   2.1. Organic Light-Emitting Diodes (OLEDs) 7262
   2.2. Organic Field-Effect Transistors (OFETs) 7263
   2.3. Organic Photovoltaic Devices (OPVs) 7263
3. Chemical Modification of Pyrene 7264
   3.1. 1-Substituted Pyrenes 7264
   3.2. 1,3,6,8-Tetrasubstituted Pyrenes 7272
   3.3. 1,6- And 1,8-Disubstituted Pyrenes 7274
   3.4. 1,3-Disubstituted Pyrenes 7275
   3.5. 2,7-Substituted Pyrenes 7275
   3.6. 4,5,9,10-Substituted Pyrenes 7277
4. Pyrenes as Active Components in Devices 7279
   4.1. 1-Substituted Pyrenes 7279
      4.1.1. Linear Structures 7279
      4.1.2. Liquid Crystalline Structures 7290
      4.1.3. Dendritic Structures 7290
      4.1.4. Organic−Inorganic Hybrids 7293
   4.2. 1,3,6,8-Tetrasubstituted Pyrenes 7293
      4.2.1. Linear Structures 7293
      4.2.2. Liquid Crystalline Structures 7294
      4.2.3. Dendritic Structures 7297
   4.3. 1,6- And 1,8-Disubstituted Pyrenes 7299
      4.3.1. Linear Structures 7299
      4.3.2. Liquid Crystalline Structures 7301
   4.4. 1,3-Disubstituted Pyrenes 7302
   4.5. 2,7-Disubstituted Pyrenes 7304
   4.6. 4,5,9,10-Substituted Pyrenes 7304
5. Conclusion 7309
Author Information 7310
Biographies 7310
References 7310

## 1. INTRODUCTION

Pyrene is the fruit fly of photochemists. Its unique properties have inspired researchers from many scientific areas, making pyrene the chromophore of choice in fundamental and applied photochemical research. Since the pioneering work of Laurent, who in 1837 discovered pyrene in the residue of the destructive distillation of coal tar,[1] this polycyclic aromatic hydrocarbon has been the subject of tremendous investigation. The name pyrene, Greek for "fire", was attributed since he believed that it was frequently obtained via the reaction of organic substances with fire. Later on, in 1871, Gräbe reported the isolation of pyrene via extraction with carbon disulfide, which left the accompanying chrysene undissolved.[2] Concentration of the solution gave a crude pyrene, which was further purified via the picrate. Decomposition of the picrate yielded pyrene as yellow plates.

Pyrene is also formed in many pyrolytic processes, for example, in the destructive distillation of soft coal tar, by pyrolysis of acetylene and hydrogen,[3] by the zinc-dust distillation of thebenol and thebenin,[4] and from petroleum by the catarol process.[5] Until 1882, an interesting source of pyrene was a special distillation of mercury ore as carried out in Idria. The byproduct, which was mixed with mercury, was called "Stupp" and contained up to 20% pyrene as well as other polycyclic hydrocarbons.

The search for an effective method to prepare pyrene lead Weitzenböck in 1913 to the first synthesis of pyrene, starting from *o,o′*-ditolyl.[6] Until the 1950s, several other preparative routes toward pyrene were presented.[7−16] Modernization of the distillation process of coal tar, as well as the destructive hydrogenation of hard coal, yielded considerable quantities of pyrene and other polycyclic hydrocarbons, making pyrene of commercial use.

Pyrene was initially used in the preparation of several derivatives, such as the pyranthrone, for the synthetic dye industry.[17] Later, in 1954 Förster and Kasper reported the first observation of intermolecular excimers in a pyrene solution.[18] This excimer formation, combined with long-lived excited states, high fluorescence quantum yield,[19] exceptional distinction of the fluorescence bands for monomer and excimer, and the sensitivity of its excitation spectra to microenvironmental changes,[20] brought pyrene to the status of a gold standard as a molecular probe of microenvironments. Thanks to this attractive combination of properties, pyrene has become one of the most studied organic molecules in terms of its photophysical properties.

The fluorescence properties of pyrene have been utilized over the last 50 years in the investigation of water-soluble polymers, making pyrene, by far, the most frequently applied dye in fluorescence labeled polymers.[21,22] The attachment of hydrophobic pyrene units to water-soluble polymers alters not only the properties of the polymer but also those of the chromophore. The pyrene chromophore is also frequently employed as a probe to measure properties of surfactant micelles, phospholipid vesicles, and surfactant/polymers aggregates. The tendency of pyrene and its derivatives to form excimers has been widely employed for supramolecular design and for probing the structural properties of macromolecular systems. Pyrene labels have

**Received:** December 14, 2010
**Published:** July 11, 2011

ACS Publications © 2011 American Chemical Society



Samsung Exhibit 1020, Page 1 of 55

been extensively used in structural studies of proteins and peptides,[23−26] but also DNA recognition[27−31] and investigation of lipid membranes.[32−39] The excimer fluorescence of pyrene and derivatives has been also utilized to sense environmental parameters such as temperature,[40] pressure,[41] or pH.[42] The change of the excimer fluorescence intensity reflects changes in the environment. In addition, it can also be used to detect guest molecules such as gases ($O_2$ or $NH_3$),[43−46] organic molecules,[47−49] metals,[50−57] or other miscellaneous analytes.[58]

In addition to excimer sensing, which propelled pyrene to the status of the most used fluorescent probe, there has been a recent increased interest in the use of pyrene as organic semiconductor for application in materials science and organic electronics. Great progress has been made, particularly in the past decade, in the search for organic materials with attractive electronic and photophysical properties for application in a new generation of electronic and optoelectronic devices.[59−61] The ability to replace inorganic semiconductors with organic materials will decrease manufacturing costs and allow fabrication of devices over large areas on lightweight and flexible substrates. The appeal of new technologies based on organic semiconductors has notably promoted the advancement of devices such as organic light-emitting diodes (OLEDs), organic photovoltaic cells (OPV), organic field-effect transistors (OFETs), organic lasers, and memory cells. These devices are being tailored for application in flat-panel displays, lighting, RFID (radio frequency identification tags), electronic skin, and solar modules. Furthermore, flexible organic electronic devices have generated entirely new design concepts for consumer electronics, since they are fully adaptable to complex surface shapes.

The key to the conception of high-performance electronic organic devices is based on the insight of clear structure−property relationships, which can be used to understand the properties of existing devices and predict the ideal material sets for utilization in the next generation of electronic devices. Subtle changes in structure or composition of an organic material can greatly alter its bulk properties. In contrast to inorganic semiconductors, the properties of organic materials such as energy gap, solubility, electron affinity and stability in ambient air can be adjusted by changing their chemical composition, giving the chemist an incomparable degree of flexibility in materials design.

Nowadays, researchers are focusing on improving organic systems through molecular tuning, interface control, and optimization of film morphologies for high-performance organic devices. The design of improved organic materials involves both the optimization of the functional units and the control of their supramolecular order. First, the properties of the individual molecules must be considered and understood. This includes electronic properties such as energy gap and charge carrier mobility and intramolecular processes such as energy and electron transfer. The interaction between these molecules is fundamental to understand how they affect the macroscopic properties. It is possible to control the molecular and supramolecular complexity by changing the chemical structure, which results in different architectures ranging from linear polymeric chains to flat disks or dendritic structures. In the case of pyrene, modification of the chemical structure by varying the substitution at different positions of the pyrene ring allows the control of the molecular architecture and thus the molecular packing, which renders the handling of pyrene substitution a key factor in pyrene-based semiconductors. The presence of electron-rich or electron-poor units is also important and permits the fine-tuning of the optical properties while also influencing the molecular packing. High spatial organization is of great importance for the construction of devices in order to control the charge carrier mobilities. Also the choice of the right processing technique is crucial for the fabrication of high-performance devices.

Conjugated organic oligomers and polymers have achieved the status of a major technologically important class of materials. Polymers have the advantages of low cost, ease of modification of properties by appropriate substitution, and solvent processability. Oligomers are of particular interest, since they generally possess good molecular-ordering properties when processed using vacuum-sublimation techniques. Since vacuum deposition is often argued to be expensive and limiting toward display size, several efforts have been made in order to make oligomers soluble in organic solvents with the introduction of proper chemical substituents. Monodisperse conjugated oligomers can be free from structural defects, possessing high purity from conventional purification methods, allowing a very accurate relationship between structure and properties. Pyrene-based low-molecular weight organic materials and polymers have been used as active components in molecular electronic devices such as OLEDs, OFETs, and, more recently, solar cells.

Herein, we provide an overview of the use of pyrene-based materials in organic electronics illustrating the increased interest of pyrene in electronic devices and highlighting their potential as organic semiconductors. In our structure-driven approach, we describe many efforts to manage the pyrene chemical challenges and, consequently, establish a new pyrene chemistry that allows the use of pyrene in organic electronics. Moreover, we also demonstrate how to control the intermolecular interactions by manipulating the complexity of the structure at the molecular level using different substitutions on the pyrene ring. The design of different pyrene-based molecular architectures is discussed, as well as the study of the optical and electronic properties plus the charge transfer processes, which are of particular interest for molecular electronics. Furthermore, our study paves the way for the evaluation of these molecular components with respect to their performance in molecular electronic devices.

Thus, in section 2 we provide a short description of the most common organic electronic devices, such as OLEDs, OFETs, and OPVs, and clarify the interest of pyrene in these electronic and optoelectronic devices, since this is the driving force for the development of the new pyrene chemistry. In section 3, we survey this chemistry regarding the chemical modification of pyrene for light-emitting and semiconducting properties with particular emphasis on the different substitutions on the pyrene ring. This includes the most frequently studied chemical reactions for the easily accessible mono- and tetrasubstituted pyrene derivatives, as well a discussion of the chemical difficulties in selectively obtaining disubstituted pyrene derivatives. Disubstitution of the pyrene ring is fundamental to achieve linear or cyclic oligomers as well as polymers. In addition, the chemical challenges in reaching inaccessible positions at the pyrene ring, such as the 2,7-positions, are also considered. Afterward, in section 4, we review the use of pyrene derivatives comprising different molecular architectures resulting from different substitution paths as active components in organic electronic devices. This section includes the monosubstitution of pyrene, which results in different molecular architectures, such as small-molecules, oligomers, and polymers, as well as in the formation of columnar structures and the incorporation of pyrene as end-groups in dendritic structures. This section also deals with the 1,3,6,8-tetrasubstituted



Samsung Exhibit 1020, Page 2 of 55

pyrenes in different molecular organizations, such as columnar liquid crystals and dendrimers. Also, the 1,6- and 1,8-disubstituted pyrene derivatives and their resulting molecular architectures in organic electronics are reviewed. We also consider the novel 1,3-disubstituted pyrene derivatives in the design of oligomers, polymers, and macrocycles. The investigation of 2-substituted pyrenes in small molecules and star-shaped derivatives, as well the 2,7-disubstituted pyrenes in oligomers and polymers, is also discussed. Our review also includes the study of the 4,5,9,10-tetrasubstituted pyrenes as small molecules and as discotic materials. It is important to emphasize that this is a structure-driven review and therefore in all sections the sequence of the described pyrene derivatives appears on the basis of the molecular structure-type as ordering principle. Finally, in section 5 we provide a summary concerning the usefulness of pyrene in organic electronics as well as an outlook.

## 2. ELECTRONIC AND OPTOELECTRONIC ORGANIC DEVICES

This section briefly describes the principles and operation processes of the most common organic electronic devices, namely OLEDs, OFETs, and OPVs and elucidates the interest of pyrene in these devices.

### 2.1. Organic Light-Emitting Diodes (OLEDs)

In 1987, a double layer OLED using thin films of 1,1-bis(4-(di-*p*-tolylamino)phenyl)cyclohexane (TAPC) as a hole-transporting material and tris(8-quinolinolato)aluminum ($Alq_3$) as the emitter material sandwiched between transparent indium tin oxide (ITO) and an alloy of magnesium and silver was reported to exhibit a luminance of over 1000 cd $m^{-2}$ at a drive voltage of ca. 10 V.[62] Subsequently, a single-layer OLED using a thin film of poly(*p*-phenylene vinylene), ITO/polymer/Ca, was reported in 1990.[63] These two reports have triggered extensive research and development of OLEDs from the standpoints of both fundamental science and potential technological applications for full-color, flat-panel displays and lighting.

The working principle of OLEDs involves charge injection from the anode and cathode into the adjacent organic layers, transport of injected charge carriers through the organic layers, exothermic recombination of holes and electrons to generate electronically excited states of molecules, often called excitons, followed by their emissive deactivation via either fluorescence or phosphorescence, which is taken out of the device as electroluminescence (EL).

The efficiency of an OLED is characterized by its quantum efficiency, the current efficiency in cd $A^{-1}$ ($\eta_L$) or the luminous efficiency ($\eta_P$) in lm $W^{-1}$. For the quantum efficiency, two different parameters have to be taken into account: the external quantum efficiency ($\eta_{ext}$) and the internal quantum efficiency ($\eta_{int}$). $\eta_{ext}$, defined as the number of emitted photons divided by the number of injected charges, is given by[64]

$$\eta_{ext} = \eta_r \varphi_f \chi \eta_{out} = \eta_{int} \eta_{out}$$

where $\eta_r$ is the probability that holes and electrons recombine to form excitons. Owing to the low mobility of the charge carriers, the probability of charge recombination or exciton formation in organic materials is nearly equal to 1. Nevertheless, the efficiency of OLEDs is determined to a significant extent by the efficiency of electron and hole injection into the organic layers, and in order to maximize $\eta_r$, a good balance between the two types of charges is desired. $\varphi_f$ is the fluorescent quantum efficiency or the fraction of excitons that decays radiatively. $\chi$ is the probability for radiative decay to occur, and generally only singlet excitons emit light. The light-emitting materials can be phosphorescent or fluorescent, small molecules or polymers. In the particular case of phosphorescent emitters, a singlet to triplet energy transfer is allowed via intersystem crossing, which leads to highly efficient devices where 100% of the excitons can produce light, in contrast to only 25% in conventional fluorescent devices. A further challenge in obtaining high external efficiencies is optical outcoupling. Thus, in conventional fluorescent OLEDs, the maximum external quantum efficiency is currently limited to 5−6%.

The current efficiency ($\eta_L$), expressed in cd $A^{-1}$, is another way to characterize the quality of a device and represents the ratio of the luminance ($L$) to the current density ($J$) flowing into the diode. The luminous efficiency ($\eta_P$) as a Lambertian emitter expressed in lm $W^{-1}$ is the ratio of the optical flux to the electrical input and is given by

$$\eta_P = \frac{L\pi}{JV} = \eta_L \frac{\pi}{V}$$

where $V$ is the working voltage. Thus, devices with high luminous efficiency have to combine high quantum (or current) efficiency with a low working voltage. Note that $\eta_L$ and $\eta_P$ are functions of the eye's sensitivity (photopic response), which is a maximum in the yellow peaking at 555 nm, and therefore, the current or luminous efficiency is lower in the blue and the red part of the spectrum in comparison with green, assuming devices with the same quantum efficiency and working voltage. The brightness of an OLED, given by the luminance in cd $m^{-2}$, is also used by several authors to estimate the performance of the device. For comparison, the brightness of a conventional laptop display reaches values of approximately 150 cd $m^{-2}$. Further critical characteristics of OLEDs are CIE color coordinates and device lifetimes.

During the last decades, great efforts were focused on the development of novel electroluminescent materials with intense luminescent efficiency, high thermal and optical stability, good charge carrier injection and transport, and desirable film morphology, as well as on the fabrication of high-performance OLED devices.[65−72] Excellent red, green, and blue emitting materials are required to achieve full color displays and lighting applications. However, the electroluminescent properties of blue-emitting materials remain challenging, particularly in terms of stability, efficiency, and color purity. It is thus important to develop high-performance blue-emitting materials with good stability and high fluorescence efficiency. Maintaining efficient carrier injection in the light-emitting device is considered to be an important factor for achieving high performance devices. It is therefore essential to synthesize light-emitting materials with a high-lying energy level of the highest occupied molecular orbitals (HOMO), to facilitate both hole injection and transport. From the manufacturing point of view, complex multilayer device structures are difficult to fabricate, and devices with fewer layers are more desirable, as they simplify the fabrication process. Thus, in order to avoid deposition of both a hole-transporting layer and an emitting layer, it is imperative to use organic materials with both light-emission and hole-transporting properties.

In this way, pyrene, as a blue-light-emitting chromophore with good chemical stability and high charge carrier mobility, appears to be a very attractive building block for light-emitting devices.



Samsung Exhibit 1020, Page 3 of 55

It is important to mention that pyrene itself is not suitable to act as blue-emitter in OLEDs due to the strong tendency to form excimers, which leads to a red-shift of the emission as well as the decrease in the fluorescence efficiency in condensed media. This fact has limited the use of pyrene as an emissive material in OLEDs. Nevertheless, several efforts in the structural modification of pyrene containing organic semiconductors have been made in order to avoid aggregation and improve the fluorescence quantum yield for application in OLEDs. As a large conjugated aromatic system, pyrene not only has the advantage of high photoluminescence efficiency[73] and high charge carrier mobility, but also shows excellent hole injection ability when compared to other chromophores.[74]

### 2.2. Organic Field-Effect Transistors (OFETs)

Organic field-effect transistors (OFETs) are expected to be a promising technology for large-area, low cost, and flexible electronics for applications in displays, sensors, and memories.[75] In addition, they have an advantage over silicon FETs in that the processing temperature is lower.

OFETs consist of conductors, that is, source, drain, and gate electrodes; an insulator, that is, a gate dielectric; and an organic semiconductor as an active element. The materials used as the gate dielectric are either inorganic dielectric materials, for example, $SiO_2$, or organic dielectric materials, such as insulating organic polymers. Two types of structures, namely, top-contact and bottom-contact electrode configurations, have been adopted for the fabrication of OFETs. When there is no voltage application to the gate electrode, only small currents flow between the source and drain electrodes; this state is referred to as the off-state of the transistor. When negative voltage, for example, is applied to the gate electrode, hole carriers in the organic semiconductor layer become accumulated at the interface with the gate dielectric, and hence, hole transport takes place from the source to the drain electrode; this state corresponds to the on-state of the transistor. This type of device is called a p-channel device. Likewise, application of positive voltage to the gate electrode causes electron transport in the case of n-channel devices. Since the so-called organic semiconductors are essentially electrical insulators, charge carriers in organic semiconductors are usually supplied by injection from the source electrode into the organic layer. The current flow ($I_{SD}$) can be modulated by the magnitude of both the gate voltage ($V_G$) and the source/drain voltage ($V_{SD}$).

The current that flows from the source to the drain electrode ($I_{SD}$) under a given $V_G$ increases almost linearly with the increasing $V_{SD}$ and gradually becomes saturated. The current ($I_{SD}$) is given by

$$I_{SD} = \frac{C_i W \mu_{FET}}{L}\left[(V_G - V_T)V_{SD} - \frac{{V_{SD}}^2}{2}\right]$$

where, $\mu_{FET}$ is the field-effect mobility of the charge carrier, $L$ is the channel length, $W$ is the channel width, $C_i$ is the capacitance per unit area of the gate dielectric, and $V_T$ is the threshold voltage. The current $I_{SD}$ in the linear and saturation regions are given by

$$I_{SD,\,Linear} = \frac{C_i W \mu_{FET}}{L}(V_G - V_T)V_{SD}$$

$$I_{SD,\,Sat} = \frac{C_i W \mu_{FET}}{2L}(V_G - V_T)^2$$

The field-effect mobility ($\mu_{FET}$) can be determined from the slope of the linear plots of $(I_{SD,Sat})^{1/2}$ versus $V_G$, according to the equation. The performance of OFETs is evaluated by $\mu_{FET}$, $V_T$, and the on/off ratio of $I_{SD}$. Not only organic semiconductors but also the gate dielectric materials greatly affect the device performance.[76]

Significant progress has been made in the development of new semiconductor materials with high charge carrier mobilities for the fabrication of high-performance OFET devices. This means devices displaying high charge carrier mobilities, high on/off ratio, and low threshold voltages. There is now a large number of solution-processed as well as vacuum-sublimed organic semiconductor materials that have been demonstrated to exhibit field-effect mobilities on the order of 0.1−1 $cm^2\ V^{-1}\ s^{-1}$.[77,59] Devices using organic single crystals of rubrene have reached extremely high mobilities of around 15 $cm^2\ V^{-1}\ s^{-1}$.[78] However, the single crystal growth on the plane of a large area substrate for device applications is not easy. Polycrystalline materials have been mostly used in OFETs, and in this case, the grain size, grain boundaries, and molecular orientations will affect the device performance. Small molecules have the advantage of high purity and high crystalline order required to obtain high mobilities; however, polymers combine high conjugation through the polymeric backbone with solution processability and ease of device fabrication.[79] Our group reported recently one of the highest mobilities for solution-processed small molecules using a high-crystallinity deposition technique ($\mu_{hole}$ = 1.7 $cm^2\ V^{-1}\ cm^{-1}$)[80] as well the highest mobility value reported so far for polymer OFETs ($\mu_{hole}$ = 3.3 $cm^2\ V^{-1}\ cm^{-1}$).[81]

The high charge carrier transporting ability of pyrene has also attracted attention for the fabrication of OFET devices. Thus, pyrene has found application as a semiconducting material for *p*-type OFETs fabricated via vacuum sublimation as well as ambipolar OFETs using a single crystal of a pyrene derivative and also in organic light-emitting field-effect transistors (OLEFETs).

### 2.3. Organic Photovoltaic Devices (OPVs)

In the case of organic solar cells, researchers, motivated by the prospect of a low-cost alternative to silicon solar cells since the first device reported by Tang in 1986,[82] have rigorously improved device efficiencies with the main focus being on the organic materials.

The basic operation processes of pn-heterojunction organic photovoltaics (OPVs) are as follows: (a) light absorption by organic semiconductors to form excitons, (b) diffusion of the excitons, (c) charge carrier generation and separation at the p/n interface, (d) charge transport through the organic layers, and (e) charge collection at both electrodes. These processes are just the opposite to those of OLEDs.

The performance of OPVs is evaluated by power conversion efficiency ($\eta$) and fill factor (FF). They are defined as

$$\eta = \frac{(VJ)_{max}}{I}$$

$$FF = \frac{(VJ)_{max}}{V_{OC}J_{SC}}$$

where $I$, $V_{OC}$, and $J_{SC}$ are the incident light power, the open circuit voltage, and the short-circuit current, respectively.

Two major concepts have been developed since the original donor/acceptor bilayer device reported by Tang, both resulting in an increased number of absorbing dye molecules that can contribute to photocurrent. The bulk heterojunction cells



Samsung Exhibit 1020, Page 4 of 55

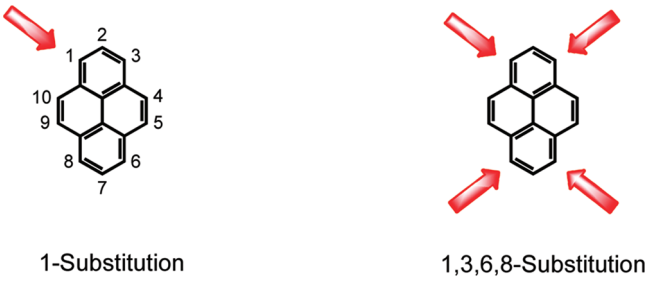


**Figure 1.** General structure of 1-substituted and 1,3,6,8-tetrasubstituted pyrenes.

(BHJ)s simply rely on an interpenetrating network of donor and acceptor phases, thereby maximizing the important interfacial area between the donors and acceptors. Polymer BHJ can be processed via solution and typically consist of a *p*-type polymer and a soluble derivative of $C_{60}$ such as [6,6]-phenyl-$C_{61}$-butyric acid methyl ester (PCBM). Just as in the case of OLEDs, solar cells can also be constructed on the basis of vacuum deposition of small molecules where similar "bulk heterojunctions" can be created. Both the polymer and small molecule solar cells have recently achieved efficiencies approaching 8%. In order to improve the performance of the solar cells, pyrene was recently used to enhance the absorption in the visible region, as well to achieve the ideal morphology in a pyrene−perylene derivative, which was then used as acceptor material in bulk heterojunction solar cells. In 1991, Oregan and Grätzel introduced the dye-sensitized solar cell (DSC) concept built on a mesoporous $TiO_2$, which separates the roles of light absorption and charge transport.[83] The first DSCs made use of an $I^-/I_3^-$ redox couple to regenerate the oxidized dye molecules and have shown efficiencies of over 11%. Problems concerning the sealing of such "liquid" cells have driven researchers to develop the solid-state analogs of these cells based on similar organic hole conductors as used in OLEDs. Such solid DSCs currently show efficiencies of 5%. Recently, a pyrene−perylene derivative was reported bearing an anchor group that allows the linkage of the dye to $TiO_2$ for the fabrication of dye sensitized solar cells (DSCs).

Despite the remarkable developments in the past decade, the design of new high-performance semiconductors and a better understanding of the relationship between molecular structure and device properties are still the major challenges in modern molecular electronics. In this context, the electronic and optical properties of pyrene have been attractive for the development of innovative semiconductor materials, making pyrene a very promising building block in organic electronics.

## 3. CHEMICAL MODIFICATION OF PYRENE

The electronic and photophysical properties of pyrene are very attractive for the design of new organic light-emitting and semiconductor materials. Although the chemistry of pyrene is well-known, there are considerable issues regarding regioselectivity and purification. The electrophilic substitution of pyrene is known to take place preferentially at the 1-, 3-, 6-, and 8-positions, based both on experimental results[84,85] and on consideration of calculations of molecular orbitals,[86,87] the only exception being the *tert*-butylation.[88] Thus, 1-substituted pyrenes and 1,3,6,8-tetrasubstituted pyrenes (Figure 1) can be easily accessible by direct electrophilic substitution of pyrene.

The ease of preparation of mono- and tetrasubstituted pyrenes combined with the relatively simple purification gives the possibility to straightforwardly introduce pyrene into different molecular architectures with interest in organic electronics. On the other hand, the selective preparation of disubstituted pyrenes is challenging but simultaneously highly required. It is crucial to obtain well-defined disubstituted pyrene building blocks for the controlled synthesis of linear or cyclic oligomers as well as polymers.

### 3.1. 1-Substituted Pyrenes

The most common chemical reactions used to prepare 1-substituted pyrenes for use in molecular electronics are metal-catalyzed cross-coupling reactions. In this way it is possible to obtain larger $\pi$-systems by coupling more than one or more pyrenes to another $\pi$-system. Among these cross-coupling reactions, one of the most employed is the palladium-catalyzed carbon−carbon bond-forming Suzuki reaction, which involves the palladium-mediated coupling of organic electrophiles, such as aryl halides, with organoboron compounds in the presence of a base. The Suzuki reaction is a particularly useful method for the construction of conjugated dienes and higher polyene systems of high stereoisomeric purity, as well as of biaryl and related systems. Thus, 1-bromopyrene, obtained without difficulty with 1 equiv of bromine at room temperature, can further be involved in Suzuki cross-couplings.[84,89] One example is the Suzuki reaction of 1-bromopyrene (**1**) and 1,4-benzene boron acid ether (**2**) in the presence of sodium *tert*-butoxide and $PdCl_2(PPh_3)_2$ in toluene to afford 1,4-di-1-pyrenylbenzene (**3**) (Figure 2).[90]

Another possibility is to use the 1-pyreneboronic acid (**4**) in the Suzuki coupling, as demonstrated in Figure 3. The 1-pyreneboronic acid (**4**) could be obtained by lithiation of 1-bromopyrene at 0 °C followed by treatment with trimethylborate at −78 °C and subsequent acidic workup.[91−93] In this case, pyrene **4** reacted with different aryl bromides in the presence of $Pd(PPh_3)_4$ and sodium carbonate in toluene to give the three dipyrenylbenzenes, **3**, **5**, and **6**, in 63−66% yields (Figure 3).[94] The use of these dipyrenylbenzenes **3**, **5**, and **6** as blue emitters for the fabrication of OLED devices will be analyzed in the next section. Depending on the attachment of different building blocks, it is possible to choose the appropriate cross-coupling reaction to afford different pyrene-based semiconductor materials.

In the case of pyrene, including thiophene derivatives, it is also common to use the Stille coupling involving organostannane-based compounds. One example is the reaction of 1-bromopyrene (**1**) with the bis(tributylstannyl) derivatives **7** in the presence of Pd(0) catalyst, which gave pyrene-containing oligothiophenes **8** in 52% ($n$ = 1) and 64% ($n$ = 2) yield (Figure 4). Oligothiophenes **8** were used in single-layer electroluminescent devices.

1-Substituted pyrenes can also be successfully obtained via the Heck coupling reaction. One example, the Heck reaction of 9,9-dihexyl-2,7-divinylfluorene (**9**) with the 1-bromopyrene (**1**) utilizing DMF as reaction medium and triethylamine as an acid acceptor afforded the fluorenevinylene **10** in 71% yield (Figure 5).[95] The photophysical properties and electroluminescence of compound **10** will be investigated in section 4.

Another possibility is the Wittig reaction involving a triphenyl phosphonium ylide. Thus, pyren-1-ylmethyltriphenylphosphonium bromide (**11**) was prepared from the 1-pyrenecarboxaldehyde.[96] The pyrenecarboxaldehyde was converted to 1-pyrenylmethanol with lithiumaluminium hydride and consequently



Samsung Exhibit 1020, Page 5 of 55

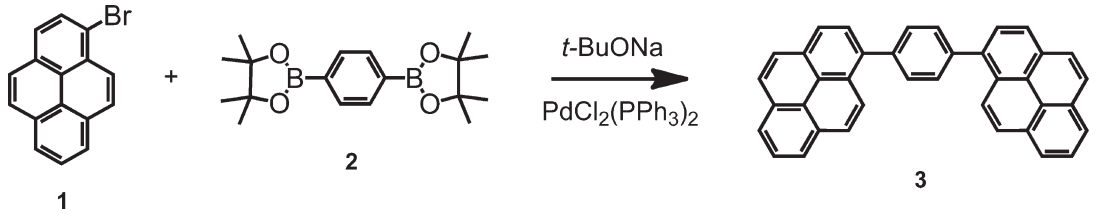


**Figure 2.** Suzuki coupling to 1,4-di-1-pyrenylbenzene (**3**).

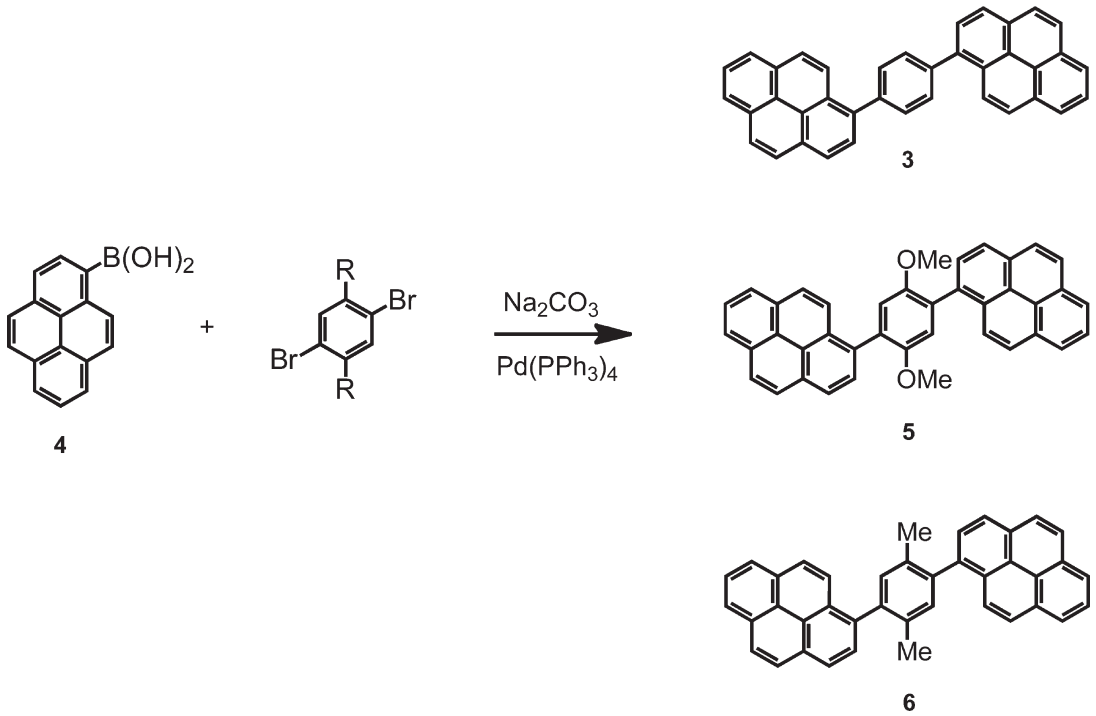


**Figure 3.** Suzuki coupling to dipyrenylbenzenes **3**, **5**, and **6**.

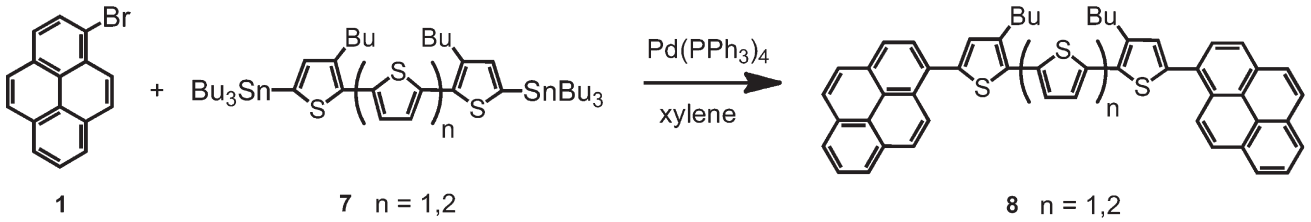


**Figure 4.** Stille coupling to pyrene-containing oligothiophenes **8**.

reacted with phosphorus tribromide in chloroform to give the 1-bromomethylpyrene. The 1-bromomethylpyrene was refluxed with triphenylphosphine in benzene to afford the corresponding phosphonium salt. Consequently, pyrene compound **13** was obtained in 30% yield via a one-step Wittig reaction between pyren-1-ylmethyltriphenylphosphonium bromide (**11**) and 2,2′-bithienyl-5,5′-dicarboxaldehyde (**12**) using lithium ethoxide as base (Figure 6).[97]

The Sonogashira reaction provides a valuable method for the synthesis of conjugated acetylenic systems, allowing the design of molecules including pyrene with interest in molecular electronic devices such as OLEDs as well in nanotechnology. 1-Ethynylpyrene (**15**) can be easily obtained from trimethyl-(pyren-1-ylethynyl)silane (**14**) in good yields (Figure 7).[98] Thus, reaction of 1-bromopyrene (**1**) with ethynyltrimethylsilane in the presence of $PdCl_2(PPh_3)_2$ and $CuI/Et_3N$ in toluene provided compound **14** in 80% yield (Figure 7). The TMS protecting group was eliminated using KOH in a mixture of THF/MeOH, giving 1-ethynylpyrene (**15**) in 86% yield (Figure 7).[98]

1-Ethynylpyrene (**15**) can be used in several Sonogashira coupling reactions to afford different pyrene semiconductors, such as the ones depicted in Figure 8.[98] In this case, 1-ethynylpyrene (**15**) reacted with 2-bromo-9-(4′-(2″-ethylhexyloxyphenyl))-9-pyrenylfluorene



Samsung Exhibit 1020, Page 6 of 55

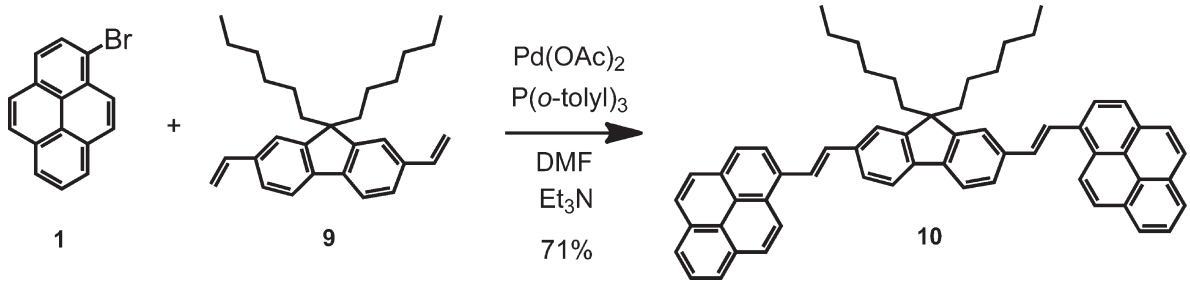


**Figure 5.** Heck coupling to fluorenevinylene **10**.

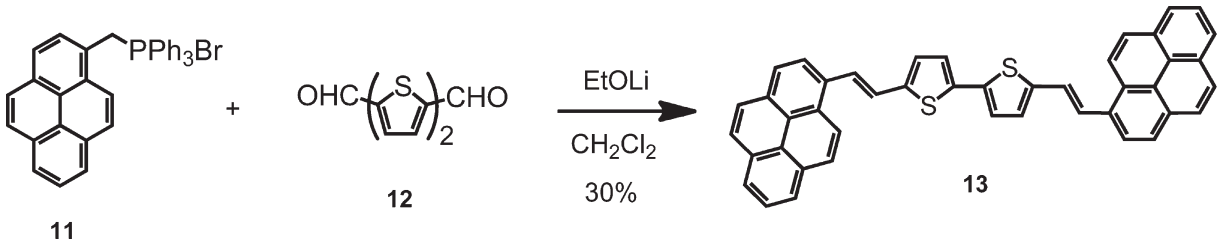


**Figure 6.** Wittig reaction to pyrene-containing thiophenevinylene **13**.

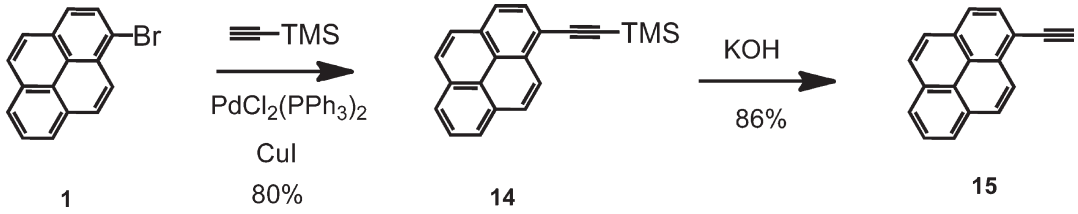


**Figure 7.** Synthesis of 1-ethynylpyrene (**15**).

and 2,7-dibromo-9-(4′-(2″-ethylhexyloxyphenyl))-9-pyrenylfluorene (**16**) in the presence of $Pd(PPh_3)_4$ and $CuI/Et_3N$ in toluene to afford the pyrene derivative **17** in 80% yield and the pyrene derivative **18** in 77% yield (Figure 8). Both compounds **17** and **18** could be used as solution processable light-emitting molecular glasses in OLED devices.

1-Ethynylpyrene (**15**) can also be involved in a Glaser coupling such as the reaction illustrated in Figure 9 using cupric acetate monohydrate in pyridine to yield 1,4-dipyren-1-ylbuta-1,3-diyne (**19**) in 36% yield.[99] The linkage of the two-pyrene units via the butadiynylene bridge produced in this case a highly fluorescent system.

The Ullmann coupling has also be used to prepare 1-substituted pyrenes with interest in molecular electronics. For example, the 10-pyren-1-yl-10*H*-phenothiazine (**22**) was prepared in 55% yield via Ullmann-type reaction of phenothiazine (**21**) and 1-iodopyrene (**20**) (Figure 10). The 1-iodopyrene (**20**) was previously prepared from the 1-bromopyrene in the presence of CuI and KI.[100] Direct iodination of pyrene is not commonly used, due to the poor yield of the reaction and insolubility of the iodide derivative. Only one reference mentions the iodine cyanide promoted iodination of pyrene to afford 1-iodopyrene.[101]

Coupling reactions involving amino groups are also possible in the presence of a palladium catalyst. 1-Aminopyrene can be prepared via the reduction of 1-nitropyrene with various reduction agents: Sn in HCl,[102] 10−40% solution of NaHS in boiling ethanol,[84] or reaction with $Ac_2O$ and $Cu(NO_3)_2.H_2O$.[103] Hydrogenation of 1-nitropyrene under $H_2$ atmosphere and in the presence of Pd/C afforded the 1-aminopyrene in good yields.[103] The coupling of pyrene with fluorene, both extensively investigated blue-emitting chromophores, seems a very interesting approach toward improved light-emitting devices. Thus, as example the reaction between an excess of the difluorene bromide **23** and 1-aminopyrene (**24**) in the presence of tris(dibenxylideneacetone)dipalladium and 1,1′-bis(diphenylphosphino)ferrocene with sodium *tert*-butoxide in toluene afforded the bis(difluorenyl)-amino-substituted pyrene **25** in 48% yield (Figure 11).[104] The solution-processable dye **25** found application as a green emitter for OLED devices.

The palladium-catalyzed amination is also possible using 1-bromopyrene (**1**) as depicted in Figure 12. Therefore, reaction between 1-bromopyrene (**1**) and phenylamines **26** using the catalyst developed by Koie and Hartwig,[105] $Pd(dba)_2/P(t\text{-}Bu)_3$ (where dba is dibenzylideneacetone) in the presence of sodium *tert*-butoxide, efficiently catalyzed aromatic C−N bond formation from an aryl halide and an aryl amine, providing pyrenylamines **27** in 78−89% yields (Figure 12) and 3,6-bis(diarylamino)carbazoles **29** in 85−94% yields (Figure 13).[106] Compounds **29** were used in the fabrication of green OLED devices.

In addition to the widely used metal-catalyzed cross-coupling reactions, a few examples of other type of reactions have also been used to achieve 1-substituted pyrene derivatives. Among these reactions, the esterification reaction has been most frequently employed. Therefore, a pyrene acid such as the butyric acid can



Samsung Exhibit 1020, Page 7 of 55

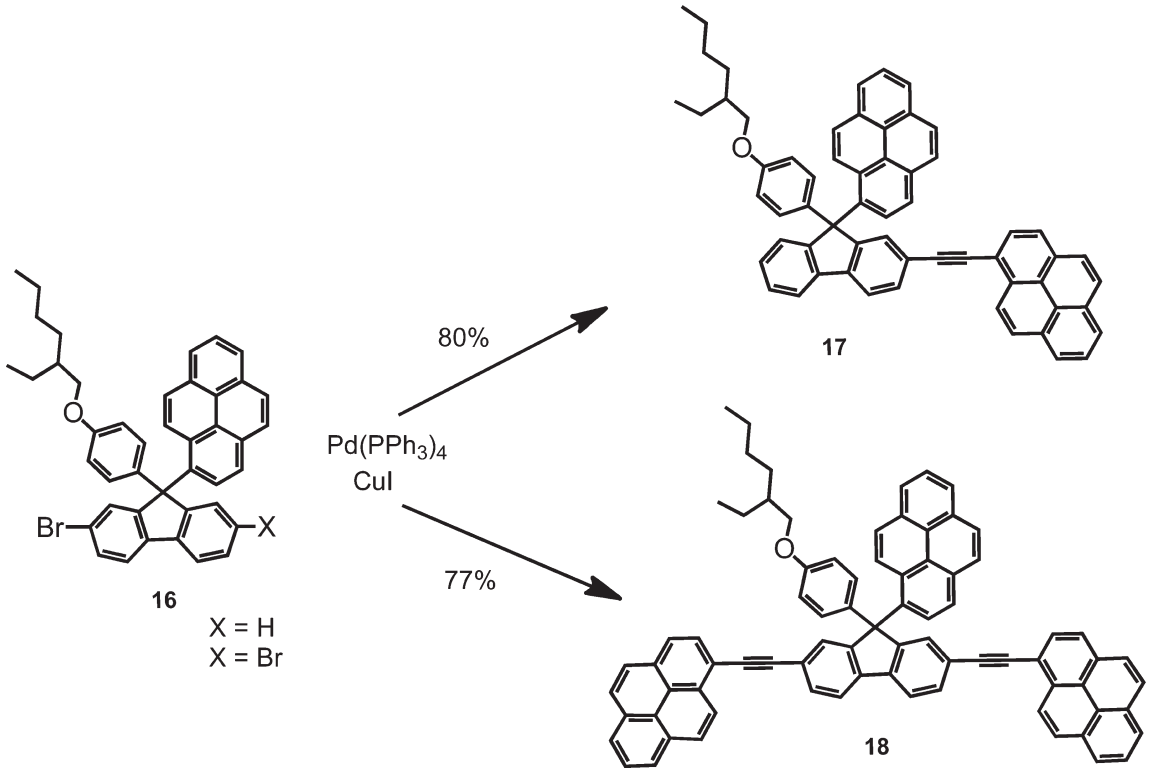


**Figure 8.** Sonogashira reaction to diarylfluorenes **17** and **18**.

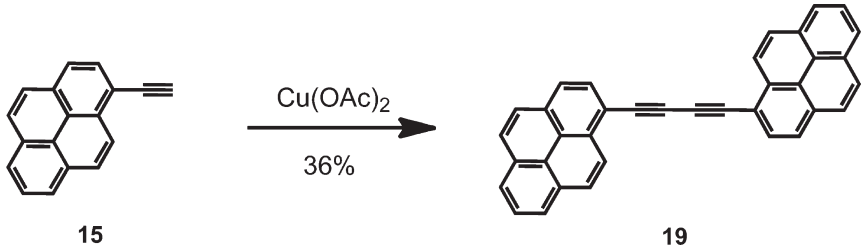


**Figure 9.** Glaser coupling to 1,4-dipyren-1-ylbuta-1,3-diyne (**19**).

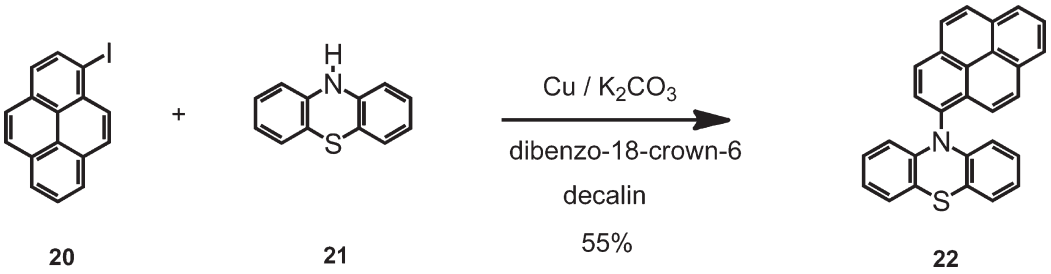


**Figure 10.** Ullmann coupling to 10-pyren-1-yl-10*H*-phenothiazine (**22**).

be prepared from the 1-iodopyrene, followed by Heck reaction with a allylic alcohol to introduce a alkanone chain, followed by the reaction with $Br_2$ and NaOH.[107] Another alternative is to obtain the 1-butyric acid directly from pyrene through a similar multistep route.[108] For instance, the multichromophore system **32** was obtained by an esterification reaction for further study of the photoinduced processes between the chromophores (Figure 14). Thus, perylene bisimide **31** was reacted with 1-pyrenebutyric acid (**30**) in the presence of DCC/DPTS to give the tetrapyrene−perylene bisimide dye **32** in 40% yield (Figure 14).

An example of an esterification reaction including a pyrene alcohol is illustrated in Figure 15. The 1-pyrenebutanol (**34**) was previously prepared by reduction of methyl 4-(1-pyrenyl)butyrate with DIBAL-H[109] and was further involved in the esterification



Samsung Exhibit 1020, Page 8 of 55

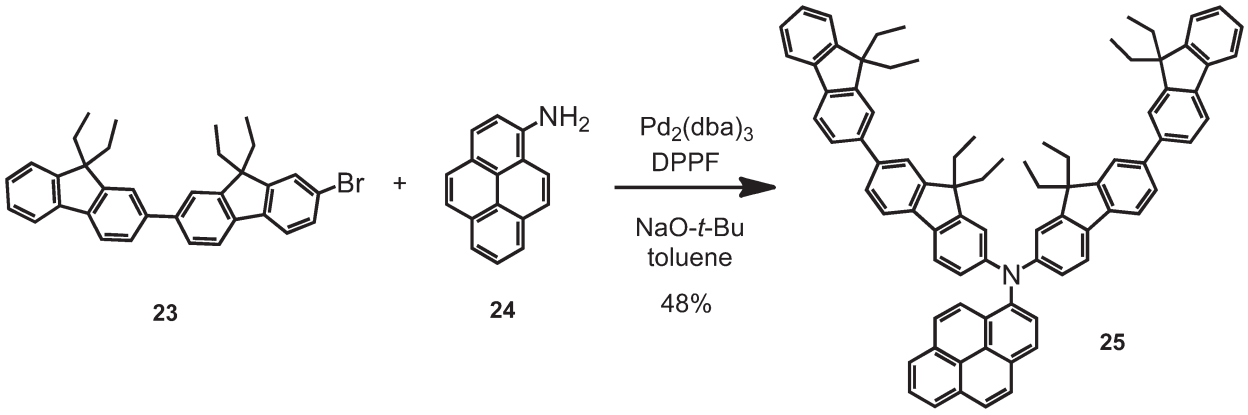


**Figure 11.** Reaction to bis(difluorenyl)amino-substituted pyrene **25**.

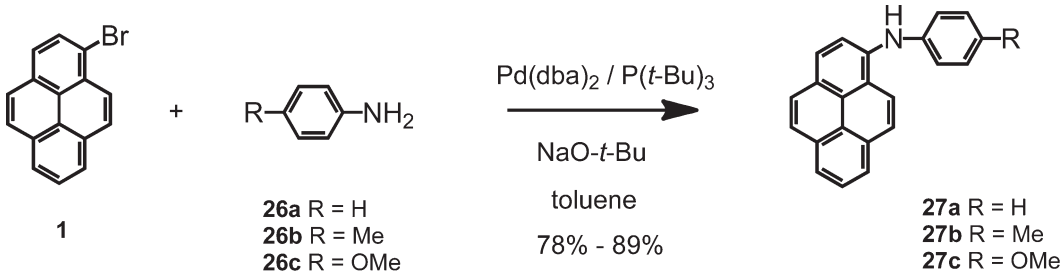


**Figure 12.** Coupling to afford pyrenylamines **27**.

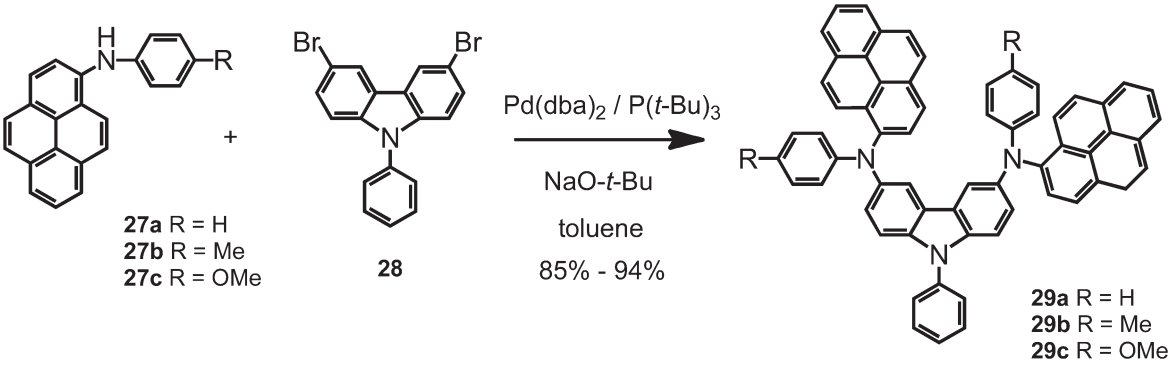


**Figure 13.** Reaction to give 3,6-bis(diarylamino)carbazoles **29**.

reaction with the benzoic acid **33** using DCC and DPTS (Figure 15). Using these reaction conditions [4-(1-pyrenyl)butyl] 3,4,5-tris(12,12,12,11,11,10,10,9,9,8,8,7,7,6,6,5,5-heptadecafluoro-*n*-dodecan-1-yloxy)benzoate (**35**) was achieved in 60% yield.

The pyrene-1-carboxylic acid can be obtained from the 1-acetylpyrene with pyridine and NaOCl,[103] with $Br_2$ and NaOH,[110] or alternatively directly from pyrene with oxalyl chloride and $AlCl_3$ which results, however, in low yield and as a mixture with the diketone.[111] Pyrene-1-carboxylic acid (**37**) can be involved in an esterification reaction, for example, with hexa-*peri*-hexabenzocoronene **36** in the presence of EDC and DMAP in $CH_2Cl_2$ to furnish the pyrenyl-HBC system **38**, which was used as a model to study the self-assembling of discotic $\pi$-system dyads (Figure 16).

The 1-pyrenecarboxaldehyde is obtainable in good yield directly from pyrene, for example, using the conditions reported by Vollmann and co-workers with methylphenylformamide and $POCl_3$.[84] Other conditions include the use of dichloromethyl methyl ether in the presence of $AlCl_3$[112] or $TiCl_4$.[113] It is also possible to obtain the carboxaldehyde by oxidation of the 1-pyrenemethanol in the presence of molecular oxygen and a ruthenium catalyst[114] or from 1-(bromomethyl)pyrene by oxidation with $MnO_2$.[115]

Afterward, the 1-pyrenecarboxaldehyde can be involved in various reactions such as in the synthesis of the monomer **41** (Figure 17). The dinitro compound **40**, containing a pyridine heterocyclic ring and a pyrene pendent group, was synthesized via a modified Chichibabin reaction. The condensation of 1-pyrenecarboxaldehyde (**39**) with 4′-nitroacetophenone in the presence of ammonium acetate gave 4-(1-pyrenyl)-2,6-bis(4-nitrophenyl)pyridine (**40**) in one step in 57% yield. Reduction of dinitro compound **40** in ethanol with hydrazine hydrate in the



Samsung Exhibit 1020, Page 9 of 55

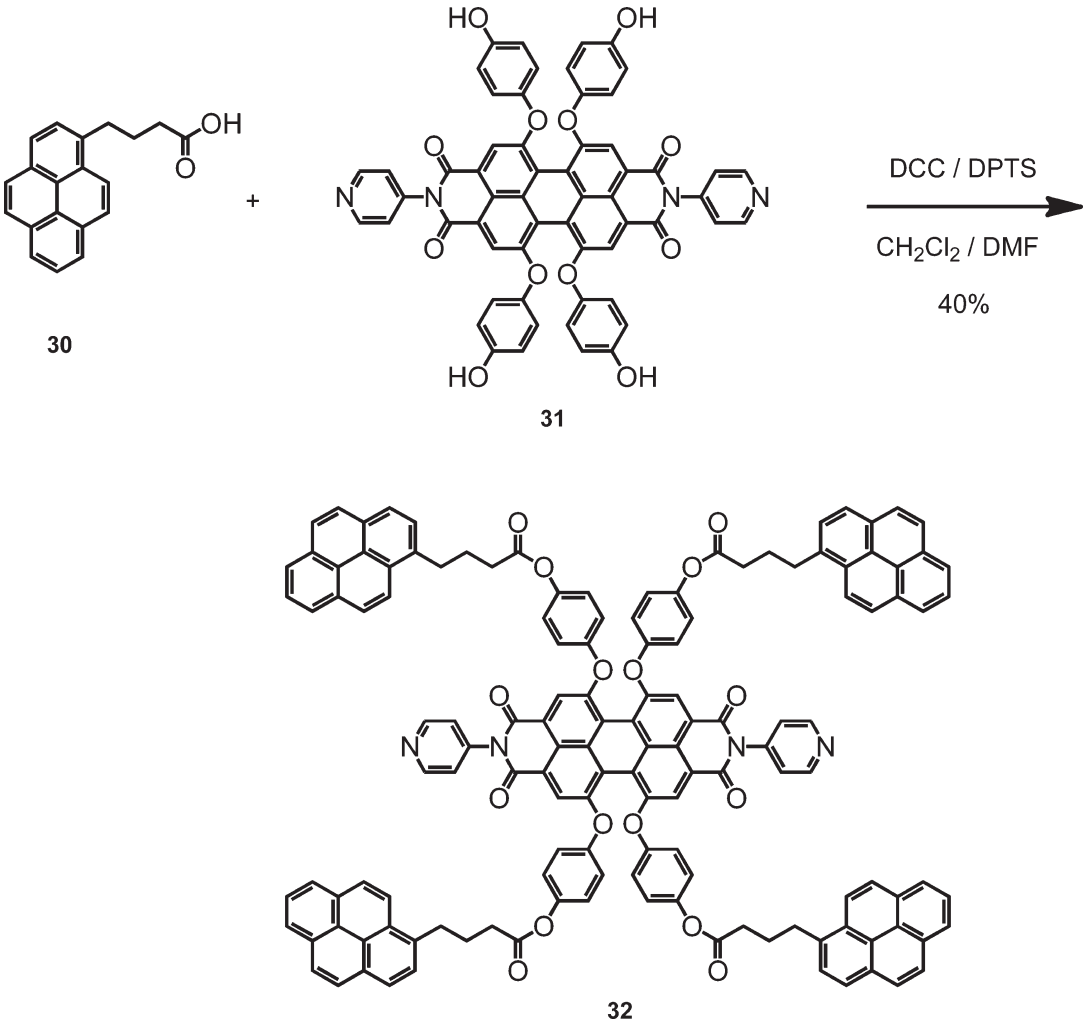


**Figure 14.** Esterification reaction to furnish tetrapyrene−perylene bisimide dye **32**.

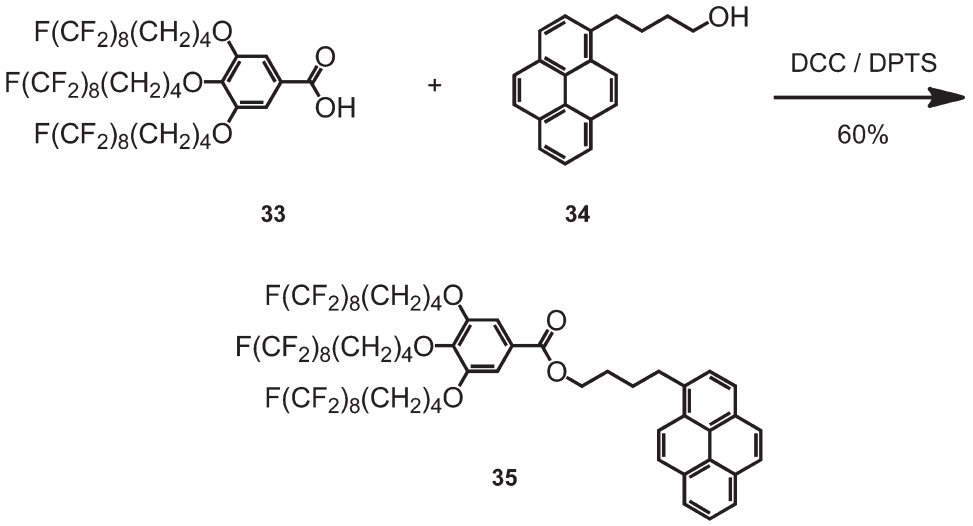


**Figure 15.** Esterification reaction to give [4-(1-pyrenyl)butyl] 3,4,5-tris(12,12,12,11,11,10,10,9,9,8,8,7,7,6,6,5,5-heptadecafluoro-*n*-dodecan-1-yloxy)benzoate (**35**).

presence of catalytic amounts of palladium on carbon produced the 4-(1-pyrenyl)-2,6-bis(4-aminophenyl)pyridine (**41**) in 67% yield (Figure 17). This pyrene monomer **41** was used to prepare the poly(pyridine-imide) for optoelectric applications. As will be



Samsung Exhibit 1020, Page 10 of 55

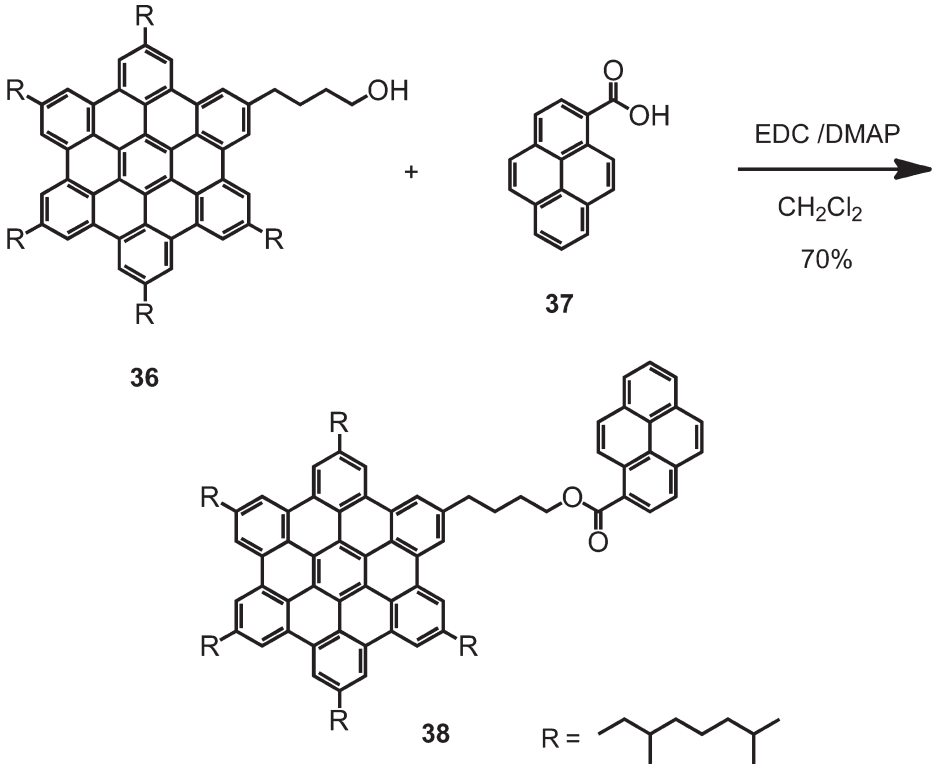


**Figure 16.** Esterification to give pyrenyl-HBC system **38**.

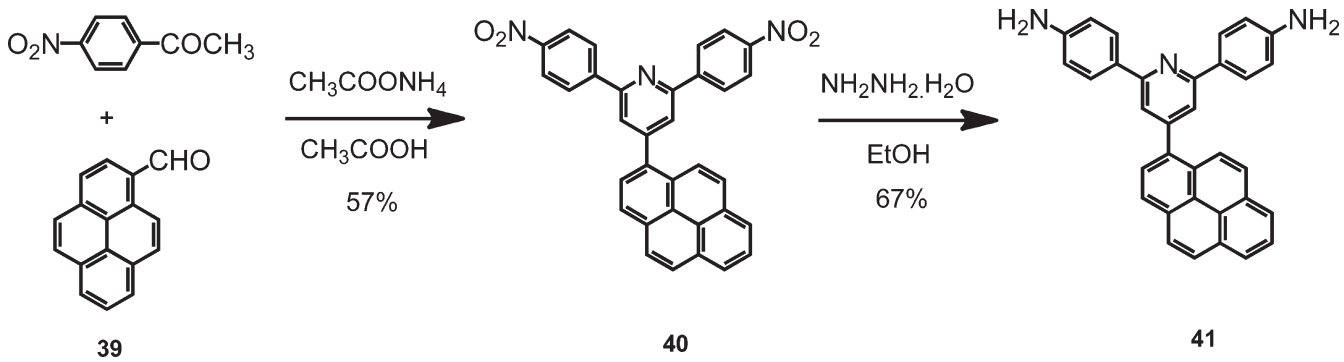


**Figure 17.** Synthetic route to 4-(1-pyrene)-2,6-bis(4-aminophenyl)pyridine (**41**).

described, the optical properties of this polymer can be modulated upon protonation of the pyridine unit.

The 1-pyrenecarboxaldehyde can also be involved in Prato's 1,3-dipolar cycloaddition reaction with $C_{60}$ and a azomethine ylide generated in situ in order to obtain a $C_{60}$−pyrene dyad, which allows the study of the photoinduced processes between pyrene and an electron acceptor. The reaction of the 1-pyrenecarboxaldehyde (**39**) with $C_{60}$ and sarcosine in toluene gave $C_{60}$−pyrene dyad **42** in 56% yield (Figure 18).

The 1-pyrenemethanol can be easily obtained by reduction of 1-pyrenecarboxaldehyde with different reduction agents, such as $Li(BH_3CN)$,[116] $NaBH_4$,[113,117−119] or $LiAlH_4$.[96] It can also be prepared from the pyrene-1-carboxylic acid with $H_2SO_4$ followed by reduction with $LiAlH_4$.[110]

1-Pyrenemethanol (**43**) can be subsequently involved in a condensation reaction, as depicted in Figure 19. The pyrene **45** was attached to a perylene bisimide building-block in order to

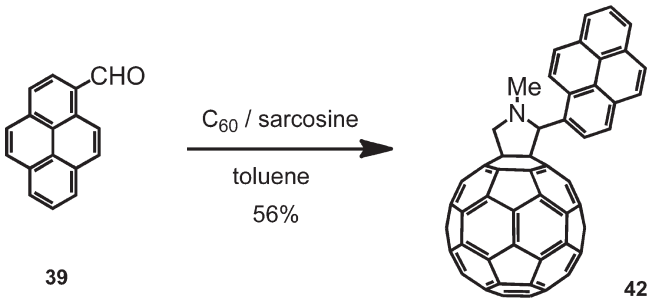


**Figure 18.** 1,3-Dipolar cycloaddition to $C_{60}$−pyrene dyad **42**.

prepare a fluorescent switch in which light-induced shuttling of a macrocycle along the thread between pyrene and perylene produces changes in the interaction between the two chromophores.



Samsung Exhibit 1020, Page 11 of 55

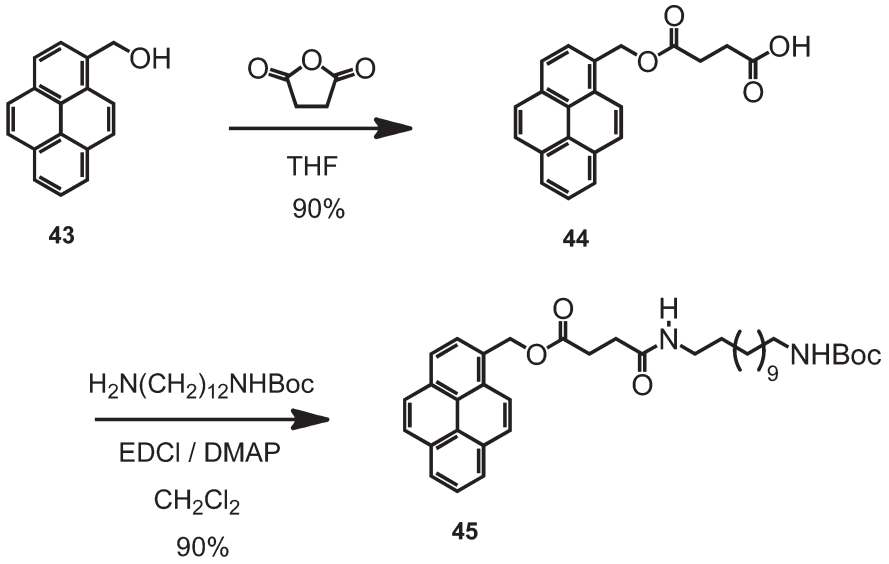


**Figure 19.** Synthetic route to pyrene-containing protected amine **45**.

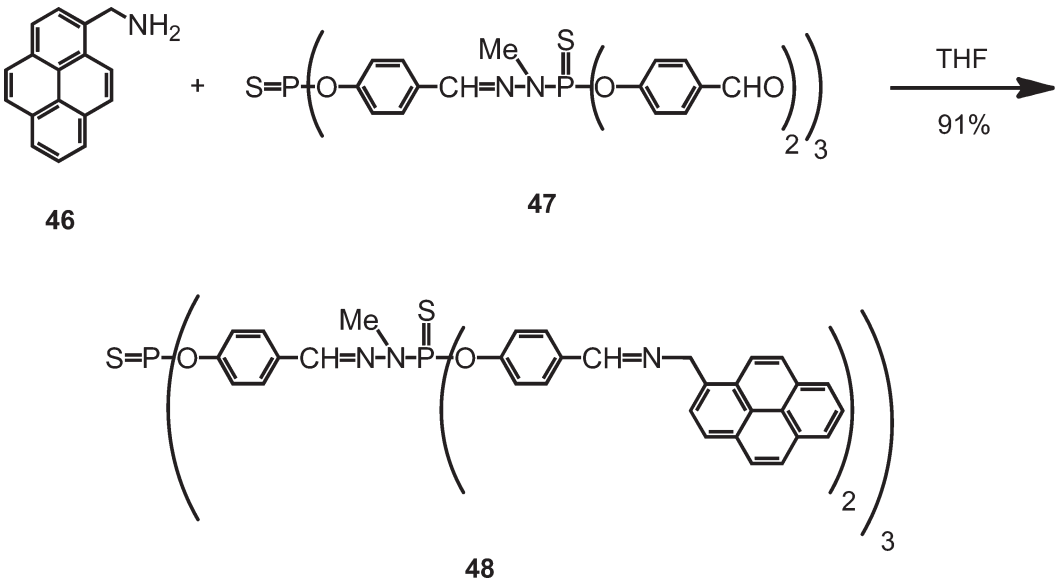


**Figure 20.** Condensation reaction to obtain first-generation dendrimer **48**.

The 1-pyrenemethylamine can be prepared by reaction of 1-pyrenecarboxaldehyde with hydroxylamine hydrochloride to afford pyrenecarboxaldehyde oxime, followed by treatment with Zn dust in acetic acid.[120] 1-Pyrenemethylamine (**46**) can be further used in condensation reactions with aldehydes, such as the one depicted in Figure 20. Compound **48** constitutes the first generation of a series of phosphorus dendrimers bearing pyrene as chromophoric end group, for the application in blue-emitting OLEDs.

The preparation of 1-substituted pyrene azides is possible starting from the 1-pyrenemethanol[121] for further employment in the CuI-catalyzed Huisgen reaction (azide–alkyne cycloaddition). Thus, the reaction of pyrene azide **49** with acetylene **50** in the presence of $CuSO_4$ and sodium ascorbate in THF/$H_2O$ furnished **51** in the excellent yield of 94% (Figure 21).[122] In the next section, we will describe the employment of compound **51** as a building-block to prepare light-harvesting antenna systems based on the excimer formation of pyrene.

The Grignard reaction can also be utilized to prepare 1-substituted pyrenes, interesting for molecular electronics. For example, the biarylmethanol **52** was synthesized in 76% yield via Grignard reaction of the 4-bromobenzaldehyde and pyrene-1-ylmagnesium bromide prepared in situ from 1-bromopyrene (**1**) (Figure 22). The following reduction of the hydroxy group using $Me_2SiHCl/InCl_3$ gave 1-(4-bromobenzyl)pyrene (**53**) in 86% yield (Figure 22).

Another possibility to prepare pyrene-based materials is the Friedel–Crafts reaction directly from pyrene. The Friedel–Crafts reaction, using aluminum chloride, between cyanuric chloride and pyrene in xylene as a halogen-free aromatic solvent in the presence of a small amount of sodium ethoxide gave



Samsung Exhibit 1020, Page 12 of 55

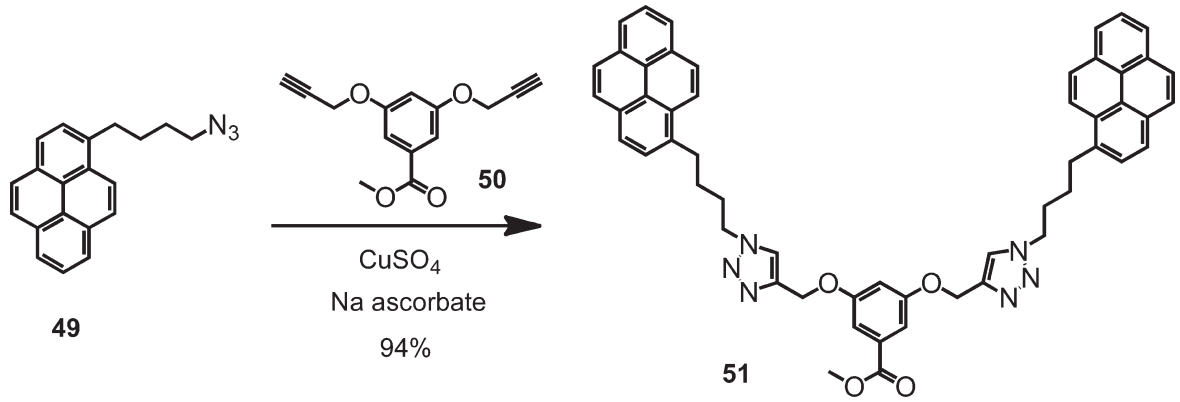


**Figure 21.** Huisgen reaction to give pyrene building-block **51**.

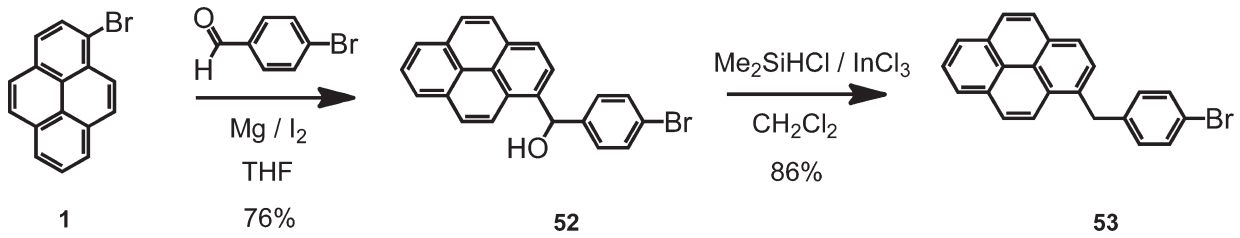


**Figure 22.** Synthetic route to 1-(4-bromobenzyl)pyrene (**53**).

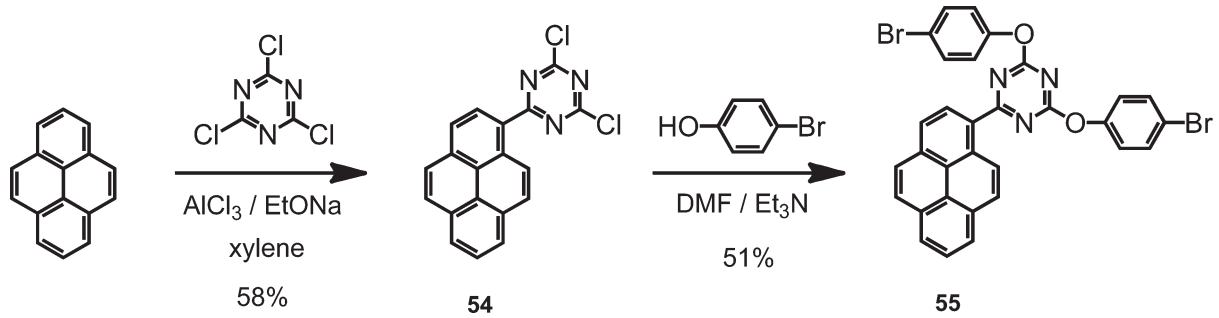


**Figure 23.** Synthetic route to 2,4-bis(4-bromophenoxy)-6-(pyren-1-yl)-1,3,5-triazine (**55**).

2,4-dichloro-6-pyren-1-yl-1,3,5-triazine (**54**) in 58% yield (Figure 23). Compound **54** reacted subsequently with 4-bromophenol in DMF utilizing triethylamine as an acid acceptor to furnish the 2,4-bis(4-bromophenoxy)-6-pyren-1-yl-1,3,5-triazine (**55**) in 51% yield (Figure 23). The pyrenyltriazine building block **55** was used to prepare two series of random copolymers with fluorene or *p*-phenylene units, which behave as blue- or green-light-emitting materials.

### 3.2. 1,3,6,8-Tetrasubstituted Pyrenes

Most pyrene derivatives are monosubstituted, but a practical precursor to tetrafunctional compounds is 1,3,6,8-tetrabromopyrene, which has been produced easily on the gram scale since 1937, by the bromination of pyrene at high temperatures.[84]

Thus, 1,3,6,8-tetrabromopyrene (**56**) can be obtained in high yield (90%) via bromination with $Br_2$ in nitrobenzene at 160 °C (Figure 24).[123]

This straightforward access to 1,3,6,8-tetrabromopyrene has opened up new routes to a broad family of C-functionalized pyrenes obtained by Suzuki or Sonogashira coupling reactions.

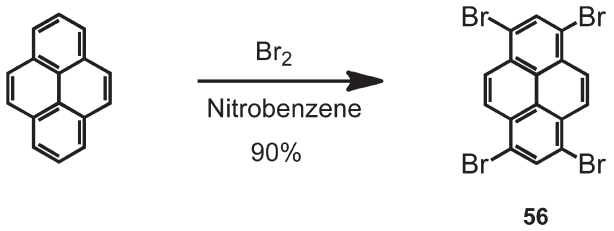


**Figure 24.** Bromination reaction to 1,3,6,8-tetrabromopyrene (**56**).

The Suzuki reaction between 1,3,6,8-tetrabromopyrene (**56**) and different boronic acids using palladium catalyst could furnish different tetrasubstituted pyrenes **57**−**60**, such the ones depicted in Figure 25.[124] The tetrasubstitution, in this case, allows a particular conformation, which avoids aggregation between pyrenes and permits the use of these pyrene-based derivatives in light-emitting devices.

1,3,6,8-Tetrabromopyrene (**56**) can also be involved in Sonogashira couplings. For example, the reaction of



Samsung Exhibit 1020, Page 13 of 55

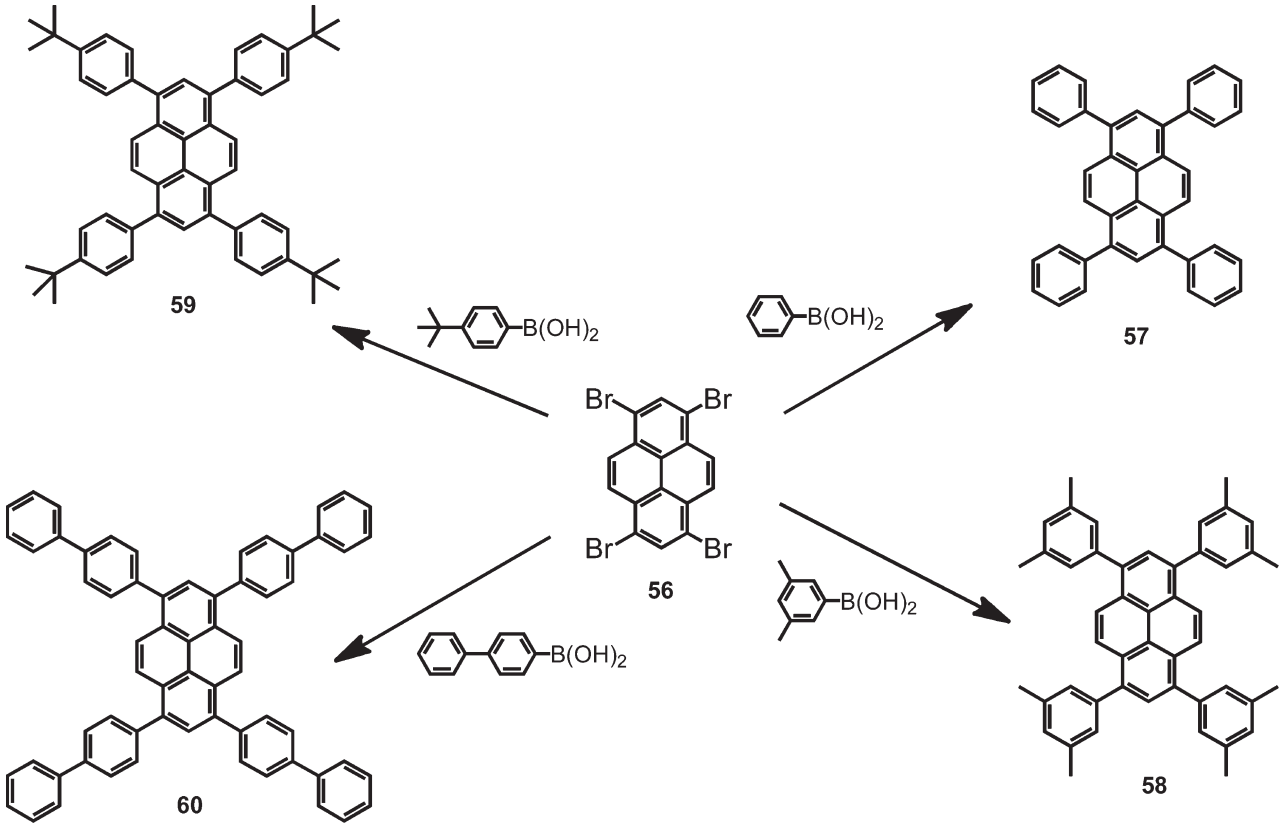


**Figure 25.** Suzuki coupling between tetrabromopyrene **56** and different boronic acids.

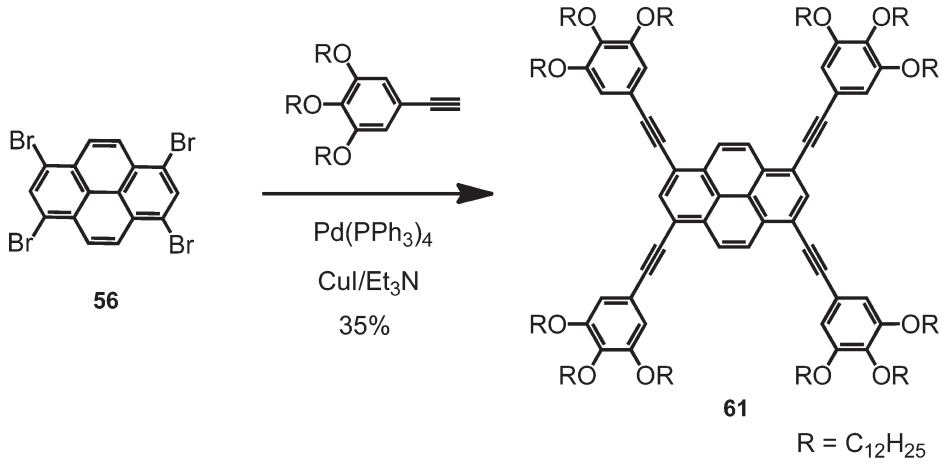


**Figure 26.** Sonogashira coupling to tetrasubstituted pyrene **61**.

3,4,5-tridodecyloxyphenylacetylene with **56** gave the tetrasubstituted pyrene **61** in 35% yield (Figure 26).[125]

A different strategy is based on the previous preparation of 1,3,6,8-tetraethynylpyrene (**63**), which constitutes an important building block for further Sonogashira couplings (Figure 27). In this way, a Sonogashira–Hagihara cross-coupling of 1,3,6,8-tetrabromopyrene (**56**) with trimethylsilylethyne afforded 1,3,6,8-tetrakis((trimethylsilyl)ethynyl)pyrene (**62**) in 83% yield, which was deprotected with $K_2CO_3$ in methanol to give the pyrene building block **63** in the high yield of 95% (Figure 27).

1,3,6,8-Tetraethynylpyrene (**63**) can be directly used in Sonogashira cross-coupling reactions[126] or in Diels–Alder cycloadditions, as depicted in Figure 28. For instance, the Diels–Alder cycloaddition between **63** and tetraphenylcyclopentadienone **64** in *o*-xylene provided the first-generation dendrimer **65** in 95% yield (Figure 28). The substitution of pyrene at the 1,3,6,8-positions allows the incorporation of pyrene as active core in dendrimers to evaluate the degree of site-isolation of the core, like in the case of pyrene dendrimer **65**.

1,3,6,8-Tetrabromopyrene (**56**) was also used in a simple nucleophilic aromatic substitution with thiolate anions in a polar solvent to achieve polysulfurated derivatives including pyrene (Figure 29).[127] Compound **66** was obtained in 90% yield from 4-methylbenzenethiol after heating in DMF at 80 °C in the



Samsung Exhibit 1020, Page 14 of 55

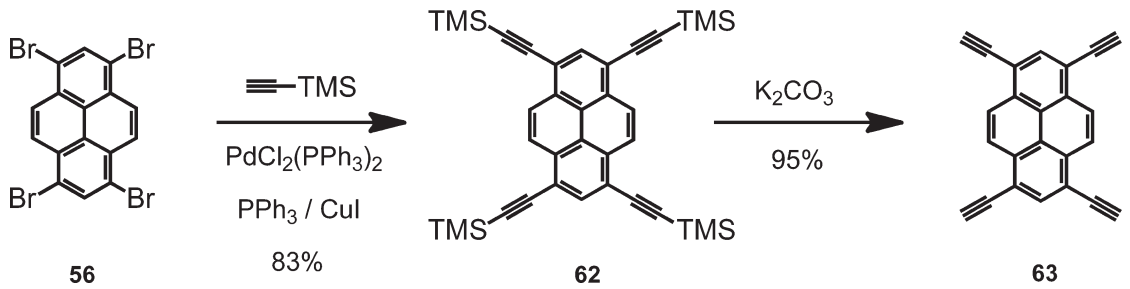


**Figure 27.** Synthetic route to 1,3,6,8-tetraethynylpyrene (**63**).

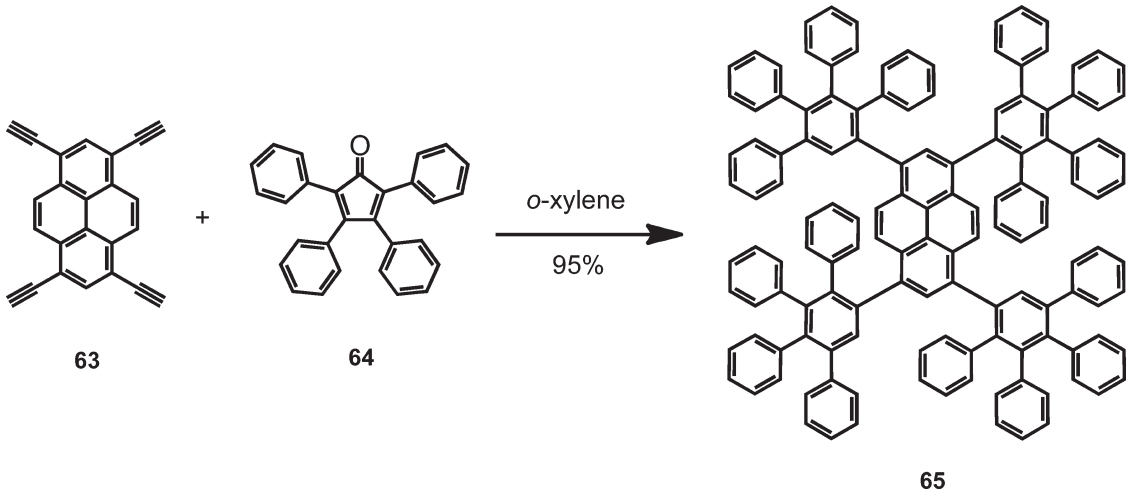


**Figure 28.** Diels–Alder cycloaddition to first-generation dendrimer **65**.

presence of a strong base (NaH). The first-generation dendrimer **66** presents interesting redox properties, such as the change of the color emission upon reversible one-electron oxidation, which may be useful for optoelectronic devices.

An approach to attach different alkyl chains to the pyrene aromatic system starts with pyrene-1,3,6,8-tetracarboxylic acid (**67**) synthesized following the procedure of Vollmann and co-workers[84] and subsequent esterification with $SOCl_2$ and different alcohols to various different pyrene esters **68** (Figure 30).[128] Some of these pyrene esters present columnar liquid crystalline behavior combined with electroluminescence.

### 3.3. 1,6- And 1,8-Disubstituted Pyrenes

The conversion of pyrene into disubstituted pyrenes always results in complex mixtures of the 1,6- and 1,8-disubstituted pyrenes (Figure 31), which are difficult to isolate.

Bromination of pyrene to provide dibromopyrene results in a mixture of 1,6- and 1,8-dibromopyrenes that can only be separated by several fractional crystallizations from toluene based on the only slight difference in solubility.[129] The tedious and difficult separation of 1,6-dibromopyrene affords a useful pyrene building block for coupling reactions such as Suzuki, Sonogashira, or Heck.

An interesting method to reach tetrasubstituted pyrenes with two different functional groups consists of the use of two Suzuki coupling reactions, as presented in Figure 32.[130] Reaction of 1,6-dibromopyrene (**69**) with 3-pyridinylboronic acid in the presence of $Pd(PPh_3)_4$ and $K_2CO_3$ in THF gave 1,6-dipyridin-3-ylpyrene (**70**) in 74% yield. Bromination of compound **70** with pyridinium hydrobromide perbromide in 1,2-dichlorobenzene furnished 3,3′-(3,8-dibromopyrene-1,6-diyl)dipyridine (**71**) in 70% yield. A second Suzuki coupling with 2-naphthylboronic acid afforded 3,3′-(3,8-dinaphthalen-2-ylpyrene-1,6-diyl)dipyridine (**72**) in 80% yield. Tetrasubstituted pyrene **72** was then used as a new electron transport material for the fabrication of blue OLED devices.

The most common reactions using 1,6-disubstituted pyrenes include Sonogashira couplings. For example, the reaction of 1,6-diethynylpyrene (**73**) with carbazole derivatives **74** and **76** under Sonogashira conditions allowed the preparation of the 1,6-disubstituted pyrenes **75** and **77**, as depicted in Figure 33.[131] These pyrene-carbazole-based organic emitters **75** and **77** were used in the fabrication of electroluminescent devices.

The Heck coupling is also frequently employed in the preparation of 1,6-disubstituted pyrene-based oligomers or polymers. One such example is the reaction of 1,6-dibromopyrene (**69**) with 1,4-didodecyloxy-2,5-divinylbenzene in the presence of $Pd(OAc)_2$ and $P(o\text{-tolyl})_3$ in DMF and $Et_3N$ to afford the fluorescent pyrene-based polymer **78** in the good yield of 80% (Figure 34).[132]

Beside the frequently employed coupling reactions, the direct oxidation of pyrene has also appeared as an alternative method to prepare 1,6- and 1,8-disubstituted pyrenes.[84] The weakness of this route lies in the fact that the obtained mixture of 1,6- and 1,8-disubstituted pyrenes cannot be easily isolated.

Pyrene-1,6-dione (**79**) and pyrene-1,8-dione (**80**) were prepared in a ratio 1:1 (55% yield) by the oxidation of pyrene with sodium dichromate in 3 M $H_2SO_4$ solution (Figure 35). It is



Samsung Exhibit 1020, Page 15 of 55

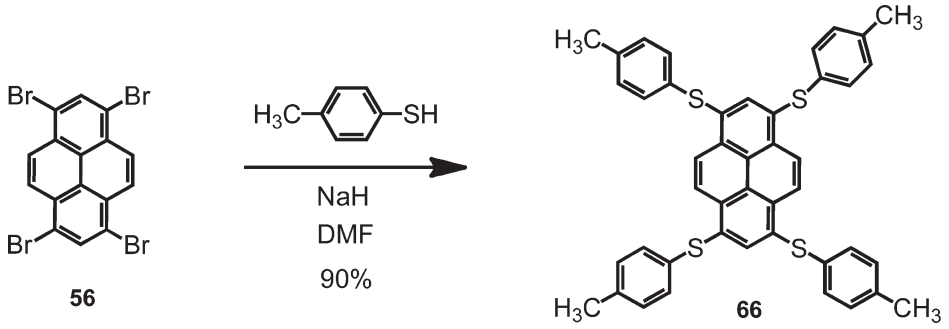


**Figure 29.** Synthesis of first-generation dendrimer **66**.

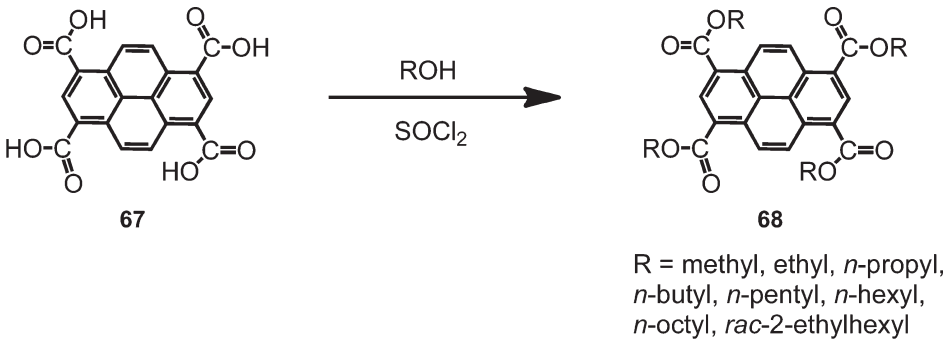


**Figure 30.** Esterification reaction to tetrasubstituted pyrene esters **68**.

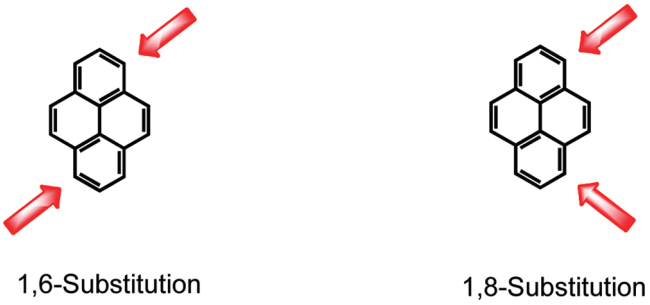


**Figure 31.** General structure of 1,6- and 1,8-disubstituted pyrenes.

common that the mixture of 1,6- and 1,8-disusbtituted pyrenes will be involved in the next reaction step, due to their highly difficult separation. Thus, the mixture was treated with an alcohol in the presence of $FeCl_3$ to prepare the corresponding alkoxy pyrene derivatives **81** and **82** in 23−38% yields. Disubstituted pyrenes **81** and **82** constitute a new class of $\pi$-acceptor discotic liquid crystalline compounds having a pyrenedione core.

### 3.4. 1,3-Disubstituted Pyrenes

Although the electrophilic substitution of pyrene occurs at the 1,3,6,8-positions, as previously mentioned, the formation of 1,3-disubstituted pyrenes is not easily accessible, since the 1,6- and the 1,8-disubstituted pyrenes are preferentially formed. Very recently, however, our group developed an innovative approach to selectively obtain 1,3-disubstituted pyrenes (Figure 36).

This synthetic concept includes the use of a *tert*-butyl group as a positional protective group and low temperature reaction conditions to provide the 1,3-disubstituted pyrene in high yield. Thus, pyrene was first mono-*tert*-butylated to give 2-*tert*-butylpyrene (**83**), which was then treated with bromine (2 equiv) in $CH_2Cl_2$ at −78 °C to furnish 1,3-dibromo-7-*tert*-butylpyrene (**84**) in 89% yield (Figure 37).[133] The monomer **84** was used to prepare the respective polymer as blue-emitter for single-layer OLEDs.

This new 1,3-dibromopyrene building block opens a new field in terms of 1,3-substitution of pyrenes, allowing many possibilities in terms of coupling reactions such as Suzuki, Sonogashira, Yamamoto, or Heck, for example.

We recently reported the Suzuki coupling reaction of 1,3-dibromo-7-*tert*-butylpyrene (**84**) with 7-*tert*-butylpyrene-1-boronic acid pinacol ester (**85**) to afford 7,7′,7″-tri-*tert*-butyl-1,1′:3′,1″-terpyrene (**86**) in 68% yield (Figure 38).[133] Compound **86** was used as a model compound to study the photophysical properties and stereoisomerism of polypyrene dendrimers.[133]

### 3.5. 2,7-Substituted Pyrenes

Substitution of pyrene at the 2- and 7-positions (Figure 39) represents a general problem, as these positions are not directly accessible by electrophilic substitution of pyrene itself, thus demanding an indirect route.

The usual approach to substitution of the 2-position of pyrene follows the lines of the early work of Vollmann,[84] who started with the carboxylic acids at the 2-position prepared from the 1,2-phtaloylpyrene in the melt with potassium. The synthesis of the acids themselves often involved unpredictable yields and tedious separation of isomers. Furthermore, this method is difficult for the introduction of halogens, in that the acid is converted to the amine, which must then be changed to the halide by the Sandmeyer reaction or a variation thereof, which normally proceeds in low yield with polynuclear aromatic amines.



Samsung Exhibit 1020, Page 16 of 55

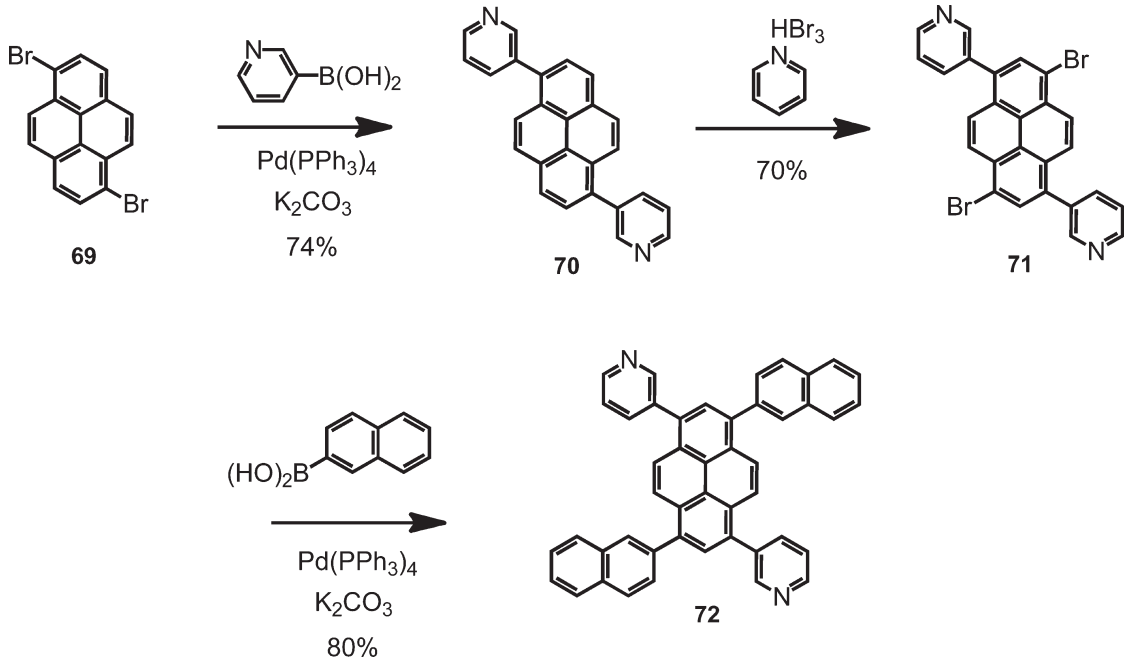


**Figure 32.** Synthetic route to 3,3′-(3,8-dinaphthalen-2-ylpyrene-1,6-diyl)dipyridine (**72**).

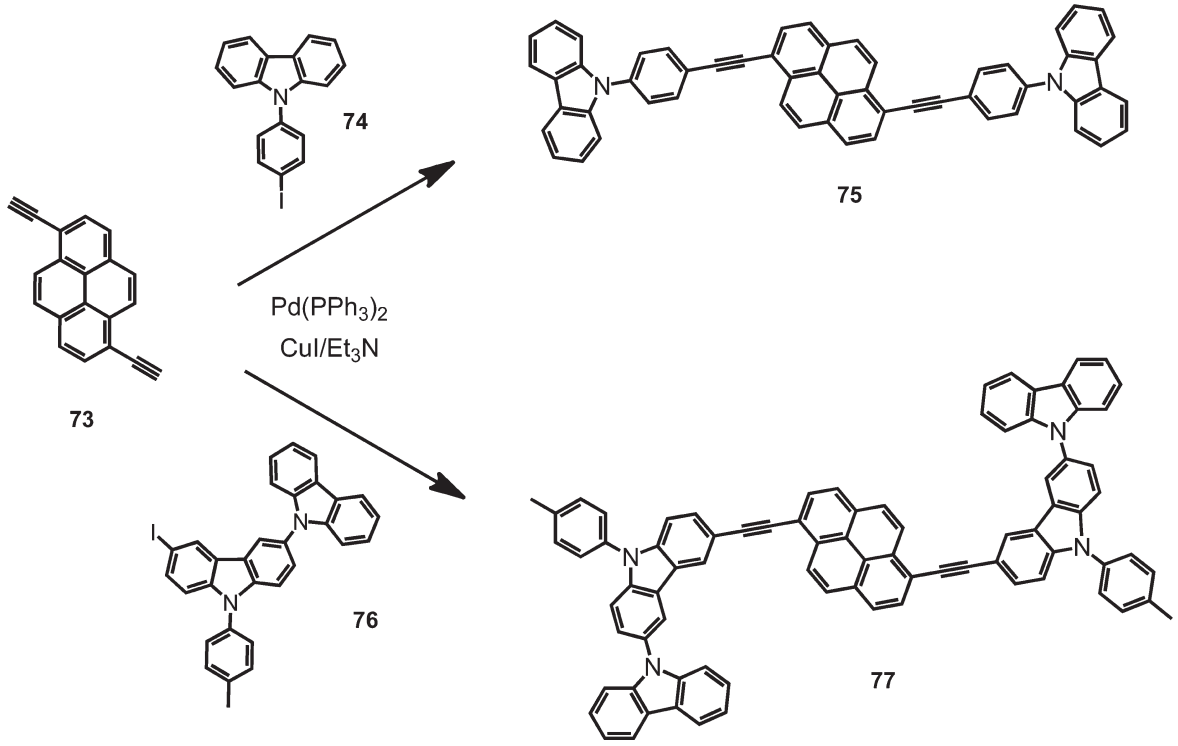


**Figure 33.** Sonogashira coupling to 1,6-disubstituted pyrenes **75** and **77**.

In an effort to circumvent these difficulties, two main approaches have been employed: (a) the reduction of pyrene to 4,5,9,10-tetrahydropyrene followed by electrophilic substitution and subsequent rearomatization and (b) use of cine substitution via a 1,2-dehydropyrene intermediate to convert 1-bromopyrene to a mixture of 1- and 2-aminopyrene, separation of the amines, and conversion to the halide. However, these are multistep and low-yielding processes, which increase the difficulty in obtaining the 2,7-substituted pyrenes.

An example of this indirect route to achieve functionalization at the 2,7-positions is depicted in Figure 40. 4,5,9,10-Tetrahydropyrene (**87**) was synthesized in 85% yield by the reduction of pyrene with $H_2$ and palladium on carbon (Figure 40). Compound **87** was converted to 2,7-dibromotetrahydropyrene (**88**)



Samsung Exhibit 1020, Page 17 of 55

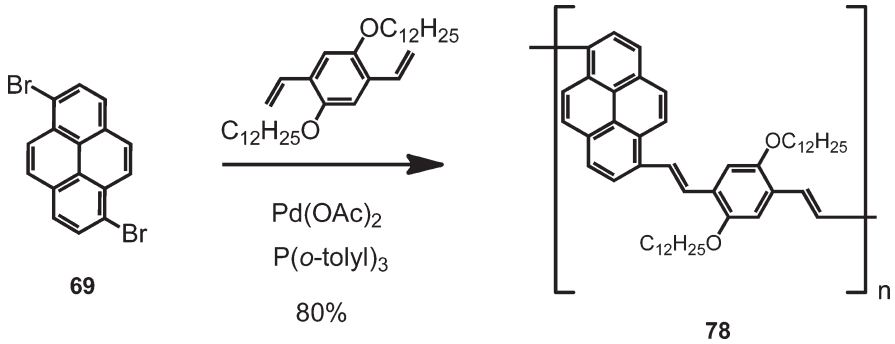


**Figure 34.** Heck coupling to pyrene-based polymer **78**.

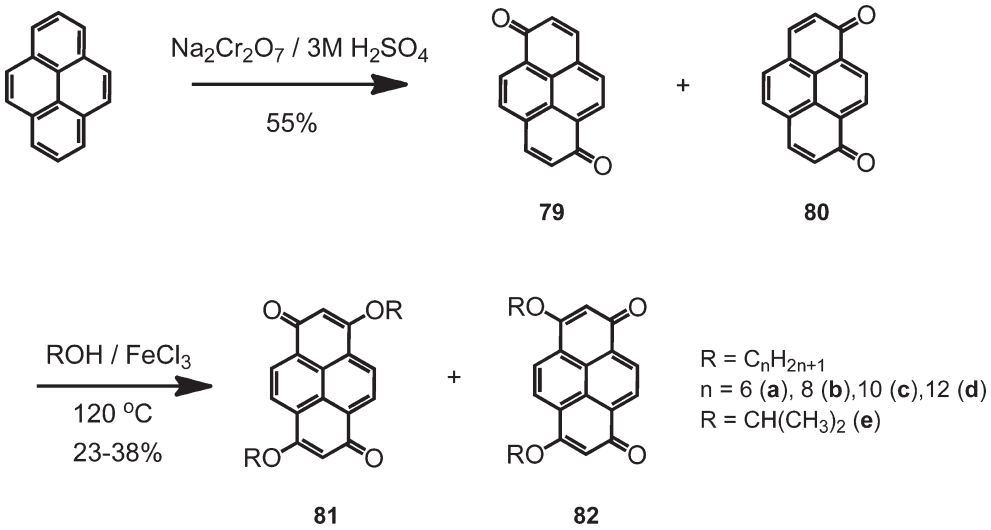


**Figure 35.** Synthetic route to pyrenediones **81** and **82**.

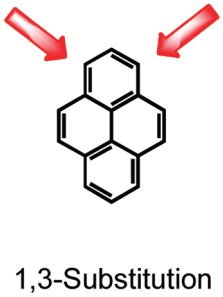


**Figure 36.** General structure of 1,3-disubstituted pyrenes.

in 55% yield following the modified bromination developed by Harvey et al., who used a solution of **87** in acetic acid. Subsequently, 2,7-dibromotetrahydropyrene (**88**) was monolithiated with *n*-BuLi at −90 °C and reacted with octyl chloroformate to yield the ester **89** in one step in 72% yield. The ester **89** was oxidized with 2 equiv of DDQ to give compound **90** in 63% yield.

Recently, a one-step synthesis was reported to obtain pyrene-2,7-bis(boronate)ester in very good yields using an iridium-based catalyst.[134] The pyrene-2,7-bis(boronate)ester and the pyrene-2-(boronate)ester obtained following this method can be directly used in several Suzuki couplings. On the basis of this boronation reaction, our group developed a new synthetic method to synthesize the 2,7-dibromopyrene in only two steps and in high yields (Figure 41). Bromination of pyrene-2,7-bis(boronate)-ester (**91**) with $CuBr_2$ afforded 2,7-dibromopyrene (**92**) in the good yield of 70%. Following the same strategy, pyrene-2-boronate ester (**93**) provided 2-bromopyrene (**94**) in 75% yield (Figure 41).

This strategy circumvents difficulties in obtaining 2,7-dibromopyrene (**92**) and 2-bromopyrene (**94**) and opens many possibilities in terms of using these attractive building-blocks in different coupling reactions.

### 3.6. 4,5,9,10-Substituted Pyrenes

The 4,5,9,10-positions of the pyrene ring are very interesting for the preparation of extended aromatic systems; however, as in the case of the 2-substituted pyrenes, these positions are difficult to reach (Figure 42).

Several attempts have been made to prepare pyrene-4,5-diones and pyrene-4,5,9,10-tetraones directly from pyrene. Pyrene-4,5-dione has been prepared in low yield by the oxidation of pyrene with the highly toxic osmium tetroxide.[135] The pyrene-4,5-dione and pyrene-4,5,9,10-tetraone have been also prepared by multistep synthetic routes.[136−138] To avoid such multistep routes to the tetraones, the oxidation of pyrene was reported using a heterogeneous mixture of ruthenium(III)chloride ($RuCl_3$) and sodium periodate ($NaIO_4$) in $CH_2Cl_2$, $H_2O$, and $CH_3CN$, which selectively provided pyrene-4,5-dione (**95**) and pyrene-4,5,9,10-tetraone (**96**), depending on the reaction



Samsung Exhibit 1020, Page 18 of 55

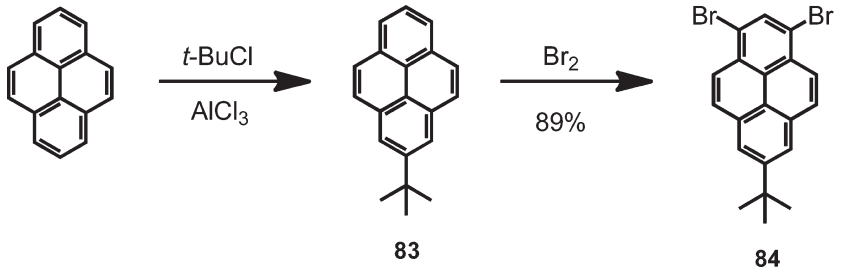


**Figure 37.** Synthesis of 1,3-dibromo-7-*tert*-butylpyrene (**84**).

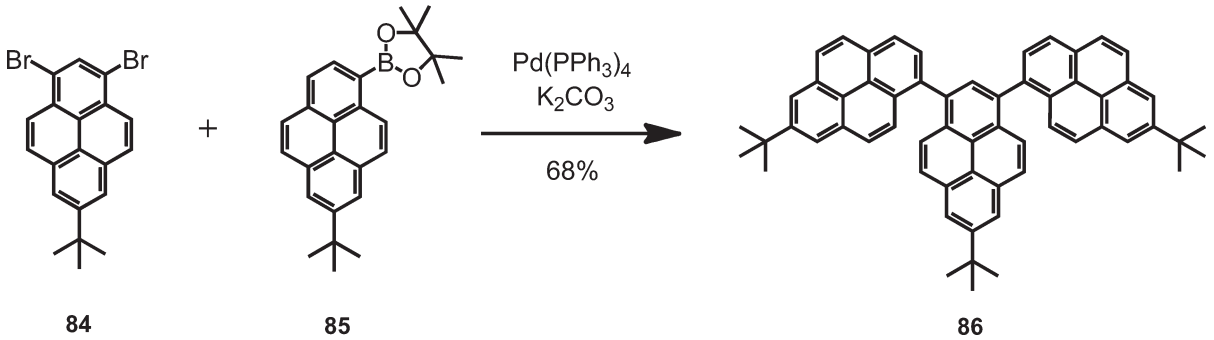


**Figure 38.** Synthesis of 7,7′,7″-tri-*tert*-butyl-1,1′:3′,1″-terpyrene (**86**).

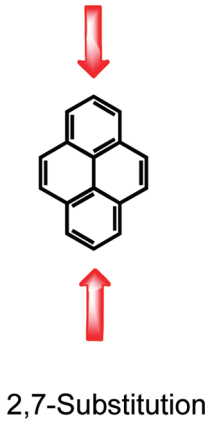


**Figure 39.** General structure of 2,7-disubstituted pyrenes.

temperature and the amount of oxidant used (Figure 43).[139] This strategy opened many possibilities in terms of extension of the pyrene conjugated system by simple condensation reactions.[140]

An example of the use of pyrene-4,5-dione (**95**) is depicted in Figure 44. Pyrene-4,5-dione was condensed with 1,3-diphenylacetone in ethanol in the presence of KOH to achieve 1,3-diphenylcyclopentapyren-2-one (**97**) in 53% yield. Sequential aryne formation from the triflate precursor triggered by TBAF (tetrabutylammonium fluoride), followed by trapping with 2 equiv of pyrene **97** afforded compound **98** in 22% yield (Figure 44). The electroluminescent pyrene **98**, also called "twistacene", was used as emitter with a host polymer to fabricate single-layer white OLEDs.

Another important strategy to reach the 4,5,9,10-position of the pyrene ring includes the use of two *tert*-butyl groups at the 2,7-positions as positional protective groups and the presence of iron in the reaction mixture. Thus, bromination of 2,7-di-*tert*-butylpyrene (**99**) with 6.0 equiv of bromine in the presence of iron powder resulted in an acid-catalyzed rearrangement of bromine atoms and gave 4,5,9,10-tetrabromo-2,7-di-*tert*-butylpyrene (**100**) in 90% yield (Figure 45).[141]

The building block **100** allows many metal-catalyzed cross-coupling reactions with the possibility of removal of the *tert*-butyl groups using acid conditions.

A special case of functionalization of the pyrene ring is achieved via direct nitration. The nitration of pyrene by means of an equivalent amount of nitric acid in glacial acetic acid affords a mixture of 2- and 4-nitropyrene **101**, which is extremely difficult to separate, since their properties are expected to be similar (Figure 46). If the properties of this mixture of isomers are expected not to interfere with the properties of the final compound, it is possible to proceed to the next synthetic step using the mixture, such as in the case depicted in Figure 46.

Reaction of the isomers mixture **101** with hydrazine monohydrate and Pd/C afforded a mixture of 2- and 4-aminopyrene **102** in 72% yield. Consequent condensation with 1,7-(4-*tert*-butylphenoxy)perylene-3,4,9,10-tetracarboxylic dianhydride (**103**) afforded the pyrene−perylene dyad **104** in 70% yield (Figure 46). This pyrene−perylene system **104** was used as an acceptor material in the fabrication of photovoltaic devices.

In the following section we will show how these pyrene-containing molecules were employed as active semiconductors in devices. Most of the structures described in section 3 will be revisited in section 4 regarding their light-emitting behavior and semiconducting properties. The design of different molecular architectures based on the different substitution patterns of pyrene will be analyzed, as well the optical and electronic properties, in addition to the photoinduced processes, which are of particular interest in molecular electronics. Furthermore, we will highlight the role of these pyrene derivatives as



Samsung Exhibit 1020, Page 19 of 55

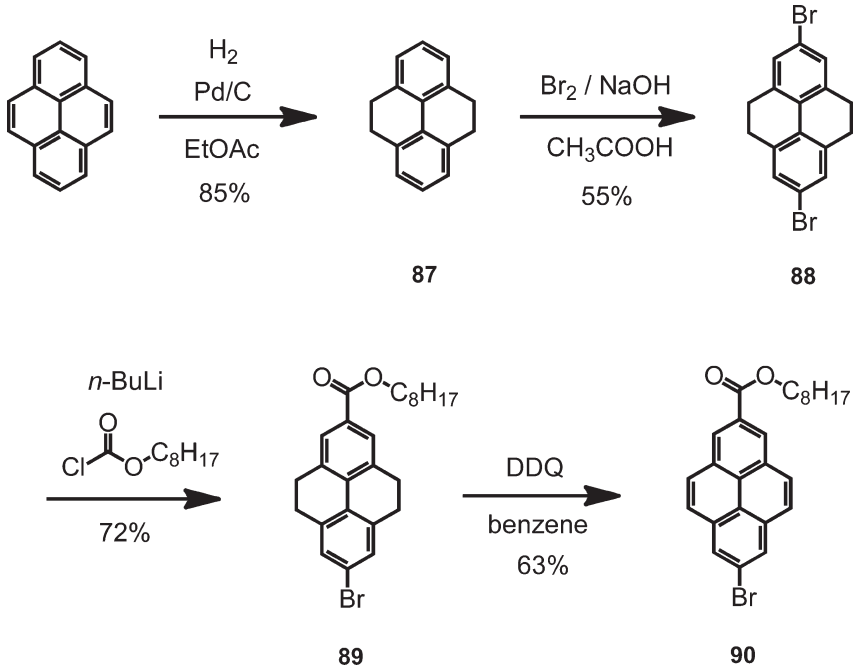


**Figure 40.** Synthetic route to achieve pyrene building block **90**.

semiconductor materials and evaluate these molecular components with respect to device fabrication and performance.

## 4. PYRENES AS ACTIVE COMPONENTS IN DEVICES

### 4.1. 1-Substituted Pyrenes

**4.1.1. Linear Structures.** Monosubstituted pyrenes are the most common pyrene derivatives and have been often involved in the preparation of small molecules and oligomers, as well as end-groups of polymers with interesting properties for organic electronic devices. Suitable modifications of the molecular structures with electro- or photoactive groups should allow the 1-substituted pyrenes to be transformed to more intelligent systems with improved charge carrier mobilities and/or photoluminescence for application in electronic and optoelectronic devices.

In molecular electronics it is also important to understand intramolecular charge transfer processes, such as energy and electron transfer, since these are fundamental processes in photochemistry. Molecular systems that contain several electron donors and/or acceptors tethered together using various types of bridge molecules have been extensively investigated. The principal aims of these studies have been to develop a better understanding of electron transfer, to mimic the very efficient electron transfer in the photosynthetic reaction centers, and to develop molecular electronic devices. Intramolecular charge transfer in organic systems has been widely investigated to identify the factors controlling the charge separation and charge recombination critical in molecular devices. Electronic interactions and charge transfer efficiencies in donor−acceptor systems based on pyrene have been investigated by comparing experimental and theoretical results. Intramolecular energy transfer processes in donor−acceptor systems including pyrene have been studied in a biphenylbisphthalimidethiophene[142] and in a fullerene−pyrene dyad.[143] Moreover, electron transfer processes have been reported in donor−acceptor systems including pyrene, such as pyrene and a xanthene dye;[144] also systems in which donor and acceptor are directly linked through a C−C $\sigma$-bond;[145] through conjugation via phenylene units;[146−148] linked via an ethynylene bridge;[149] or in a anion-bound supramolecular complex.[150]

In addition to the study of the photophysical properties and charge-transfer processes, which are of particular importance for the further development of electronic devices, many pyrene-based semiconductors have effectively been tested in the fabrication of devices such as OLEDs, for example.

Recently, it was demonstrated how the fine-tuning of the molecular structure can have a deep impact on optical and electronic properties by simple insertion of a phenylene group between two pyrene rings.[90] The 1,1′-dipyrenyl[151−154] and the 1,4-dipyrenylbenzene were synthesized from 1-bromopyrene under Suzuki coupling conditions and used as emitters for greenish blue OLED devices. Multilayer devices fabricated with 1,4-dipyrenyl benzene showed a power efficiency of 5.18 lm/W at a voltage, current density, and luminance of 5.2 V, 20 mA/cm$^2$, and 1714 cd/m$^2$, respectively. For the same device configuration, but using 1,1′-dipyrenyl, the best power efficiency was 4.09 lm/W at a voltage, current density, and luminance of 5.6 V, 20 mA/cm$^2$, and 1459 cd/m$^2$, respectively. The device fabricated with 1,4-dipyrenylbenzene shows better brightness and higher luminescence efficiency and power efficiency relative to the device with 1,1′-dipyrenyl. These values show that the pyrenyl group is a good luminescent center, and the insertion of a phenylene group between two pyrenes improves the performance of the device.

Similar dipyrenylbenzene derivatives and their application as extremely efficient blue emitters for electroluminescent devices were studied as well.[94] The three dipyrenylbenzenes **3**, **5**, and **6** prepared by Suzuki coupling present twisted structures (Figure 47), which results in a low degree of $\pi-\pi$ stacking in the solid state, and their emission wavelengths can be fine-tuned from 463 to 446 nm in thin films with high fluorescence quantum yields of 63−75%.

Furthermore, the nondoped devices based on 1-(2,5-dimethyl-4-(1-pyrenyl)phenyl)pyrene (**6**) as a host emitter can reach an



Samsung Exhibit 1020, Page 20 of 55

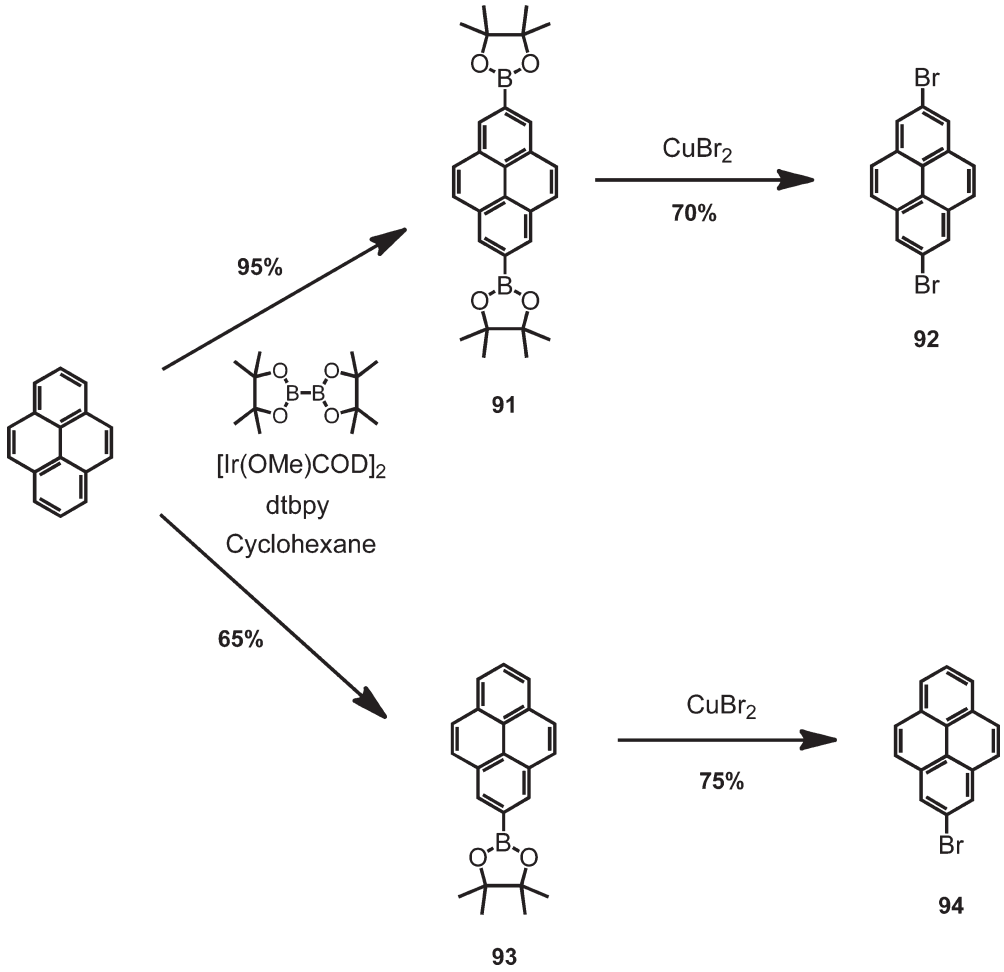


**Figure 41.** A new method to prepare 2-bromopyrene (**94**) and 2,7-dibromopyrene (**92**).

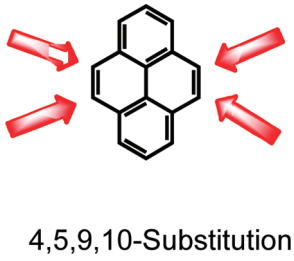


**Figure 42.** General structure of 4,5,9,10-tetrasubstituted pyrenes.

remarkably high external quantum efficiency ($\eta_{ext}$) of 5.2% in the deep-blue region with CIE coordinates of (0.15, 0.11) and a very high luminance of 40 400 cd $m^{-2}$ at 14 V. These materials have been shown to be excellent charge transporters and host emitters in OLED applications. These light-emitting characteristics are among the highest values reported so far for nondoped blue OLEDs and particularly correspond to the best performance achieved for nondoped pyrene-based blue OLEDs.

Beside the application of pyrene derivatives as light-emitting or light-emitting and transporting materials, pyrene-based systems have also find application as host materials in OLEDs. 1,3,5-Tri-1-pyrenylbenzene (**105**) was designed as a host material for blue emitters (Figure 48).[155]

A highly efficient blue OLED device was produced using compound **105** as host material. This fact comes from the favorable relation in the energy diagram in which both HOMO and LUMO levels of the dopant are enclosed in the band gap of the host material. The long lifetime of the device with **105** is due to the stable morphology of **105**, due to the high $T_g$ of **105**.

The design of innovative molecular structures combining pyrene and fluorene moieties has appeared as an important approach for the fabrication of blue-light-emitting OLED devices. Pyrene and fluorene are both widely investigated blue-emitting chromophores. However, pyrene in addition to its high photoluminescence efficiency and high charge carrier mobility, is a large planar aromatic system with better hole-injection ability than conjugated fluorene derivatives, because of its electron-rich character.

A series of fluorene derivatives, namely, 2,7-dipyrene-9,9′-dimethyl fluorene (**106**), 2,7-dipyrene-9,9′-diphenylfluorene (**107**), and 2,7-dipyrene-9,9′-spirobifluorene (**108**), constituted exclusively by carbon and hydrogen atoms was investigated (Figure 49).[156]

The pyrene units were introduced because they are highly emissive, bulky, and rigid, in order to improve the fluorescence quantum yield and thermal stability of the fluorene derivatives. These compounds containing pyrene groups at the C2,7-positions showed blue light emission with high fluorescence quantum yields. Further modification at the C9-position with dimethyl,



Samsung Exhibit 1020, Page 21 of 55

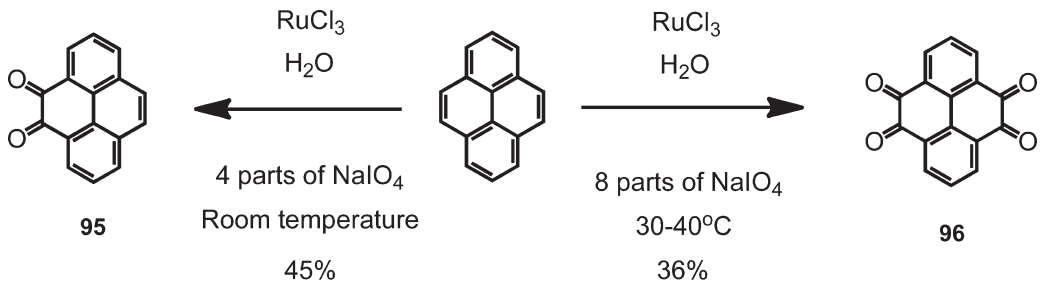


**Figure 43.** One-step synthesis to pyrene-4,5-dione (**95**) and pyrene-4,5,9,10-tetraone (**96**).

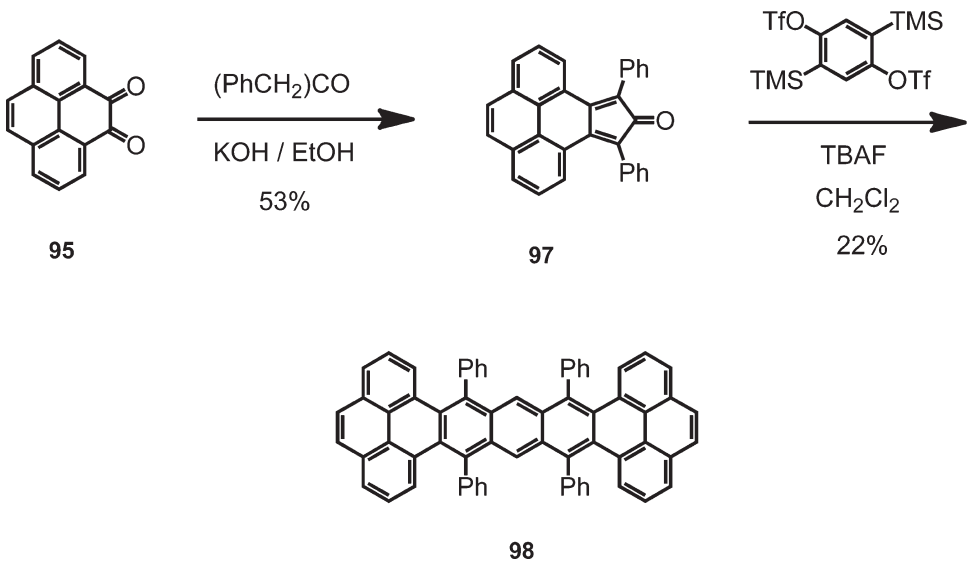


**Figure 44.** Synthetic route to twistacene (**98**).

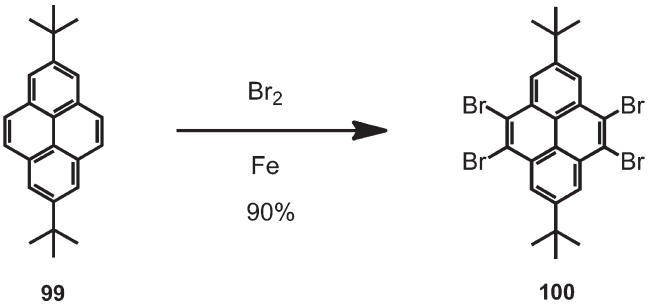


**Figure 45.** Bromination to afford 4,5,9,10-tetrabromo-2,7-di-*tert*-butylpyrene (**100**).

diphenyl, or spiro substituents allowed the fine-tuning of the thermal stability. As the size of the substituents at the C9-position increases from two methyl groups to a fluorene group, the glass-transition temperature ($T_g$) of the compounds increases from 145 to 193 °C. The blue-light-emitting OLEDs based on these compounds showed excellent efficiencies of 5.3 cd $A^{-1}$ and 3.0 lm $W^{-1}$ in nondoped OLED devices. This high efficiency arises from the molecular structure of the materials, which results in appropriate HOMO and LUMO levels for both hole and electron injection. Also, the good charge-carrier-transport properties and the high fluorescence efficiency contribute to the high performance of the devices.

A related system **10** bearing a vinylene unit was synthesized via Heck coupling as previously described in Figure 5.[95] The two hexyl chains at the C9-position of the fluorene enhance the solubility. A high photoluminescence efficiency of $\phi_{PL} = 0.64$ was measured in solution, while the photoluminescence efficiency of the thin films was significantly lower, resulting in $\phi_{PL} = 0.02$. This is due to the strong photoluminescence quenching caused by excimer formation. OLED structures with ITO/PEDOT:PSS/**10**/Mg:Ag/Ag displayed green electroluminescence with a brightness of up to 240 cd $m^{-2}$, which is a low value. Very poor EL characteristics were observed in the OLED devices, i.e., $\eta_{EL}$ was $4.3 \times 10^{-5}$ % at 30 V. This low $\eta_{EL}$ results from the high-energy barrier for hole injection and the poor film quality of the thin-film layer. As demonstrated, modification of the molecular structure by including vinylene units resulted in a strong propensity toward excimer formation and concentration quenching, leading to low emission efficiency.

Recently, a series of well-defined, pyrene-modified oligo(2,7-fluorene ethynylene)s was synthesized in order to study the influence of pyrene on the photo- and electroluminescence properties of the pyrene−fluorene oligomers **109**−**111** (Figure 50).[157]

These pyrene-containing oligomers were obtained via Pd/Cu-catalyzed Sonogashira couplings and exhibit good solubility, stable thermal properties, and high photoluminescence emission. The extended structure between pyrene and fluorene, resulting from the triple bonds, reduced the steric hindrance of the bulky



Samsung Exhibit 1020, Page 22 of 55

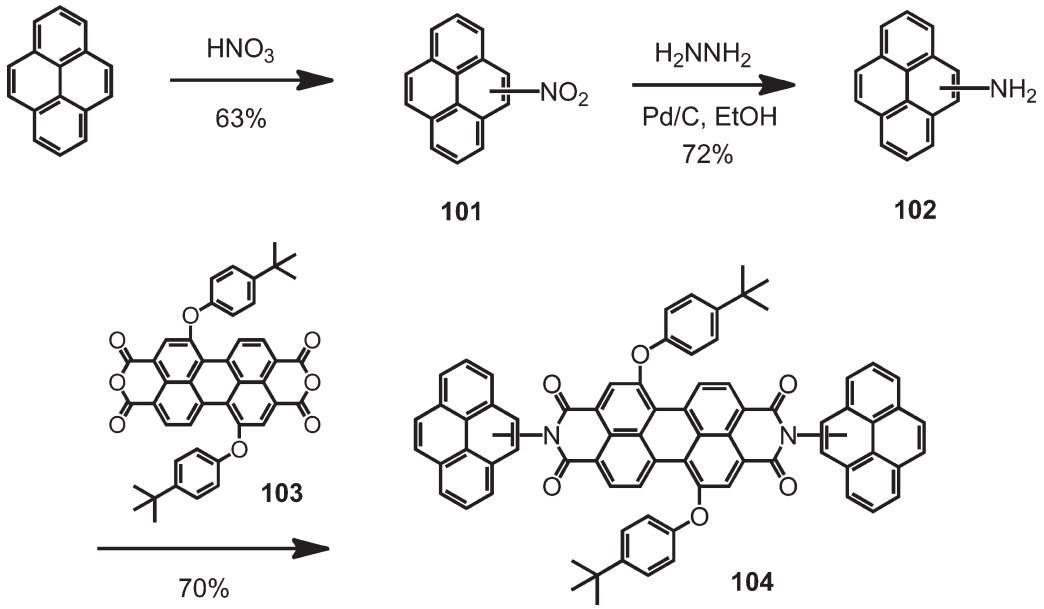


**Figure 46.** Synthetic route to pyrene−perylene dyad **104**.

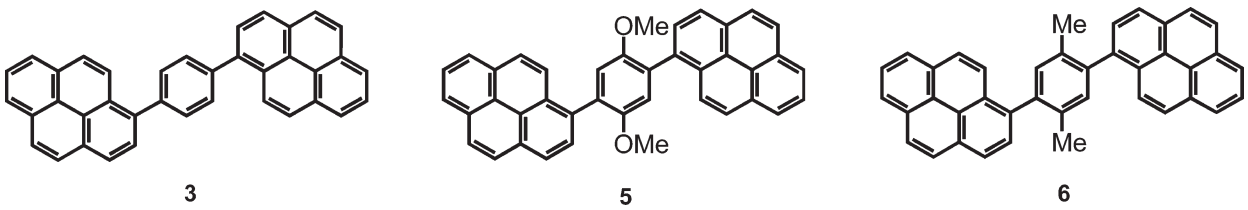


**Figure 47.** Dipyrenylbenzenes **3**, **5**, and **6**.

rigid pyrene and made the molecules more planar, relative to a C−C single bond. The strongly red-shifted emission of **109** in a thin film, compared to solution, is due to the formation of excimers between pyrene units, which caused the low-energy emission. The PL quantum yields of the oligomers were in the range of 0.78−0.98, which became higher with increasing length. Moreover, **111** ($\phi$ = 0.98) exhibited a higher quantum yield than oligomers with similar chain length. The difference in quantum yields might be due to the excitons extended over the whole backbone of **111**. Multilayer OLEDs using these materials as emissive layers showed that for oligomers **109**, **110**, and **111**, the EL emissions were observed from green to blue with an increasing number of fluorene moieties. Interestingly, the performance of the devices decreased as chain length increases. One possible explanation for this phenomenon was that the oligomers with more fluorene units crystallized more readily than the oligomers with fewer fluorene units. It is well-known that crystallization is disadvantageous to the electroluminescent properties of organic materials. As a result, the maximum luminance of these oligomers decreased with the chain length. On the other hand, the current density became higher with increasing oligomeric length. This result is in accordance with the previously reported dependence of carrier mobility on oligomer length, that is, the mobilities of both carriers increased with the backbone length. By comparison, relatively greater current density could also be observed in oligomers with more pyrene moieties.

The design of a different trimer system including pyrene and fluorene as bulky and highly blue emissive groups and

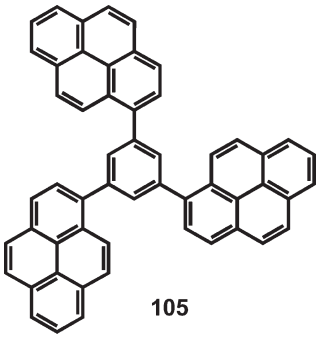


**Figure 48.** Chemical structure of 1,3,5-tri-1-pyrenylbenzene (**105**).

triphenylamine as hole-transporting moiety was achieved using Suzuki coupling, which resulted in a novel class of blue-light emitting materials **112** and **113** (Figure 51).[158]

These compounds have a three-dimensional conformation, which is beneficial for inhibiting self-aggregation and/or excimer formation in the solid state. In thin films, a blue emission with a peak at 440−470 nm without the unwanted long-wavelength emission was observed. The photoluminescence spectra exhibited excellent thermal stability upon annealing in air. The introduction of the triphenylamino groups at the C9-positions of the fluorene molecule resulted in a suitable HOMO energy level, which allowed effective hole injection. The attachment of



Samsung Exhibit 1020, Page 23 of 55

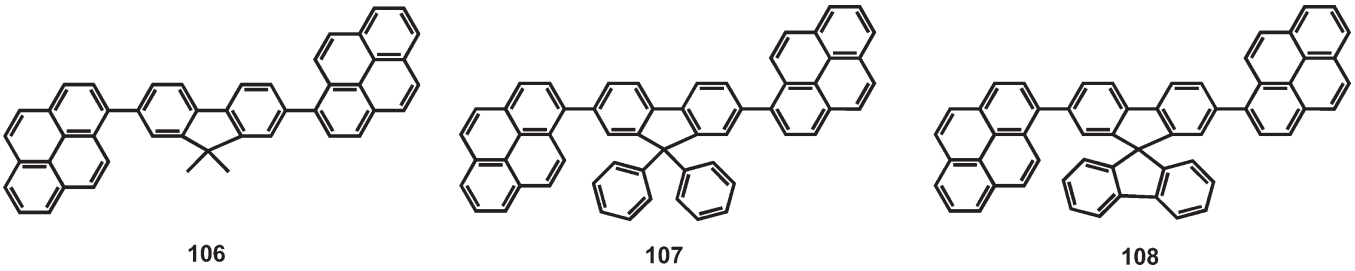


**Figure 49.** Chemical structure of fluorenes **106**−**108**.

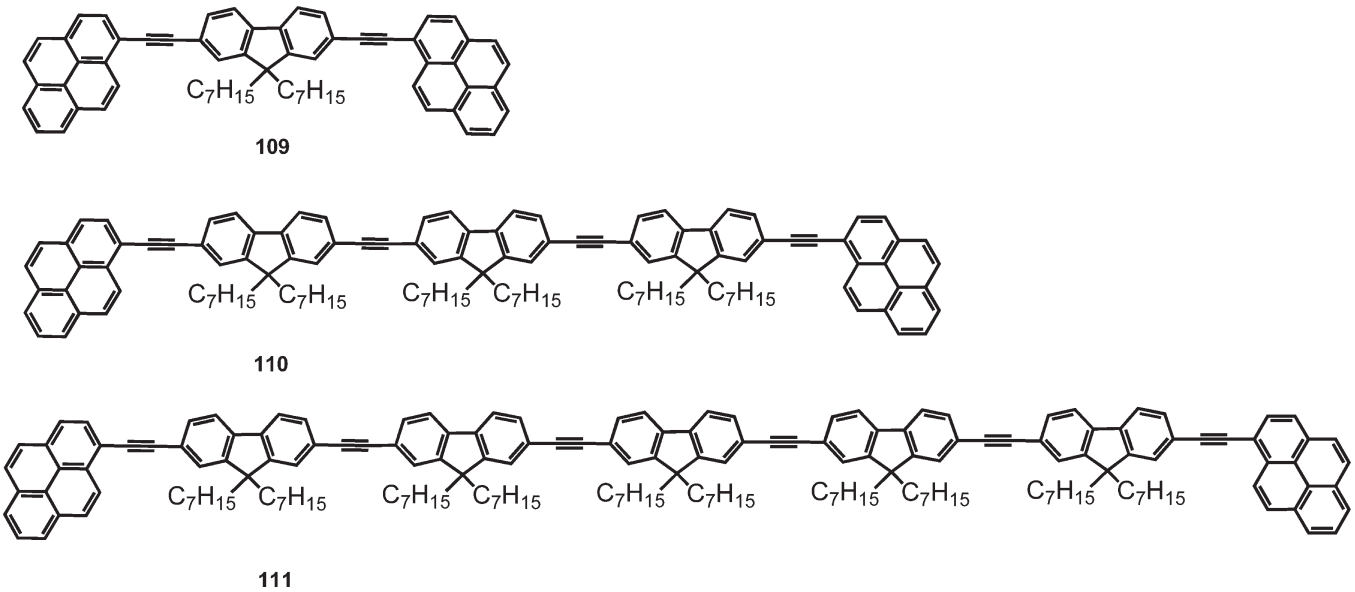


**Figure 50.** Pyrene-modified oligo(2,7-fluorene ethynylene)s **109**−**111**.

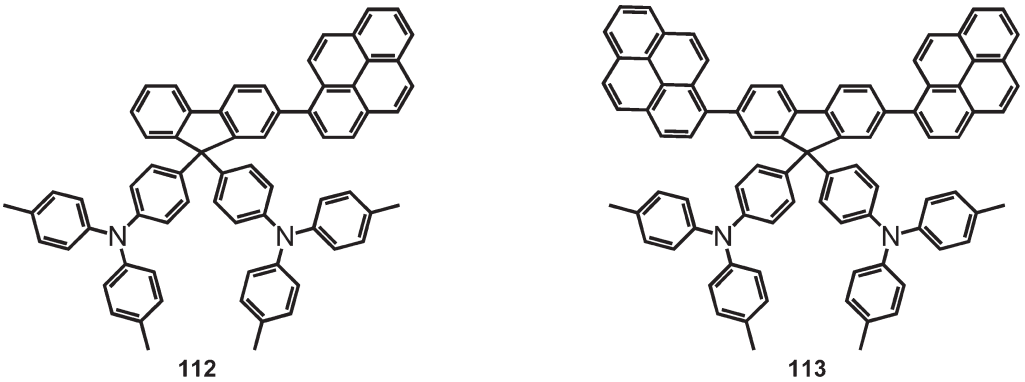


**Figure 51.** Chemical structure of **112** and **113**.

pyrene as a highly emissive moiety increases the fluorescence quantum yield. These trimer systems presented outstanding thermal stability with decomposition temperatures from 453 to 509 °C and showed high glass-transition temperatures of 153−174 °C.

Novel fluorene-substituted pyrenes including a pyrene unit at the C9-position of the fluorene moiety were investigated, namely, the new nonplanar 9-phenyl-9-pyrenylfluorenes **114** and **115** (Figure 52).[159] These pyrene-fluorene derivatives **114** and **115** were obtained via Suzuki coupling.

These materials combine the high thermal stability of the fluorene moiety with the high efficiency, high carrier mobility, and hole-injection advantage of pyrene. A OLED device, ITO/TCTA/**115**/BCP/Mg:Ag, without the need for hole-injection layer, showed very bright blue electroluminescence (EL) (19 885 cd $m^{-2}$), with the low turn-on voltage of 3.5 V, current efficiency of 3.08 cd/A, and power efficiency of 1.17 lm/W, which is competitive with the best doped and nondoped blue OLEDs. This high performance of a nondoped blue OLED uses a simple



Samsung Exhibit 1020, Page 24 of 55

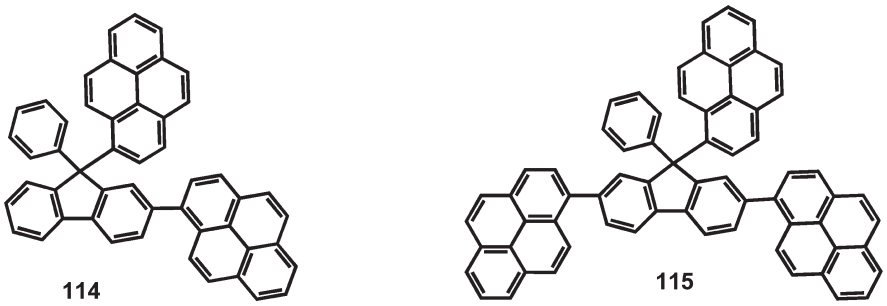


**Figure 52.** Chemical structure of 9-phenyl-9-pyrenylfluorenes **114** and **115**.

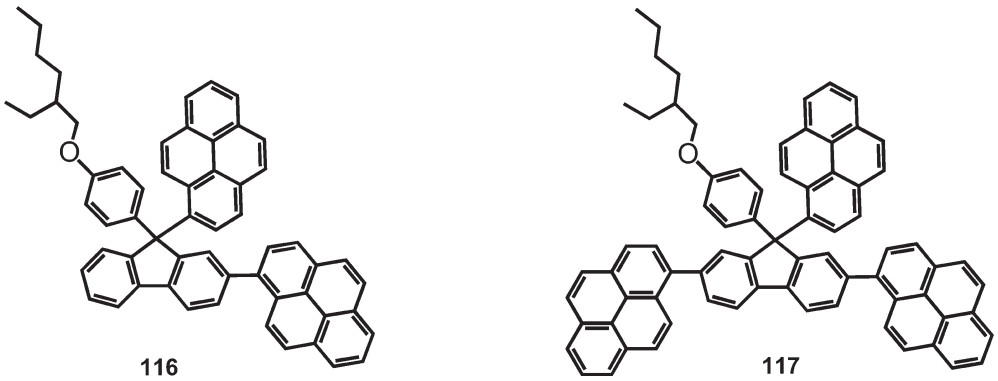


**Figure 53.** Chemical structure of fluorene-substituted pyrenes **116** and **117**.

device architecture, avoiding the need for hole-injection layers, thereby simplifying device fabrication. The introduction of a long alkyloxy chain in 9-alkylphenyl-9-pyrenylfluorene substituted pyrenes results in a better solubility and a lower tendency to crystallize in the devices.[160]

Very recently, it was demonstrated how to take advantage of the supramolecular $\pi-\pi$ stacking in new pyrene-functioned fluorenes **116** and **117**, as efficient solution-processable small molecules for blue and white organic light-emitting diodes (Figure 53).[161]

Modification of the molecular structure by incorporating only one 2-ethylhexyloxyl solubilizing chain allowed the formation of smooth films by spin-coating. The photophysical measurements revealed that the $\pi-\pi$ aggregation of pyrene increased the film-forming ability. In solution these molecules exhibit deep blue emission from the isolated molecules, and in thin film, their emission is dominated by supramolecular $\pi-\pi$ stacking of pyrene rings, which is located in the sky-blue region and is very broad. A single layer OLED using **116** as the bulk emitter showed efficient sky blue emission with the maximum brightness over 3600 cd/m$^2$ and peak efficiency up to 1.30 cd/A. Furthermore, a white electroluminescent device was obtained by doping MEH-PPV into the host **116**. Single layer white OLEDs displayed a maximum brightness of 5710 cd/m$^2$ and peak efficiency of 1.84 cd/A. The performance of these devices is reasonable for single layer OLEDs with emission of blue and white light; however, they have the advantage of using solution-processable small molecules.

Insertion of ethynylene units into the previous molecular structure via Sonogashira coupling as previously demonstrated in Figure 8 resulted in solution-processable molecular glasses with green light emission (compounds **17** and **18**).[98] These pyrene-functionalized diaryl-fluorenes present high thermal and morphological stabilities for optoelectronic applications. Single- and double-layered devices displayed efficient green emission, and the emission color remained fairly stable with increasing current. A single-layered device using CsF as the cathode showed a maximal current efficiency up to 2.55 cd/A and a maximal brightness over 8000 cd/m$^2$, which is relatively high for a solution-processed small molecule OLED.

Another solution-processable light-emitting dye reported recently is the bis(difluorenyl)amino-substituted pyrene **25**, synthesized via a palladium-catalyzed C−N coupling, as earlier shown in Figure 11.[104] Simple double-layer devices from a solution process showed green emission with external quantum efficiency of 1.06%.

Another way to increase thermal stability and/or a glassy state durability of organic compounds is the addition of carbazole moieties into the molecular structure. Therefore, the new molecular structures **118** were designed and synthesized via palladium-catalyzed amination (Figure 54).[106]

The high decomposition temperatures ($T_d$ > 450 °C) of **118a**−**c** suggest that the presence of carbazole and pyrene moieties is definitely beneficial to their thermal stability. The ability of **118a**−**c** to form stable glasses is likely due to the asymmetry of the amines in these compounds, as reported before for similar asymmetric diamine compounds. The most unusual feature of these compounds is their rather high glass transition temperature ($T_g$ = 180−184 °C), which may offer improved lifetime in devices. Compounds **118a**−**c** are green light emitters in both solution and the solid state. The solution fluorescence quantum yields were found to be 0.12, 0.11, and 0.19, respectively, for **118a**, **118b**, and **118c**. Double-layer EL devices were fabricated using compound **118a** as the hole-transport layer as



Samsung Exhibit 1020, Page 25 of 55

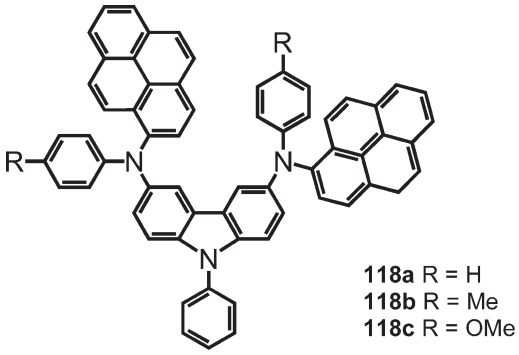


**Figure 54.** Chemical structure of carbazole-substituted pyrenes **118**.

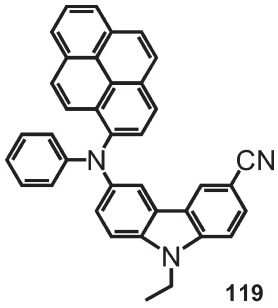


**Figure 55.** Chemical structure of 3-cyano-9-diarylamino carbazole **119**.

well as the emitting layer and TPBI [1,3,5-tris(*N*-phenylbezimidazol-2-yl)benzene] as the electron-transport layer. Green light emission from **118a** at 530 nm was observed. Preliminary measurements showed promising physical performance: turn-on voltage of 5 V, maximum luminescence of 38 000 cd/m$^2$ at 13.5 V, external quantum efficiency of 1.5% at 5 V, and luminous efficiency of 2.5 lm/W at 5 V.

Modification of the molecular structure via introduction of a cyano substituent on the carbazole moiety allowed a better balance of the electron- and hole-transport rates for high-performance electroluminescent devices.[162] This 3-cyano-9-diarylamino carbazole **119** emits in the green region, with $\phi_{PL}$ of 0.54; in addition it combines hole-transport/light-emitting/electron-transport functions (Figure 55) and therefore results in highly efficient EL devices. This type of three-in-one device material is particularly interesting for the easy fabrication of single-layer OLEDs.

A new type of molecular structure, achieved via Pd/Cu-catalyzed Sonogashira coupling, combines pyrene, carbazole, and fluorene moieties, such as compounds **120** and **121** (Figure 56).[163]

Here, pyrene was incorporated for its electron-accepting nature, while carbazole has the common hole-transporting function. Two heptyl groups were introduced at the 9-position of fluorene in order to increase the solubility for easier device fabrication. The introduction of two heptyl groups could inevitably decrease the intermolecular interactions and afford higher emission efficiency in thin films. The device structure fabricated via the spin-coating technique was ITO/PEDOT:PSS/**121**/TPBI/Al, where PEDOT:PSS and TPBI were used as the hole-injection and electron-transport layer, respectively. The device showed green emission, a low turn-on voltage of about 4.6 V, and a low operation voltage with low brightness for

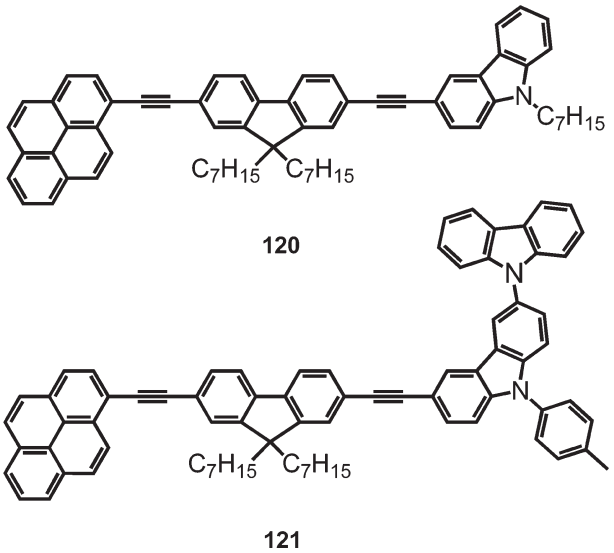


**Figure 56.** Chemical structure of pyrenes **120** and **121**.

green emission (100 cd m$^{-2}$ at ≈7 V, 1000 cd m$^{-2}$ at ≈9 V), as well as an external quantum efficiency of 0.41%. These devices, based on pyrene−fluorene−carbazole derivatives, showed low turn-on voltages, however, also a low brightness, which corresponds to an inferior device performance relative to the standard green emitting ITO/α-NPB/Alq$_3$/Mg:Ag device reported in literature and other systems here previously mentioned. However, these systems have the advantage of solution processability.

Electroluminescent materials **122** and **123** were reported comprising electron-deficient quinoxalines, electron-rich triarylamine segments, and fluorophores such as carbazole, fluorene, and pyrene, whose preparation involved a key step Pd-catalyzed C−N coupling reaction (Figure 57).[164] OLED devices were fabricated with the configuration ITO/**122**/TPBI/Mg:Ag and showed green emission at 504 nm with (0.20, 0.53) CIE coordinates, an external quantum efficiency of 1.53%, and a maximum luminance of 49 120 cd/m$^2$. The same device configuration using compound **123**, revealed also a green emission at 512 nm with (0.23, 0.57) coordinates, an external quantum efficiency of 1.88%, and a maximum luminance of 70 850 cd/m$^2$. These green-emitting devices show promising parameters such as exceptional brightness and are better relative to the standard green-emitting ITO/α-NPB/Alq$_3$/Mg:Ag devices reported in the literature.[165] The incorporation of fluorene and pyrene greatly improves the brightness of the emission in the devices, while pyrene and carbazole units strengthen the thermal properties such as glass transition temperature and decomposition temperature.

Pyrenyl-substituted fluorenes **124** with a novel structure including hexanyl as the linker between two fluorene moieties have been synthesized via Suzuki cross-coupling (Figure 58).[166]

These pyrenyl-substituted fluorenes tend to form amorphous structures arising from the high steric hindrance. DSC results suggested that these pyrene derivatives are more suitable for making stable films for organic electronic devices. Optical properties revealed that these derivatives have high molar extinction coefficients and can prevent severe aggregation in the film state due to the particular molecular structure. The cyclic voltammetric curves showed that these derivatives could be used as strong electron-donating materials.



Samsung Exhibit 1020, Page 26 of 55

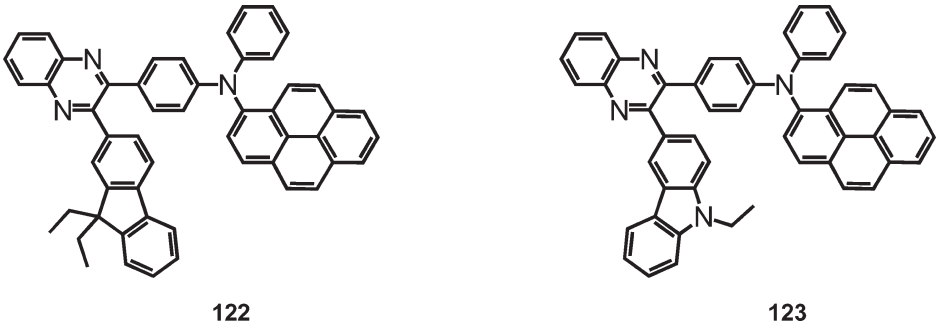


**Figure 57.** Chemical structure of **122** and **123**.

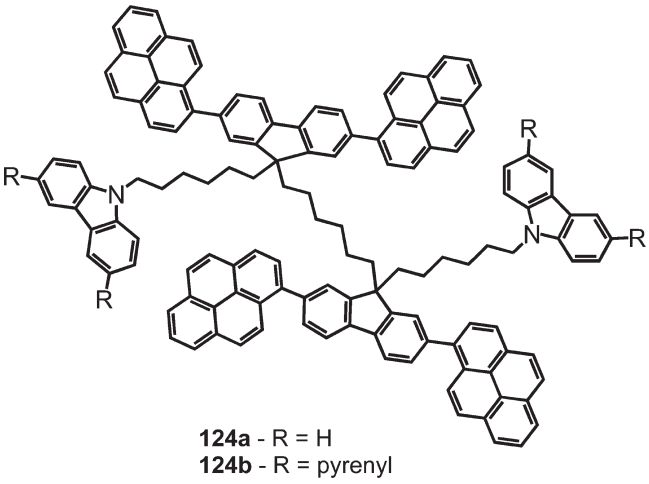


**Figure 58.** Chemical structure of pyrenyl-substituted fluorenes **124**.

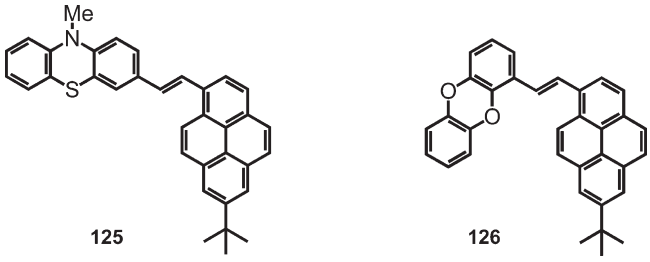


**Figure 59.** Chemical structure of **125** and **126**.

In order to understand how molecular structure and supramolecular arrangement determine the efficiency of the transformation of electrical into photonic energy, two multifunctional dyes **125** and **126** containing phenothiazine and dibenzodioxine as electron-donor group and pyrene as emissive subunit and electron acceptor (Figure 59) were synthesized and their optical properties investigated in solution and in a polymer-embedded single-layer OLED.[167]

The phenothiazine **125** exhibits almost identical emission spectra upon photochemical or electrochemical activation. In the case of the dibenzodioxine **126**, the electrochemically generated luminescence is significantly weaker than the photochemically generated luminescence (as expected from the lower stability of the radical ions) and shifted to a longer wavelength. Obviously, the excimer emission of **126** is preferentially generated. Therefore, **125** appears to be a better candidate for OLED fabrication, because it gives stable radical ions and has a comparatively more efficient luminescence. Single-layer OLED devices showed low external quantum yields of $\Phi_{(125)} = 3.5 \times 10^{-3}\%$ and $\Phi_{(126)} = 3.0 \times 10^{-4}\%$. The addition of a hole-blocking layer and variation of the polymer matrix resulted in higher quantum yields reaching 0.12%, which is still low. The electrochemiluminescence of **125** is more efficient than that of **126**.

Several pyrene-containing oligothiophene systems were reported as active components in organic electroluminescent devices.[168] In oligothiophenes, the high conjugation causes substantial red-shifts of the electronic absorption and emission transitions into the visible region, considerably lowering the oxidation potentials and high stabilization of the resulting radical cationic species, which constitutes beneficial features for electronic materials.[169]

For the purpose of improving the emissive properties, oligothiophenes **8**, **127**, and **128** (Figure 60) were modified with fluorescent pyrenes at the 1- or 2-positions.[168] The attachment of the pyrene units was achieved via Stille coupling as previously mentioned.

The insertion of pyrenes has the advantage of not only enhancing the fluorescence but also the thermal stability and charge-transport capability of the oligothiophene films. The single-layer EL devices of the pyrene-bearing oligothiophenes sandwiched between an ITO electrode and an Al/LiF bilayer electrode emitted versatile visible light depending on the chain lengths and the substitution positions (**8**, $x = 1$, yellow; **8**, $x = 2$, orange; **127**, green; **128**, orange; Figure 60), and the EL spectra have close resemblance to the respective PL spectra. The maximum brightnesses of these EL devices, except for that of **8** ($x = 1$), were, however, rather low, despite the high current density: **8** ($x = 1$), 1860 cd m$^{-2}$ at a driving voltage of 12.5 V; **8** ($x = 2$), 53 cd m$^{-2}$ at 13.7 V; **127**, 130 cd m$^{-2}$ at 9.5 V; **128**, 37 cd m$^{-2}$ at 14.5 V. Comparison of these devices in the respective 1- or 2-substitution series evidently indicates that the EL performance tends to decrease with increasing chain lengths of oligothiophenes. The low brightness of the EL devices is understandable in terms of the inherent p-type semiconducting character of oligothiophenes, which favor hole injection from the anode more effectively than electron injection from the cathode. The chain extension of the oligothiophene backbone probably strengthens the p-type character much more to promote a charge imbalance in the single-layer structure. Consistent with this explanation, the maximum luminance of the pyrene-bearing oligothiophenes can be enhanced by 1 order of magnitude by the fabrication of double-layer structures, where 2,9-dimethyl-4,7-diphenyl-1,10-phenanthroline (BCP) is incorporated as a hole-blocking layer.



Samsung Exhibit 1020, Page 27 of 55

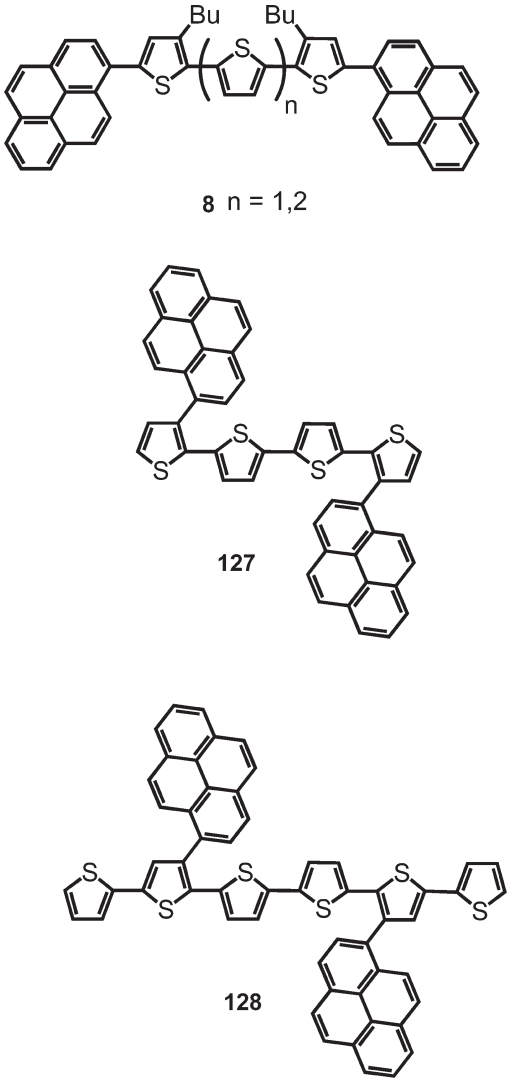


**Figure 60.** Chemical structure of pyrene-modified oligothiophenes **8**, **127**, and **128**.

Related pyrene-substituted oligothiophene derivatives **129** and **130** (Figure 61) synthesized via Wittig reactions were utilized as p-type semiconducting layers in OFETs.[97]

OFETs were fabricated using the top contact geometry with Au contacts, and thin films of the two conjugated oligomers were produced by vacuum evaporation. The devices performed as p-type transistors with hole mobility values in the range of $10^{-5}$–$10^{-3}$ $cm^2\ V^{-1}\ s^{-1}$. These values are much lower than those obtained for related 1,4-distyryl oligothiophenes. Although spectroscopic studies in solution show that the introduction of the pyrene moieties induces a significant extension of electronic conjugation and, consequently, a reduction of the gap value, it is likely that they have a nonplanar structure, in contrast to the case of their distyryl analogues, which could hamper efficient $\pi$-stacking in the solid state. It was also observed that the pyrene-containing oligomers form highly disordered crystalline thin films. All together, these features could account for the inferior transistor performances of the pyrene-compound-based OFETs.

Optimized FET devices utilizing a pyrene organic radical derivative resulted in low operating voltages and excellent p-type FET characteristics. OFET devices were fabricated with a layer of

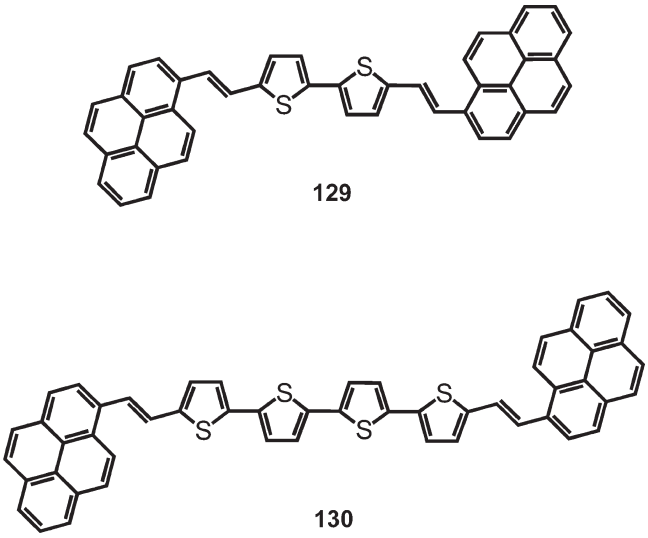


**Figure 61.** Chemical structure of pyrene-modified oligothiophenes **129** and **130**.

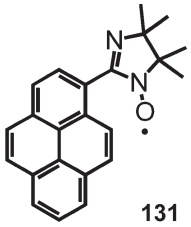


**Figure 62.** Chemical structure of 1-imino nitroxide pyrene (**131**).

vacuum-deposited 1-imino nitroxide pyrene (**131**) (Figure 62) as semiconductor on a $SiO_2$/Si substrate with top-contact configuration.[170,171]

The devices gave rise to a hole mobility of about 0.1 $cm^2\ V^{-1}\ s^{-1}$ with an on/off ratio of nearly $5 \times 10^4$. This is the OFET with the highest performance for the examples of OFETs based on an organic radical. A low threshold voltage of about −0.6 V and inverse subthreshold slope of about 540 mV $decade^{-1}$ was also obtained, which are much lower values than those of OFETs based on many organic semiconductors with $SiO_2$ as the gate insulator, such as pentacene or P3HT. These values are acceptable when compared to other OFETs using vacuum-deposited small molecules; however, they corresponds to the best performance achieved so far for OFET devices based on pyrene derivatives.

OFETs based on pentacene have attracted much attention in the last years since pentacene has shown the highest charge-carrier mobility in polycrystalline films (up to 5 $cm^2\ V^{-1}\ s^{-1}$). Because pentacene is almost insoluble in the common organic solvents, it is processed only by vacuum deposition. When appropriately functionalized, pentacene can offer high charge carrier mobilities combined with stability and processability. These reasons make pentacene derivatives a very rich source of discovery and excitement in the field of organic semiconductors. Anthony and co-workers introduced substituted ethynyl groups at the 6- and 13-positions of pentacene, for further substitution with alkyl or trialkylsilyl groups.[172,173] Recently, the related pyrene−pentacene dyad **132** (Figure 63) was reported, from which the absorption was tuned in the visible region of the



Samsung Exhibit 1020, Page 28 of 55

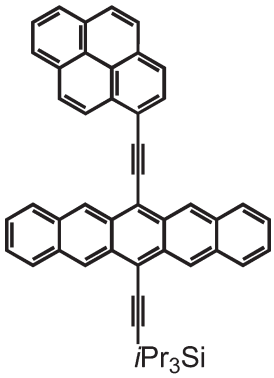


132

**Figure 63.** Chemical structure of pyrene−pentacene dyad **132**.

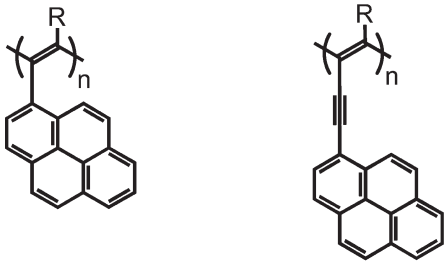


**133a**, R = H
**133b**, R = $SiMe_3$

**134a**, R = H
**134b**, R = $SiMe_3$

**Figure 64.** Chemical structure of pyrene containing polyacetylenes **133** and **134**.

spectrum relative to the pentacene-TIPS previously described by Anthony.[174] The design of this dyad was based on three key factors. First, pyrene was attached to the pentacene through an ethynyl linker at the 13-position to provide extended conjugation and enhance absorption in the 300−475 nm range. Second, the increased $\pi$-surface provided by pyrene was expected to offer improved $\pi$-stacking interactions in the solid state. Finally, a triisopropylsilylethynyl group appended to the 6-position was expected to maintain the solubility of the product.

The absorption range was improved in comparison to the model compound without pyrene; however, no crystals could be obtained to study the solid-state packing of these dyads.

Thin films of pyrene in a polystyrene matrix have also been prepared by spin-coating, and their optical properties were studied.[175] It was shown that these pyrene films could be used in the fabrication of blue- and green-light-emitting diodes. Although this technique has advantages such as ease of fabrication and low cost, it is ideal to chemically bond the pyrene to the polymeric chain, since such polymers would have advantages over doping polymer hosts with respect to processability and stability. Thus, beside small molecules and oligomers with a few repeat units, conjugated polymers bearing 1-substituted pyrene derivatives as end groups have also been reported.

While pyrene has been extensively used for the investigation of water-soluble polymers with the fluorescence technique, a literature survey revealed only a small number of investigations concerning polymers with pending 1-pyrenyl units for organic

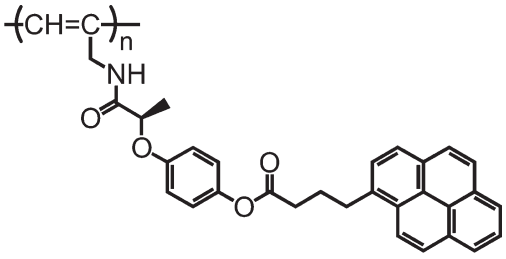


135

**Figure 65.** Chemical structure of pyrene-functionalized polyacetylene **135**.

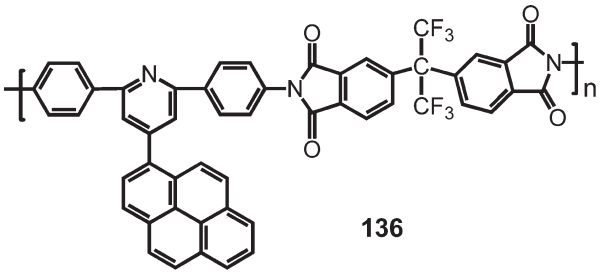


136

**Figure 66.** Chemical structure of pyrene-functionalized poly(pyridine-imide) **136**.

electronic applications. The pyrene moieties were attached to the polymeric backbone in order to increase thermal stability, extend the conjugation, or improve the fluorescence for application in OLED devices.

Polyacetylene is a conjugated polymer that shows metallic conductivity upon doping. However, the insolubility and instability of this polymer, as well as its improcessability, limit its practical application as a functional material. Addition of some substituents, however, can remarkably improve its stability. A series of mono- and disubstituted polyacetylenes **133** and **134** with pending 1-pyrenyl groups was synthesized and characterized (Figure 64).[176]

All polymers possess high thermal stability. Among these polymers, poly(1-ethynylpyrene) displayed high molecular weight and extended conjugation. The presence of a trimethylsilyl group or an additional triple bond in the monomers decreases the degree of conjugation of the resulting polymers. The addition of another triple bond, however, increases significantly the thermal stability of the polymers. All of these polymers display intramolecular interactions between pyrene units, giving rise to nonassociated and associated pyrene unit emissions. From excitation spectra and fluorescence decay profiles, measured at the maximum of both fluorescence bands, it was shown that ground state interactions (static) are responsible for the long wavelength emissions observed. It was also observed that steric effects created by pendant groups along the polymer backbones greatly affect the electronic interactions between pyrene moieties.

The copolymerization of a pyrene-containing achiral *N*-propargylamide with chiral *N*-progargylamides was studied.[177,178] The copolymers with certain compositions take a helical structure with predominately one-handed screw sense, which is tunable by the composition of the chiral units. This enables the



Samsung Exhibit 1020, Page 29 of 55

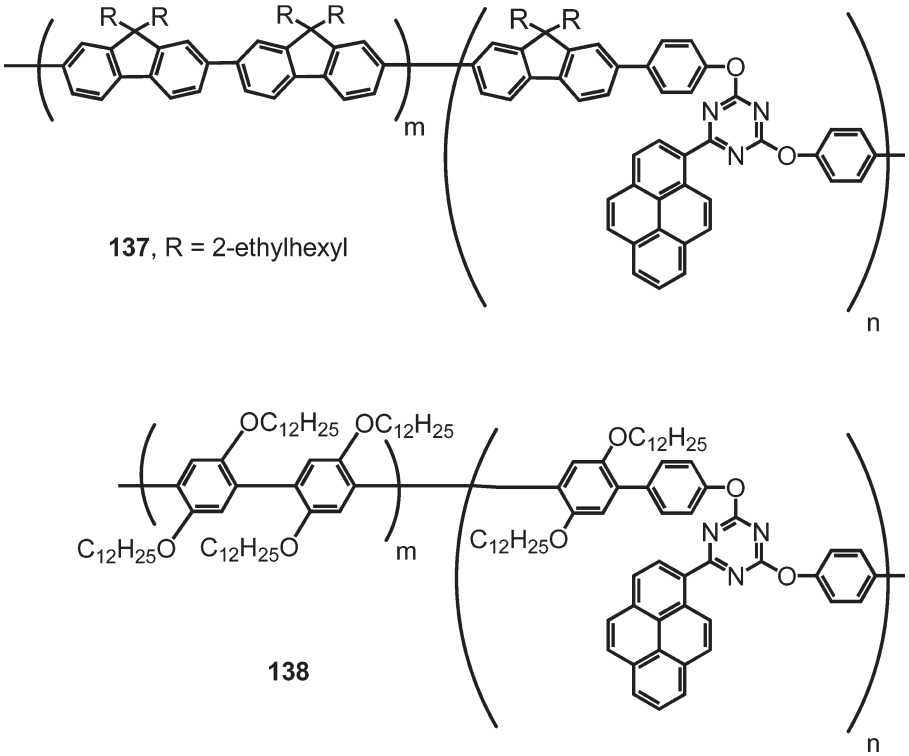


**Figure 67.** Chemical structure of poly(fluorene)s **137** and poly(*p*-phenylene)s **138** containing pyrenyltriazine moieties.

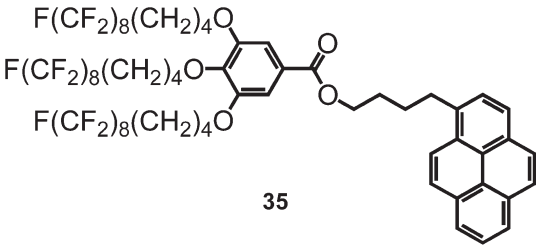


**Figure 68.** Chemical structure of pyrene-containing fluorinated chains **35**.

control of the orientation of pyrene moieties along the helical polymer backbone. The copolymers emit weak fluorescence when they form a helix. On the other hand, they emit strong fluorescence when they take a randomly coiled structure. The fluorescence properties of the pyrene-carrying copolymers greatly depend on the secondary structure.

The same authors reported a novel helical fluorescent polymer based on polyacetylene with pendent pyrene groups (Figure 65).[179] The monomer was obtained by the esterification reaction between the chiral alcohol derivative and 1-pyrenebutyric acid using EDC and DMAP. The polymerization was conducted in $CH_2Cl_2$ and catalyzed with (nbd)Rh$^+$[$\eta_6$-$C_6H_5B^-$ $(C_6H_5)_3$]. The polarimetric and CD spectroscopic data indicated that polymer **135** formed a helical structure with predominantly one-handed screw sense, and the helical structure was very stable upon heating and addition of MeOH. Polymer **135** showed very large excimer-based fluorescence compared to the monomer. It was considered that the helical structure was favorable for the pendent pyrene groups to form excimers. Thus, the photoluminescent polymer is stable to heat and MeOH. The stereoregular helical main chain of the polyacetylene with pyrene chromophores is expected to increase nonlinear optical response and lower the requirement for polar ordering.

The synthesis and characterization of a new poly(pyridine-imide) **136** derived from a new monomer, 4-(1-pyrene)-2,6-bis(4-aminophenyl)pyridine (PBAPP), containing heterocyclic pyridine and pyrene substituents was reported (Figure 66).[180] The combination of nonconjugated polymers such as polyimides with electron-transporting layers has placed these polymers among efficient electroluminophores. Compared to a benzene ring, pyridine is an electron-deficient aromatic heterocycle, with a localized lone pair of electrons in the $sp^2$ orbital on the nitrogen atom; consequently, the derived polymers have increased electron affinity and improved electron-transporting properties and offer the possibility of protonation or alkylation of the lone pair electrons as a way of modifying their properties.

The obtained poly(pyridine-imide) **136** exhibits good solubility in common organic solvents, a high dielectric constant, and good thermooxidative stability higher than 500 °C, and excellent mechanical properties. The polymer exhibits blue emission in neutral solution and orange emission after protonation, which indicates that this polymer can be used for optoelectric applications.

Two new series of poly(fluorene)s **137** and poly(*p*-phenylene)s **138** containing pyrenyltriazine moieties were investigated (Figure 67).[181]

The purpose was to combine pyrene with 1,3,5-triazine, which is an electron transport material and has been used to improve the OLED efficiency. The copolymers with polyfluorene **137** emitted blue light in solution with PL maximum between 414 and 444 nm (PL quantum yields 0.42−0.56) and green light in a thin film with PL around 520 nm. The green emission in the solid state of these copolymers was a result of the energy transfer from the fluorene to the pyrenyltriazine moieties. Copolymers with



Samsung Exhibit 1020, Page 30 of 55

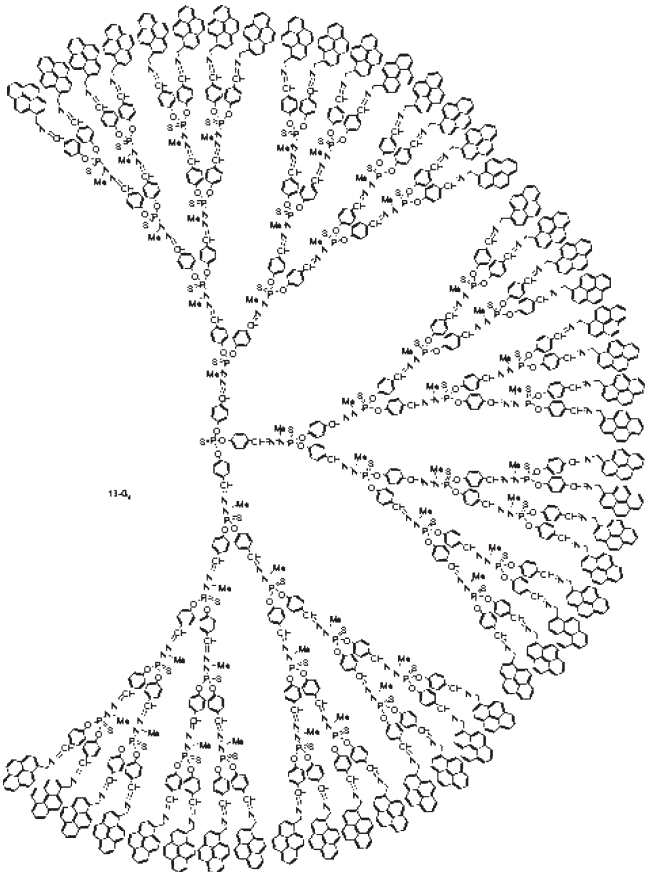

**Figure 69.** Fourth generation of phosphorus-containing dendrimers (**G4**).

poly(*p*-phenylene)s **138** emitted blue-light both in solution and thin film with PL maximum between 385 and 450 nm and PL quantum yields in solution of 0.27−0.35. The PL maximum was red-shifted by increasing the pyrenyltriazine content in the copolymer.

Modification of polysilanes was achieved via the attachment of pyrene units to the polymeric backbone.[182] These polymers were used in the fabrication of single-layer and double-layer OLED devices, and their photophysical properties were analyzed. An increase in the visible PL emission intensity was observed in these modified polysilanes. OLED devices emitted white light, and the electroluminescence spectra differed from the photoluminescence spectra. Charge trapping in the radiative recombination centers plays an important role in EL emission. An EL efficiency up to 0.06% was detected in double-layer devices, which is 1 order of magnitude higher than that in single-layer devices. Chemical substitution with pyrene units improved the photostability of polysilane; therefore, the modified polysilanes can be use in polymer-blend OLEDs to modify transport and injection properties and/or to prevent aggregation of the conjugated polymers. The same authors reported an increase in the EL efficiency and stability in blue OLED devices based on a polymer blend composed of the modified polysilane including pyrene and poly(9,9-dihexadecylfluorene-2,7-diyl).[183] Such blending significantly improved the OLED performance.

**4.1.2. Liquid Crystalline Structures.** The spontaneous organization of molecules into columnar superstructures via $\pi$-stacking interactions is very promising for organic electronic devices, since it results in high charge-carrier mobilities along the columnar stacks.[184−186] Only a few examples of 1-substituted pyrene derivatives have been reported to self-assemble in supramolecular columnar liquid crystalline structures.

The effects of the ordering and alignment of perfluorinated supramolecular columns containing conjugated cores on the photoluminescence properties were reported. As mentioned before, the semifluorinated supramolecule **35**, containing a monosubstituted pyrene unit as the core, was found to self-assemble into columns (Figure 68).[187]

The pyrene was used as a probe to study the self-aggregation phenomena. Slow cooling from an isotropic state resulted in a high degree of ordering and a vertical alignment of the columns with respect to the substrate. In contrast, rapid cooling leads to planar alignment of weakly ordered columns on the same substrates. UV−vis and PL spectra showed that less efficient packing of the $\pi$-conjugated molecules resulted in the production of a broad emission band and a second weak shoulder, which indicates the presence of isolated molecules. However, highly ordered columns with vertical and planar alignments produce excimer spectra that are typical of pyrene and a decrease in vibronic features due to isolated molecules. The fluorescence spectra are attributed to the increase in the conjugation length that results from the formation of a cylindrical structure with perfect ordering. From the surface anchoring of the material, it was concluded that ordering has a more important influence on the PL spectra than alignment.

One class of organic molecular materials deserving particular attention is discotic liquid crystalline derivatives of hexa-*peri*-hexabenzocoronene (HBC),[188] a polycyclic aromatic hydrocarbon (PAH)[189−191] with a large $\pi$-conjugated core consisting of 42 carbons. These discrete synthetic nanographenes self-assemble into highly ordered columnar structures in the bulk and crystalline monolayers at interfaces.

As earlier mentioned, we reported an alkyl-substituted hexa-*peri*-hexabenzocoronene **38** (Figure 16) with a covalently tethered pyrene unit that serves as a model to study self-assembling discotic $\pi$-system dyads both in the bulk and at a surface.[192] Wide-angle X-ray scattering, polarized light microscopy, and differential scanning calorimetry revealed bulk self-assembly into columnar structures. Relative to a control without a tethered pyrene, the new dyad exhibits a more ordered columnar phase at room temperature but with dramatically lowered isotropization temperature, facilitating homeotropic alignment. These two features are important for processing such materials into molecular electronic devices, e.g., photovoltaic devices. Scanning tunneling microscopy (STM) at a solution−solid interface revealed uniform nanoscale segregation of the large from the small $\pi$-systems, leading to a well-defined two-dimensional crystalline monolayer, which may be employed in the future to study intramolecular electron transfer processes at surfaces, on the molecular scale.[193]

**4.1.3. Dendritic Structures.** The photophysical properties of poly(propylene imine) (PPI) dendrimers modified on their periphery with fluorescent pyrene moieties were analyzed.[194] Four generations of poly(propylene imine) dendrimers have been covalently modified with pyrene moieties and examined by fluorescence spectroscopy. Emission and excitation spectra were obtained so that the generational dependence of the dendrimers, especially the extent of steric crowding, could be correlated to the photophysical properties of pyrene. In particular, the effect of dendrimer concentration and generation on pyrene−pyrene



Samsung Exhibit 1020, Page 31 of 55

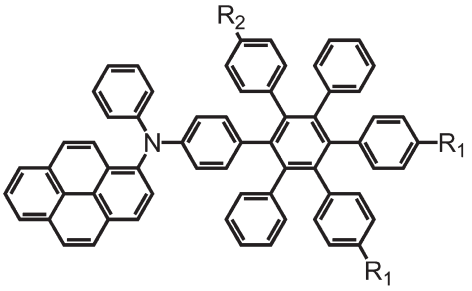


**139a,** $R_1$=$R_2$ = *t*-Butyl
**139b,** $R_1$=$R_2$ = OMe
**139c**, $R_1$=OMe, $R_2$=*t*-Butyl

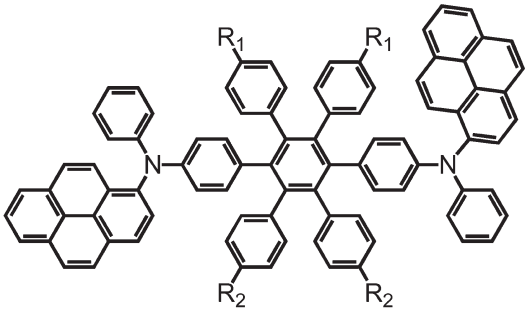


**140a,** $R_1$=$R_2$ = *t*-Butyl
**140b,** $R_1$=$R_2$ = OMe
**140c**, $R_1$=OMe, $R_2$=*t*-Butyl

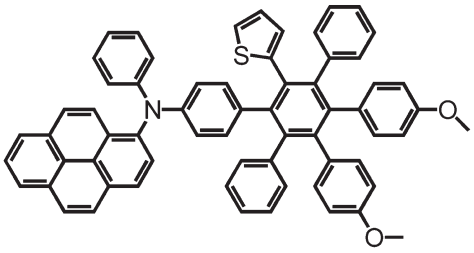


**141**

**Figure 70.** Chemical structure of hexaphenylphenylene dendronized pyrenylamines **139**−**141**.

interactions was evaluated. More excimer emission was observed for higher generation dendrimers, while little or no evidence for interdendrimer interactions was observed over more than 2 orders of magnitude in dendrimer concentration. Excitation spectra revealed the presence of preassociated pyrene moieties. Protonation of the tertiary amine units was shown to increase monomer fluorescence significantly, while only slightly increasing the observed excimer fluorescence.

These results indicate that the extent of interaction between terminal pyrene groups, which correlates to excimer fluorescence, depends on the generation of the dendrimer structure. Specifically, more excimer fluorescence arises from higher generation dendrimers, which are more sterically crowded on their surfaces.

A similar study was performed on a different series of dendrimers including only one pyrene unit per dendron.[195] This means that the observed excimers must be formed from different branches of the dendrimer and cannot originate from the nearest neighbors being attached to the same monomer unit. By a selective synthesis, only one pyrene moiety per dendron was attached, resulting in a dendrimer with three fluorophores per molecule.[195] The molecular dynamics of the dendrimer branches was studied by observing the excimer formation of pyrenyl end-groups. By time-resolved measurements of the excimer and monomer fluorescence an increased mobility of the end-groups was observed. The relative intensity of the excimer fluorescence increases with increasing size of the dendrimer.

Toward organic blue-light-emitting diodes, the grafting of pyrene as end-groups of several types and generations of phosphorus-containing dendrimers was investigated (Figure 69).[196,197]

However, the loss of fluorescence observed in several cases shows that the fluorophore must not be linked to the dendrimer through a heteroelement (oxygen or nitrogen) but through an alkanediyl linkage. As previously mentioned for the first-generation dendrimer (Figure 20), the condensation of 1-pyrenemethylamine with the aldehyde end-groups of the dendrimer led to a series of compounds fluorescent even in the solid state and thermally stable up to 320 °C. This series of dendrimers was tested in OLED devices exhibiting threshold voltages for emission of light too high for practical purposes (18−20 V) but clearly displaying electroluminescent properties.

Novel and well-defined pyrene-containing eight-arm star-shaped dendrimer-like copolymers with pentaerythritol core were synthesized.[198] These pyrene-containing dendrimers present unique thermal properties and crystalline morphologies. Fluorescence analysis indicated that the pyrene-containing dendrimer presents slightly stronger fluorescence intensity than 1-pyrenebutyric acid when the pyrene concentrations were the same. The pyrene-containing eight-arm star-shaped dendrimer-like copolymer has potential applications in optoelectronic devices.

Using thiol−ene "click" chemistry, a series of dendrimers with pyrene at the periphery was synthesized.[199] A facile and efficient synthesis of poly(thioether) dendrimers using thiol−ene addition reactions for the construction of both the dendritic backbone, as well as functionalization of the chain ends, was reported using pyrene as end-groups.

Solution processable blue fluorescent dendrimers, based on cyclic phosphazene (CP) cores incorporating aminopyrene moieties, have been prepared and used as emissive layers in OLEDs.[200] These dendrimers have high glass transition temperatures, are monodisperse, have high purity via common chromatographic techniques, and form defect-free amorphous films via spin/dip-coating. The solution processable blue-light-emitting OLEDs reach current efficiencies of 3.9 cd/A at brightness levels near 1000 cd/m$^2$. Depending on the molecular bridge used to attach the fluorescent dendron to the inorganic core, the emission wavelength changes from 470 to 545 nm, corresponding to blue and green light, respectively. Via dilution experiments it was shown that this shift in emission wavelength is likely associated with molecular stacking of the aminopyrene units.

A series of dendritic compounds bearing pyrene units at the periphery to afford light-harvesting antennae was reported on the



Samsung Exhibit 1020, Page 32 of 55

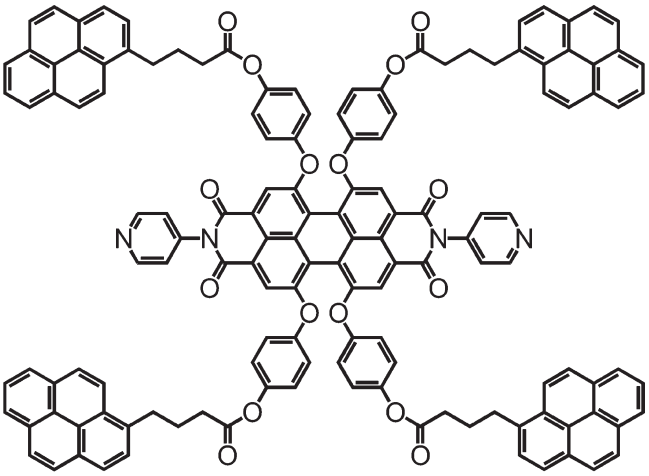

32

**Figure 71.** Chemical structure of tetrapyrene−perylene bisimide dye **32**.

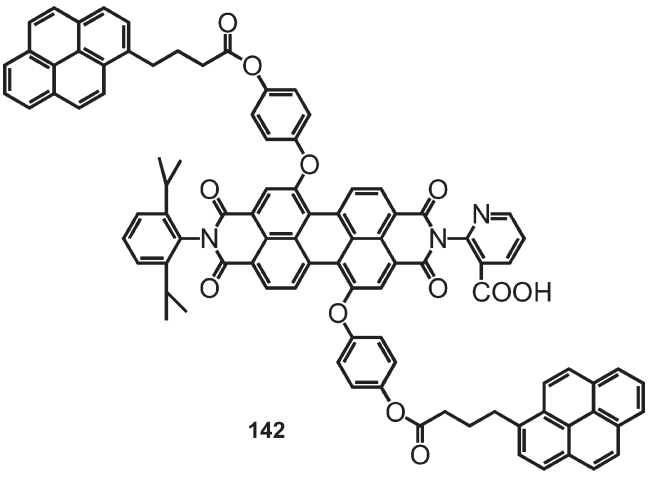


142

**Figure 72.** Chemical structure of dipyrene−perylene bisimide dye **142**.

basis of the formation of intramolecular excimers.[122] Thus, the Huisgen reaction between pyrene azides and terminal alkynes, as previously depicted in Figure 21, allowed the preparation of first-, second-, and third-generation dendrons (first-generation dendron **51** is depicted in Figure 21). For the production of light-harvesting antenna systems, a suitable acceptor chromophore has to fulfill the main requisite of the Förster theory, which is that the fluorescence spectra of the donor chromophore should overlap with the absorption spectrum of the acceptor one. For this reason, a fluorophore with a maximum absorption at around 500 nm should be linked to the dendrons. Thus, nitrobenzofurazane and a styrylpyridinium derivative were identified as suitable candidates and consequently anchored to the dendritic structure. The modified structures showed that the efficiency of the acceptor emission increases with generation and reaches the fluorescence quantum yield of 0.13 for the third-generation antenna in the solid state. These systems show to be very efficient light-harvesting dendritic materials in the solid state with energy transfer without any dissipation from the pyrene to the red-emitting acceptor. The screening performed by the pyrenes units on the acceptor site reduces the quenching due to intermolecular

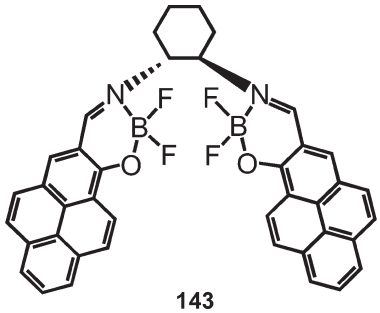

143

**Figure 73.** Structure of boron complex with pyrene ligand **143**.

interactions, giving films that display bright red emission for the third dendron generation. Single-layer devices fabricated with the dendrons and donor molecules show unstable electroluminescence due to charge trapping processes at the acceptor site. Charge injection into molecular blends in PVK generates excitons on the polymer that are subsequently transferred by energy transfer to the dendrons. Single-layer devices of the dendron molecules blended in PVK show both the blue EL components from the polymer and the monomeric pyrenes and the red emission of the acceptor. Donor molecules in the blend provide the green EL of the pyrene excimer, allowing one to finely tune the emission color by changing donor and dendron concentrations.[201]

A similar pyrene-labeled dendron as light-harvesting antenna was investigated as a model compound for the respective dendrimer.[202] In this case, pyrene was used as the electron acceptor at the periphery and the electron donor was located at the growth focal point. Intramolecular quenching in the dendrons bearing covalently attached donors was demonstrated through steady-state and time-resolved fluorescence measurements and was attributed to intramolecular photoinduced electron transfer. The amount of quenching observed is a function of dendrimer generation and of solvent polarity.

A new series of hexaphenylphenylene dendronized pyrenylamines **139**−**141** (Figure 70) was studied for application in organic light-emitting diodes.[203] The molecular design leads to high $T_g$ blue-emitting materials possessing good hole-transporting capabilities. The high $T_g$ recorded for these compounds is attributed to the presence of the rigid pyrene segment and the hexaphenylbenzene core in the molecular architecture. For each compound, the HOMO values were calculated from the oxidation potentials, and the LUMO values were deduced from the band gap calculated from the optical edge. The closeness of the HOMO of these materials to the work function of ITO ($E_f$ = 4.7 eV) indicates that hole injection into the molecular layer of these compounds will be effective. The use of an appropriate electron-transporting layer is essential to restrict recombination inside the hole-transporting layer. OLED devices using TPBI and $Alq_3$ as electron-transporting materials were tested.

Bright-blue-emitting devices were realized for both TPBI- and $Alq_3$-based devices, while the latter OLEDs require a thin hole-blocking layer to achieve recombination inside the hole-transporting layer. The best performance was achieved for OLEDS with the configuration ITO/**139a**/TPBI/Mg:Ag, which showed a low turn-on voltage of 3.0 V, a maximum luminance of 21 150 cd/m$^2$ at 14 V, an external quantum efficiency of 2.7%, and (0.13, 0.21) CIE coordinates. These values are good and rival certain anthracene-based blue-emitting materials and amine−oxadiazole conjugates previously reported.



Samsung Exhibit 1020, Page 33 of 55

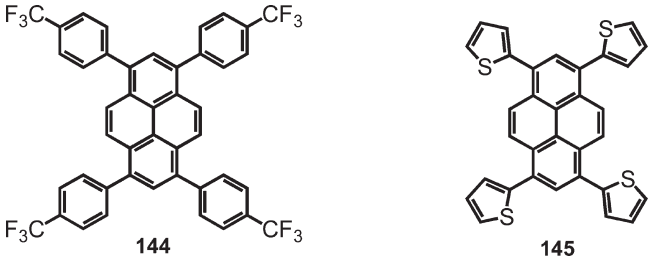


**Figure 74.** Tetrasubstituted pyrenes with trifluoromethylphenyl (**144**) and thienyl groups (**145**).

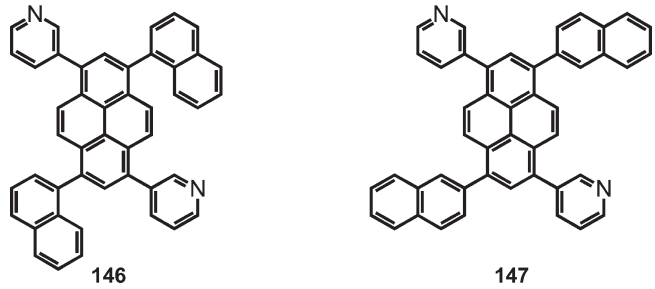


**Figure 75.** Structure of tetrasubstituted pyrenes **146** and **147**.

The synthesis of the pyrene−perylene bisimide dye **32**, as well the study of the occurring photoinduced processes, was reported (Figure 71). The understanding of the photoinduced processes is of great interest for the construction of more complex structures by means of coordination of the pyridine units to metal ions, leading to molecular squares.[204]

Analysis of the photophysical data showed the presence of both photoinduced electron and energy transfer processes. A high yield (>90%) and fast photoinduced energy transfer ($k_{en} \approx 6.2 \times 10^9\ s^{-1}$) is followed by efficient electron transfer (70%, $k_{et} \approx 6.6 \times 10^9\ s^{-1}$) from the pyrene units to the perylene bisimide moiety. The energy donor−acceptor distance, $R$ = 8.6 Å, was calculated from the experimental energy transfer rate using Förster theory. Temperature-dependent time-resolved emission spectroscopy showed an increase of the acceptor emission lifetime with decreasing temperature. This light-harvesting system displaying the two processes, energy and electron transfer, constitutes an important system to understand more complex or similar systems and can as well be used for the realization of artificial photosynthetic systems.

A similar pyrene−perylene derivative (**142**) including only two pyrene moieties and a carboxylic acid as anchor group was recently reported (Figure 72).[205] The anchor group allows the linkage of the pyrene−perylene dye to $TIO_2$ for the fabrication of dye-sensitized solar cells (DSC).

The intention of this pyrene−perylene system is to have a dye in which the absorption spectra covers the entire visible region of solar spectra as well a good energy distribution of the HOMO/LUMO orbitals to enhance the solar cell efficiency. In a detailed photophysical analysis, it was found that perylene diimide dyes containing pyrene moieties show fast photoinduced energy transfer as well as efficient electron transfer from the pyrene to the perylene diimide moiety. Fast decay components, low fluorescence quantum yields at the excitation of pyrene quencher, long wavelength emission peaks, and high values of fluorescence rate constants for **142** dye support the formation of charge-separated states of **142** dye in solution. Therefore, pyrene units in the 1,7-bay positions slightly narrow the band gap energies and raise the HOMO energy level of the perylene diimide as compared to a model compound. This pyrene-substituted perylene diimide can be used to fabricate DSCs.

**4.1.4. Organic−Inorganic Hybrids.** In the continuous search for innovative materials, organic−inorganic hybrids based on pyrene-functionalized octavinylsilsesquioxane cores for application in OLEDs were reported.[206] This class of solution-processable amorphous materials displays many attractive properties for application in OLED technology, such as ease of synthesis, high glass-transition temperatures, good film-forming properties, low polydispersity, and high purity via column chromatography. Preliminary nonoptimized OLED devices exhibited an external quantum efficiency of 2.62% and a current efficiency of 8.28 cd/A, demonstrating that these materials are efficient emitters in OLEDs.

A boron complex bearing a pyrene ligand (**143**) was synthesized and introduced as the first example of a binuclear boron complex in organic light-emitting diodes (Figure 73).[207] In the solid state, **143** exhibited strong red emission. In the polymer OLEDs fabricated with **143** blended with PVK, red emission with CIE coordinates of (0.57, 0.42) was obtained by tuning the weight concentration of **143**. Derivative **143** behaved as both an emitting and an electron-transporting material.

### 4.2. 1,3,6,8-Tetrasubstituted Pyrenes

**4.2.1. Linear Structures.** A successful effort in the prevention of aggregation in small molecules was achieved with tetrasubstituted highly sterically congested pyrenes, which can emit blue light in solution as well in the solid state and with high quantum yield.[124] The optimized geometry of 1,3,6,8-tetraphenylpyrene, according to molecular orbital calculations, shows the twisting of the phenyl groups relatively to the pyrene plane. This twisted structure prevents excimer formation that causes the concentration quenching of fluorescence in the solid state. It should be noted that unsubstituted pyrene is not a strong fluorescent emitter, whereas the 1,3,6,8-tetraphenylpyrene showed a high fluorescence quantum yield of 0.90 in the pure blue region. OLED devices were fabricated using 1,3,6,8-tetraphenylpyrene as emissive dopant.[124] The devices exhibited efficient blue emission with a current efficiency of 1.87 cd/A, external quantum efficiency of 2.1%, and (0.17, 0.09) CIE coordinates. The performance of the devices is good but uses a high dopant concentration (10%).

A bright organic light-emitting field-effect transistor (OLEFET) using 1,3,6,8-tetraphenylpyrene derivatives as the active layer was reported.[208,209] Specifically, a 1 wt % rubrene-doped tetraphenylpyrene codeposited layer had an ultimate photoluminescence efficiency $\phi_{PL}$ of 99% ± 1% and a hole mobility of about $10^{-5}\ cm^2\ V^{-1}\ s^{-1}$, leading to bright electroluminescence (EL) with a $\eta_{ext}$, however, of only 0.5%.

OFET devices using tetraphenylpyrene single crystals were also fabricated.[210,211] An ambipolar behavior in the single crystal device was observed with high charge carrier mobilities. For Au electrodes, the tetraphenylpyrene single-crystal FET exhibited an ambipolar characteristic with predominating hole injection. The hole mobility was as high as $0.27\ cm^2\ V^{-1}\ s^{-1}$. This value is much higher than the hole mobility exhibited in tetraphenylpyrene thin-film FET, which is on the order of $10^{-5}\ cm^2\ V^{-1}\ s^{-1}$. The electron mobility obtained was $2.9 \times 10^{-3}\ cm^2\ V^{-1}\ s^{-1}$. Using an asymmetric electrode configuration with Au and Mg, the



Samsung Exhibit 1020, Page 34 of 55

highest hole mobility of 0.34 $cm^2 V^{-1} s^{-1}$ was obtained. This value is low relative to other single crystal FETs based on pentacene, for example, which can reach hole mobilities of 5 $cm^2 V^{-1} s^{-1}$; however, this value corresponds to the highest mobility reported so far for a single crystal FET based on pyrene. In addition to the efficient injection of holes and electrons in this ambipolar FET, the high photoluminescence efficiency of the single crystal allows the fabrication of ambipolar light-emitting FET devices.

The 1,3,6,8-tetraphenylpyrene was also used as a blue fluorescent dye together with tris(1-phenylisoquinoline) iridium(III) [$Ir(piq)_3$] as red phosphorescent dye for the fabrication of white organic light-emitting diodes.[212]

The molecular structure of 1,3,6,8-tetraphenylpyrene was also modified with methyl or methoxy groups, resulting in tetramesitylpyrene, tetradurylpyrene, and *p*-anisyl pyrene derivatives, which were used as blue emissive materials.[213] All these pyrene derivatives emitted bright blue fluorescence, even at concentrations as low as $10^{-6}$ M. Multilayer OLED devices with the configuration ITO/NPB/tetrasubstituted pyrene/TPBI/LiF/Al were fabricated. These vacuum-sublimed devices exhibited bright blue light emission with $\lambda_{max}$ at ca. 450 nm. The maximum external quantum efficiency achieved for the nondoped device fabricated for *p*-anisyl derivative was 3.3% with a maximum luminance efficiency of 2.7 cd/A. This value is comparable to commonly used blue-emitting materials based on spirobifluorene (3.2 cd/A),[214] diarylanthracenes (2.6−3.0 cd/A),[215,216] diphenylvinylbiphenyls (1.78 cd/A),[217] or biaryls (4.0 cd/A).[218]

Two butterfly pyrene derivatives with trifluoromethylphenyl **144** and thienyl **145** aromatic groups were synthesized via Suzuki couplings and used in thin-film field-effect transistors (Figure 74).

Thanks to the twisted structure, a strong fluorescence in the solid state was obtained. The molecules pack in the herringbone motif, similar to pentacene. OFET devices were fabricated on $SiO_2$/Si substrates using a top-contact geometry. Thin films were deposited on the $SiO_2$ by high vacuum evaporation at room temperature. The device based on **144** did not show any FET performance; however, the FET device using compound **145** as active material exhibited *p*-type performance with hole mobility of $3.7 \times 10^{-3}$ $cm^2 V^{-1} s^{-1}$, on/off ratio of $10^4$, and the threshold voltage of −21 V. These values are low for a thin-film OFET processed by vacuum deposition, compared to typical values of around 1 $cm^2 V^{-1} s^{-1}$ and on/off ratio larger than $10^6$. However, these values are among the best for thin-film OFETs based on pyrene derivatives.

The pyrene-based electron-transport materials, namely, 1,6-dipyridin-3-yl-3,8-dinaphthalen-1-ylpyrene (**146**) and the 1,6-dipyridin-3-yl-3,8-dinaphthalen-2-ylpyrene (**147**), were investigated (Figure 75).[130]

The external quantum efficiencies of the blue OLED devices with these electron-transport materials increased by more than 50% at 1 mA $cm^{-2}$ compared with those of the device with the standard $Alq_3$ as electron-transport material. The enhanced quantum efficiency is due to a balanced charge recombination in the emissive layer. Electron mobilities of **146** and **147** films are 3 times higher than that in $Alq_3$. A highly enhanced power efficiency is achieved due to a low electron injection barrier and a high electron mobility. It was also demonstrated that the luminance degradation in the blue OLEDs is correlated with the HOMO energy levels of the electron transport materials.

The enhancement of electrogenerated chemiluminescence (ECL) efficiency of organic materials by improving radical stability was reported.[219] This approach uses D−$\pi$−A systems that contain a centered acceptor and peripheral multidonors in contrast to the conventional linear type D−$\pi$−A compounds. Thus, a series of alkynylpyrene derivatives **148**−**152** that consist of pyrene as an acceptor moiety and *N*,*N*-dimethylaniline as the peripheral donor moiety linked by an ethynyl bridge were prepared via Sonogashira coupling (Figure 76).

The five D−$\pi$−A compounds were chosen according to the number and substitutent position of peripheral donor moieties. Although, pyrene shows poor ECL properties, because of the electrochemical instability of its cationic radical, the ECL efficiencies of the pyrene derivatives increased in proportion to the number of the peripheral donors. Compound **152**, bearing four donor units, exhibits a marked enhancement in ECL intensity compared to the other compounds; this is attributable to its highly conjugated network that gives an extraordinary stability of the cation and anion radicals in oxidation and reduction processes, respectively. This result is relevant for the development of highly efficient light-emitting materials for applications such as OLEDs.

The two-photon absorption properties of compounds **148**−**152** were also investigated.[220] Comparison of the two-photon cross section ($\delta_{max}$) with related compounds revealed that pyrene is as efficient a $\pi$-center as anthracene in two-photon materials. Moreover, the two-photon cross section increased with the number of substituents, reaching the maximum value of 1150 GM for the tetrasubstituted pyrene **152**. The two-photon action cross section ($\phi\delta_{max}$) of **152** is comparable to that the most efficient two-photon materials. This result is useful for the design of efficient two-photon materials bearing pyrene as the $\pi$-center.

Very recently, a highly efficient solid emitter created by decorating a pyrene core with tetraphenylethene peripheries by Suzuki coupling was reported (derivative **153**) (Figure 77).[221]

Tetraphenylethene is an example of a chromophore that shows an unusual effect of aggregation-induced emission. Its molecules are nonemissive when dissolved in a good solvent but become highly luminescent when aggregated in a poor solvent. The aggregation-induced emission effect of tetraphenylethene is caused by the restriction to its intramolecular rotations. In solution, the active rotations of its multiple phenyl blades nonradiatively deactivate its excitons. In the aggregate state, however, the restriction of intramolecular rotations effectively blocks the nonradiative channel and hence makes tetraphenylethene highly emissive. The attachment of tetraphenylethene units to the pyrene core results in an aggregation-induced emission enhancement effect, efficient solid photoluminescence ($\phi$ = 70%), and excellent thermal stability ($T_d$ = 485 °C). Multilayer OLED devices using the tetraphenylethenepyrene exhibit green emission with low turn on voltage (3.6 V), high luminance (36 300 cd $m^{-2}$), high current efficiency of 12.3 cd $A^{-1}$, power efficiency of 7.0 lm $W^{-1}$, and high $\eta_{ext}$ of 4.95% at 6 V. The green OLEDs fabricated from tetraphenylethenepyrene show a better performance than the same devices using $Alq_3$ as emitter. The devices with tetraphenylethene pyrene show an excellent performance as multilayer fluorescent green OLEDs.

**4.2.2. Liquid Crystalline Structures.** In the continuous search for organic semiconductors for improved electronic devices, discotic liquid crystals have attracted considerable interest due to their self-organization and electronic properties. These mesogens are usually composed of flat aromatic cores substituted in the periphery with long, flexible alkyl chains, which



Samsung Exhibit 1020, Page 35 of 55

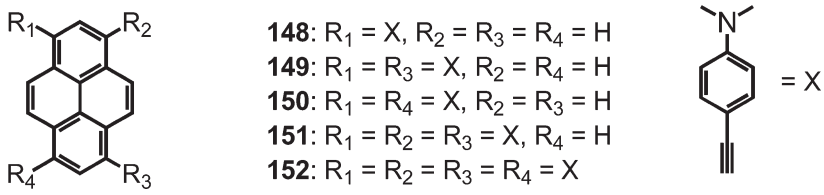


**Figure 76.** Chemical structure of alkynylpyrenes **148**−**152**.

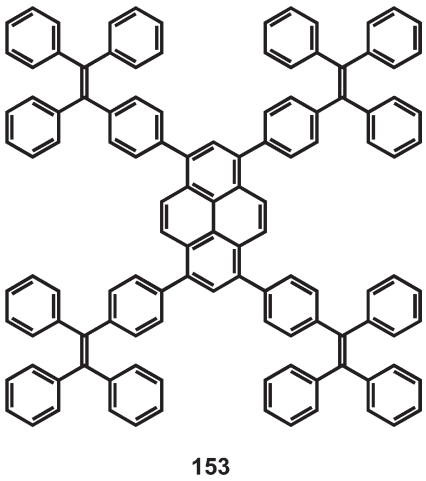


**Figure 77.** Chemical structure of tetrasubstituted pyrene **153**.

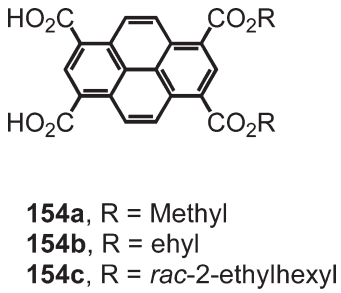


**Figure 78.** Chemical structure of pyrene-based liquid crystalline aromatic esters **154**.

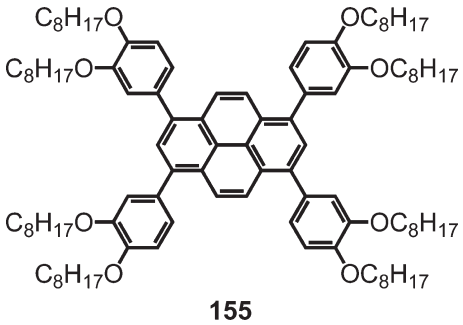


**Figure 79.** Chemical structure of tetraphenylpyrene **155**.

provide solubility and influence the association between the molecules. These self-assembled structures revealed high charge carrier mobilities along the columnar stacking axis, which make them a promising class as active components in electronic devices.

Important factors that govern the performance of discotic liquid crystals in device applications are charge injection/collection at the interfaces and charge transport within the bulk material. The degree of order within the columnar stack and therefore the overlap between the $\pi$-orbitals affects this charge transport in the material. For device fabrication, besides adequate electronic properties, the morphology of the material is a crucial property in forming distinct columnar pathways over large domains, which is thus closely related to the device performance. Controlling the interactions between the molecules and therefore the self-association by changing the chemical composition is the key factor tailoring the solubility and the thermal properties.

In this context, the substitution at the 1,3,6,8-positions of the pyrene aromatic system with flexible side chains represents a very interesting approach to form liquid crystalline columnar superstructures. Moreover, the excellent fluorescent properties of pyrene, combined with supramolecular organization in a columnar liquid-crystalline phase, is very interesting for potential application in organic electronic devices such as OLEDs.

A series of luminescent pyrene-based liquid crystalline aromatic esters was reported.[128] These pyrene derivatives combine theexcellent charge transport and film-forming properties of columnar liquid crystals with the ability to emit light. Dilute solutions of the pyrene derivatives emit in the blue region, while the pure compounds show a green to yellow emission due to the formation of molecular aggregates. The pyrene-1,3,6,8-tetracarboxylic acid was synthesized following the procedure of Vollmann et al. and esterified with $SOCl_2$/ROH, as previously mentioned (Figure 30). The pyrene liquid crystal derivatives contained as side chain a methyl (**154a**), ethyl (**154b**), or *rac*-2-ethylhexyl (**154c**) group (Figure 78).[128]

Compound **154a** is monotropic, meaning that the liquid crystal behavior exists only when the compound is heated up from the solid state, and **154b** and **154c** are enantiotropic, which means that the liquid crystal state exists by heating and by cooling the material. Both **154a** and **154b** crystallize with loss of the homeotropic alignment, while **154c** does not crystallize and is a mesomorphic fluid at room temperature. These compounds were used in two-layer OLED devices containing a hole-transporting layer.[222,223] Devices with **154b** show electroluminescence if the voltage exceeds a threshold value of about 5−6 V. These simple pyrene derivatives are interesting examples of fluorescent liquid crystals taking advantage of the pyrene aromatic system as the core.

In the search for luminescent liquid crystals, the synthesis of tetraphenylpyrene derivatives with strong emission in solution and in the solid state was studied. However, these pyrene derivatives did not form any columnar mesophases. This has been attributed to the steric hindrance associated with the four orthogonal phenyl substituents that prevents the close stacking of the pyrene cores.[224] To obtain the desired combination of intense fluorescence and columnar mesophase formation, the flat



Samsung Exhibit 1020, Page 36 of 55

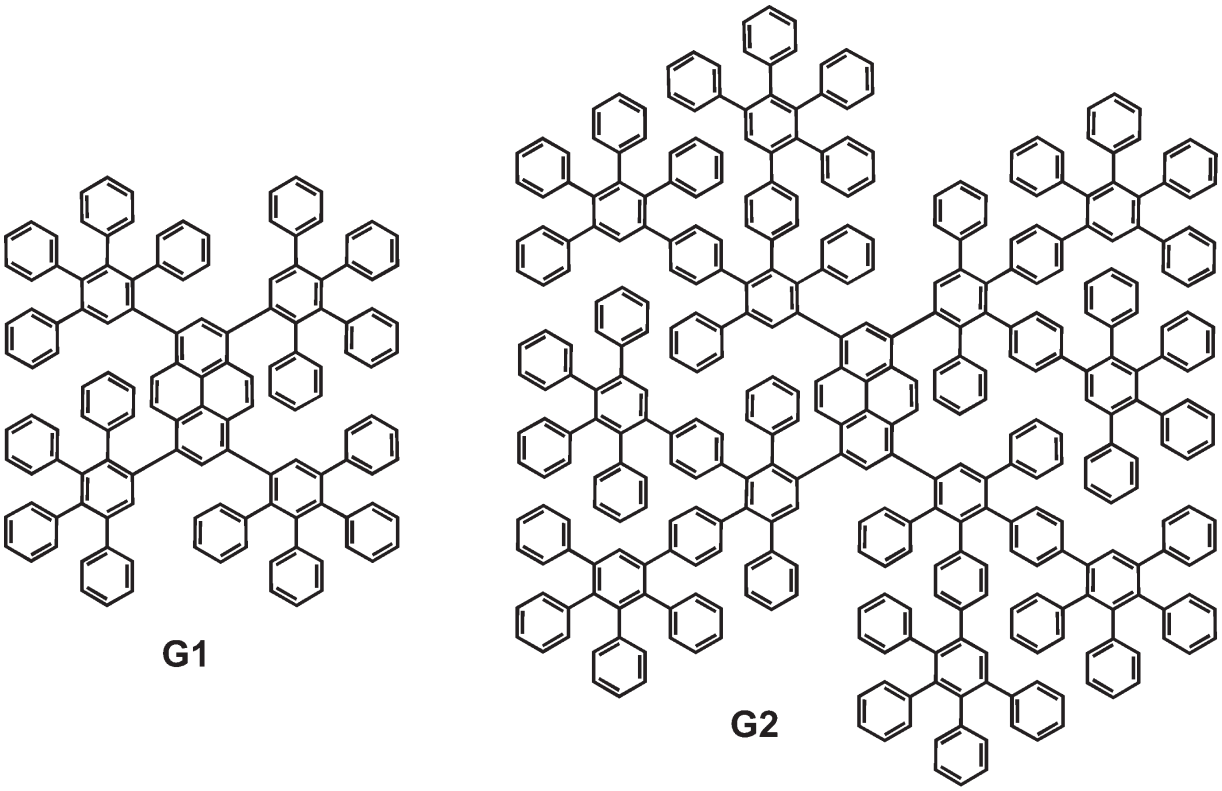


**Figure 80.** First (**G1**) and second generation (**G2**) of pyrene-cored polyphenylene dendrimers.

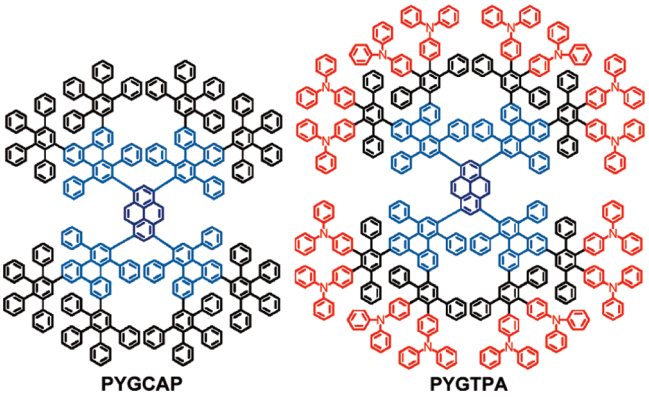


**Figure 81.** Pyrene-cored polytriphenylene dendrimers (PYGCAP and PYGTPA).

tetraethynylpyrene unit was substituted with promesogenic side groups. These side groups have a high tendency to induce a liquid crystalline behavior. A new derivative based on the tetraethynylpyrene core was then prepared via Sonogashira coupling as previously mentioned (Figure 26): 1,3,6,8-tetrakis(3,4,5-trisdodecyloxyphenylethynyl)pyrene (**61**).[125] It forms columnar liquid crystal phases over a substantial temperature range. In addition to a high fluorescence quantum yield in solution, this molecule exhibits a quantum yield in the crystalline phase as high as 62 ± 6%. This value is one of the highest fluorescence quantum yields reported for discotics, since normally due to the $\pi-\pi$ stacking the fluorescence is quenched. This high efficiency coupled with the columnar arrangement generated upon self-assembly might prove beneficial in optoelectronic applications, for example, for excitation energy transfer over large distances. Concentration-dependent studies show excimer-type emission at high concentration in solution. The absorption and emission characteristics measured for the different solid phases at various temperatures point to the formation of cofacial stacks with the chromophores rotated by 70°−80°. This mutual rotation of the chromophores promotes an optically allowed lowest excited state for aggregated molecule species, which is at the origin of the high fluorescence quantum yield.

The photoconductive properties and phase characterization of the pyrene discotic liquid crystal **155**, which contains four 3,4-dioctyloxyphenyl substituents each, were reported (Figure 79).[225] Photoconductive properties of pyrene were investigated in pure crystals,[226] in thin films,[227] and also in solutions of liquid hydrocarbons.[228]

A standard TOF (time-of flight) measurement revealed a hole mobility in unaligned samples of compound **155** on the order of $10^{-3}$ cm$^2$ V$^{-1}$ s$^{-1}$, which is typical for many other discotic mesogens in the Col$_h$ phase. Measurements of the electron charge mobility for pyrene **155** at several temperatures gave values that are close to those of the hole mobility. Such ambipolar charge-transport behavior is consistent with a hopping transport mechanism. Pyrene derivative **155** supercools to room temperature, forming a rigid glass with structural features of the preceding Col$_h$ phase and without disruption of the charge transport tunnels.

Several pyrene derivatives with acyloxy groups were reported as discotic liquid crystalline compounds with a low melting temperature and high solubilities. Although crystalline themselves, they form columnar phases as charge-transfer complexes with a strong electron-acceptor core such as tetranitrofluorenone, and they also change their textures depending on the side-chain



Samsung Exhibit 1020, Page 37 of 55

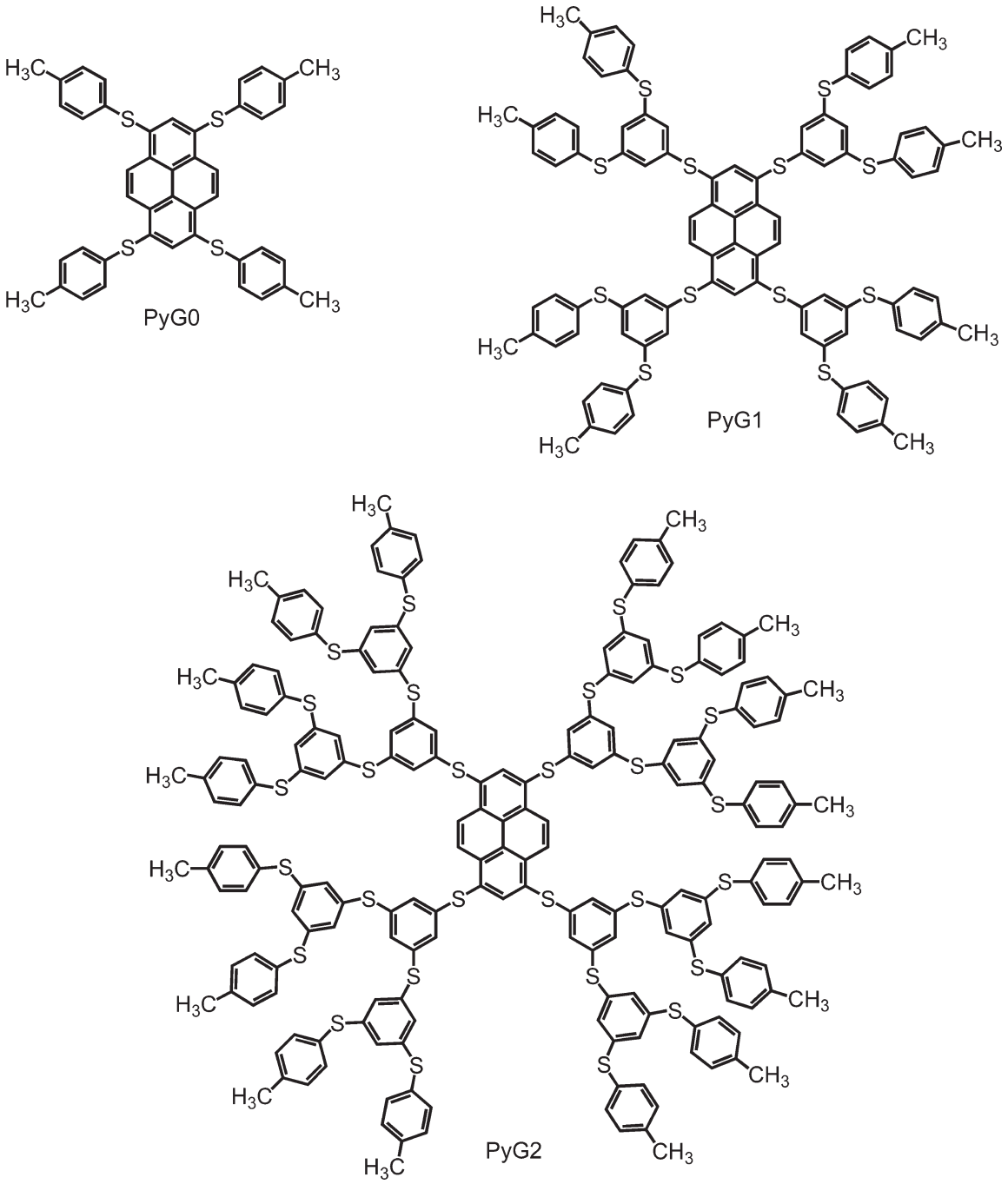


**Figure 82.** Polysulfurated dendrimers including pyrene, **PyG0**, **PyG1**, and **PyG2**.

structures.[229] On the basis of these results, the same group synthesized quinone−hydroquinone charge transfer liquid crystalline systems that form segregated columnar structures and show high electroconductivity using a pyrene moiety as the core.[230] These liquid crystals correspond to $\pi$-acceptor liquid crystalline aromatic compounds having *anti*- and *syn*-pyrenedione moieties.

**4.2.3. Dendritic Structures.** Dendrimers as hyperbranched macromolecules with size increasing by generation generally combine the merits of well-defined structures and superior chemical purity possessed by small molecules with the simple solution-processing advantage of polymers.

Among the interesting properties of pyrene, its sensitive solvatochromic shift has been used to exploit the inner structure and polarity of dendrimers. The substitution of pyrene at the 1,3,6,8-positions allows the incorporation of pyrene as active core in dendrimers to evaluate the degree of site isolation of the core. Several pyrene-containing dendrimers have also shown interesting photo- and electroluminescence properties for possible application in OLED devices.

In order to have a better insight into the relationship between dendrimer structure and core encapsulation, our group employed a pyrene moiety as the core of polyphenylene dendrimers from first to fourth generation.[123] These dendrimers were



Samsung Exhibit 1020, Page 38 of 55

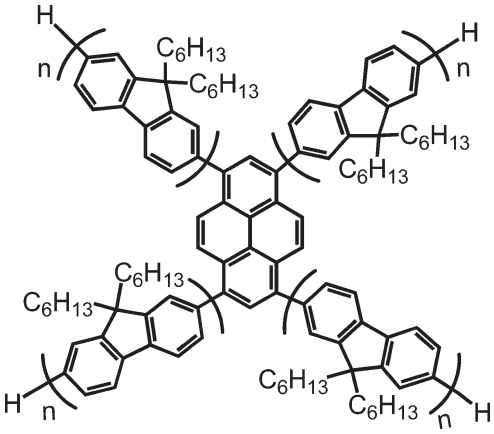

**156a**, n = 1
**156b**, n = 2
**156c**, n = 3

**Figure 83.** Starbust oligofluorenes including pyrene **156**.

obtained using the Diels–Alder cycloaddition reaction, as mentioned above (Figure 28). First- and second-generation denfrimers, **G1** and **G2**, respectively, are depicted in Figure 80.

This is expected to separate the chromophores from each other due to the stiff dendritic arms and therefore suppress aggregation in solution and in the solid state. Since amorphous glassy films are a prerequisite for several electronic devices, a large number of peripherally attached, branched alkyl chains were introduced to improve the film-forming ability of the dendronized pyrenes. The influence of the polyphenylene dendrons on the optical properties of the pyrene core was investigated by UV/vis absorption and fluorescence spectroscopy. Additional insight into the relationship between dendrimer structure and core encapsulation was derived from alkali-metal reduction of the pyrene dendrimers with pyrene as electrophore.

Stern–Volmer quenching experiments and temperature-dependent fluorescence spectroscopy indicated that a second-generation dendrimer shell is sufficient for efficiently shielding the pyrene core and thereby preventing aggregate formation. Alkali-metal reduction of pyrene dendrimers yielded the corresponding pyrene radical anions. Thereby, hampered electron transfer to the core was observed with increasing dendrimer generation, which further verifies the site-isolation concept. It is interesting that the improvements of the optical properties, such as high quantum efficiency in solution ($\phi_{PL} > 0.92$), were already achieved by applying a second-generation dendrimer shell. These shape-persistent macromolecules are exciting new materials that combine excellent optical features and an improved film-forming ability, for possible application in OLED devices.

Encouraged by our previous work on blue-emitting polytriphenylene dendrimers, which resulted in high performance OLED devices,[231] we decided to incorporate a pyrene moiety at the core of such polytriphenylene dendrimers in a novel core–shell-surface multifunctional structure using a blue fluorescent pyrene core with triphenylene dendrons and triphenylamine surface groups.[232] We found efficient excitation energy transfer from the triphenylene shell to the pyrene core, substantially enhancing the quantum yield in solution and the solid state (4-fold) compared to dendrimers without a core emitter, while TPA groups facilitated the hole-capturing and injection ability in the device applications. With a luminance of up to 1400 cd/m$^2$, a saturated blue emission with CIE of (0.15, 0.17) and high operational stability, these dendrimers (PYGCAP and PYGTPA) belong to the best reported fluorescence-based blue-emitting organic molecules (Figure 81).

Recently, the synthesis, characterization, photophysical behavior, and redox properties of a novel class of dendrimers (**PyG0**, **PyG1**, and **PyG2**, Figure 82) consisting of a polysulfurated pyrene core was presented, namely, the 1,3,6,8-tetrakis-(arylthio)pyrene moiety with appended thiophenylene units prepared as previously described in Figure 29.[127]

The novelty of this work is due both to the incorporation of an uncommon tetrathiopyrene core into a dendritic structure and to the presence of polysulfurated dendrons containing thioether functions. The photophysical and redox properties of the three dendrimers are fine-tuned by the length of their branches: (1) the dendron localized absorption band at around 260 nm increases strongly in intensity and moves slightly to the red on increasing dendrimer generation; (2) in $CH_2Cl_2$ solution, the quantum yield and lifetime of the fluorescence band, and the values of the half-wave potentials increase with dendrimer generation; and (3) the dendrimer branches partially protect the core from oxidation by $AuCl_4$. The strong blue fluorescence and the yellow to deep blue color change upon reversible one-electron oxidation.

Since it is known that oligofluorene possesses favorable characteristics for OLEDs such as high quantum yield and good optical stability and film-forming ability, a new series of pyrene-centered starbust oligofluorenes **156** was synthesized via Suzuki coupling and characterized (Figure 83).[233] The effect of different arm lengths on the optical, thermal, and morphological properties of the materials, as well as preliminary device characteristics, was investigated.

All the starbursts showed good film-forming properties and sky blue fluorescence. The single layered device made of **156c** exhibited a maximun brightness of over 2700 cd/m$^2$ and a maximum current efficiency of 1.75 cd/A. The morphology of **156a–c** demonstrated that starbursts of different arm lengths take on distinctive microstructures, which might affect the device performance.

In the search for new electronic materials, a series of solution-processable stiff dendrimers consisting of a pyrene core and carbazole/fluorene dendrons prepared via Sonogashira coupling (first-generation dendrimer **157**, Figure 84) was reported.[234] Pyrene was chosen as the core of such stiff dendrimers because of its excellent PL efficiency and high charge carrier mobility. Moreover, it allows the study of the generation effect on the aggregation of dendrimers, since pyrenes are prone to excimer formation in concentrated solutions and in solid state. Since the combination of carbazole/fluorene units has been shown to result in a strong blue fluorescence, carbazole/fluorenes were chosen as dendrons.

These dendrimers exhibit good thermal stability, strong fluorescence, efficient photon-harvesting, and excellent film-forming properties. Although the acetylene-linked dendrimers are generally considered as nonpromising materials for OLEDs, these show high EL efficiency in single-layer devices due to proper structural design and engineering. A good control over the degree of intermolecular interactions through generation modulation is important in order to maximize carrier transport but minimize excimer formation. With an optimization of spin speed, the second-generation dendrimer-based OLED device exhibited yellow EL (CIE, 0.49, 0.50) with a maximum



Samsung Exhibit 1020, Page 39 of 55

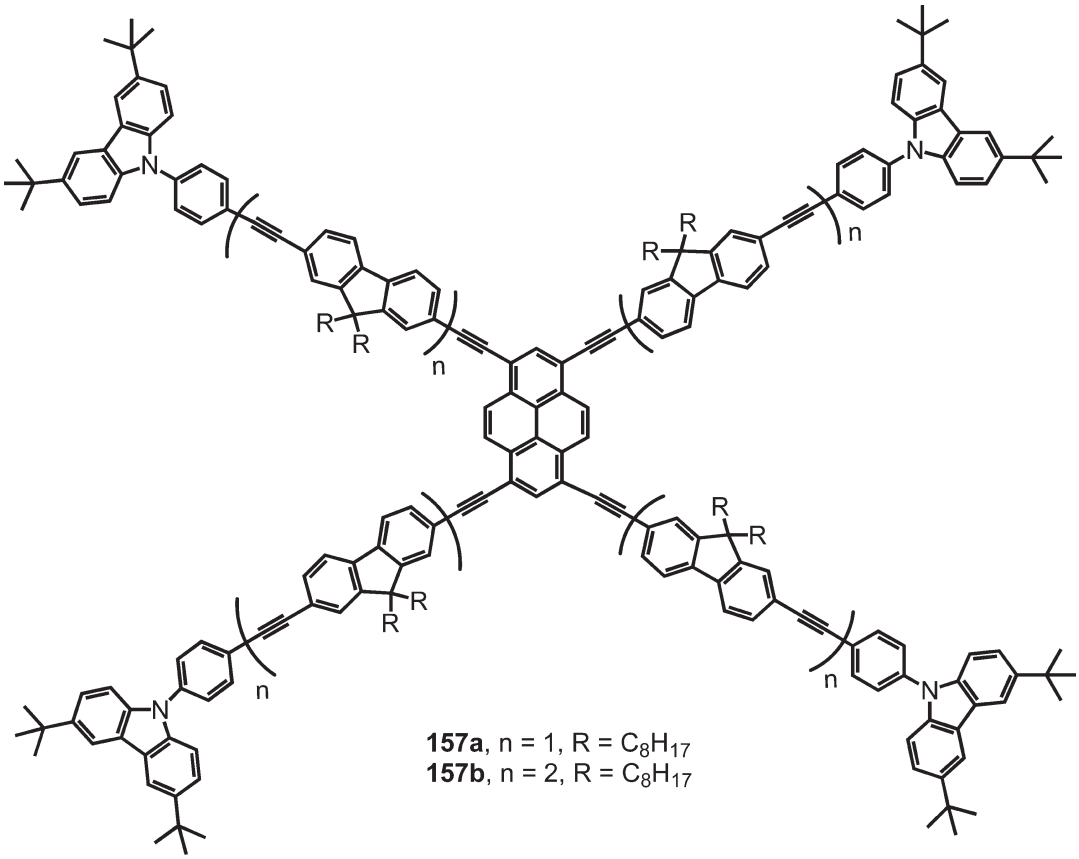


**Figure 84.** First-generation carbazole/fluorene dendrimer with pyrene at the core (**157**).

brightness of 5590 cd/m$^2$ at 16 V, a high current efficiency of 2.67 cd/A at 8.6 V, and an external quantum efficiency of 0.86%. These values are low for OLED devices; however, these dendrimers have the advantage of solution processability.

Similar solution-processable acetylene-linked dendrimers, this time including fluorinated terminal groups, were also investigated.[235] The shortest dendrimer easily self-assembles into nanofibers under simple conditions. The longest dendrimer exhibits yellowish green (CIE, 0.38, 0.61) EL emission. When compared with dendrimers with similar structures, second-generation dendrimers with $n = 2$ based single-layer LEDs exhibit improved performances with a maximum efficiency of 2.7 cd/A at 5.8 V and a maximum brightness of 5300 cd/m$^2$ at 11 V. These values are comparable to the ones reported for the acetylene-linked dendrimers without the fluorinated groups, but with the advantage of lower voltages.

A literature survey revealed only a very few investigations regarding dendrimers containing pyrene both at the core and in the periphery.[236] Recently, our group reported polypyrene dendrimers as a new type of dendrimer made exclusively of pyrene units.[133] First-generation dendrimer **Py(5)**, consisting of five pyrene units, and the second-generation dendrimer **Py(17)**, comprising 17 pyrene units, were synthesized via Suzuki coupling and their photophysical properties studied (Figure 85).

The large steric hindrance between pyrenes at the 1-position results in a high degree of twisting, as shown by the computed structures (AM1). These new fully aromatic dendrimers are relevant for artificial light-harvesting in a spatially well-defined three-dimensional architecture, comprising only one type of chromophore. Thus, we have reported a new type of stiff multichromophoric system, polypyrene dendrimers, incorporating a well-defined number of pyrene units in a confined volume. The rigid and strongly twisted 3D structure allows a precise spatial arrangement in which each unit is a chromophore. This highly twisted structure leads to high solubility and no aggregation, which resulted in high fluorescent quantum yields, more precisely 0.70 for the first-generation and 0.69 for the second-generation dendrimer. The absorption and fluorescence spectra of the dendrimers in toluene at 25 °C were measured. In the absorption spectra, the vibrational structure of 1-methylpyrene is still visible. From **Py(5)** to **Py(17)**, a broad absorption band is red-shifted from the structured part of the spectrum and increases in relative intensity. This broad band reflects the intramolecular interaction between the pyrene moieties in the dendrimers, which becomes stronger from the first- to the second-generation dendrimer. An intramolecular energy transfer is expected in the second-generation dendrimer from the second dendrons to the first dendrons and subsequently to the core. A small overlap between the absorption and emission spectrum is the first obtained evidence; however, a detailed study of the excited-state processes in these new pyrene systems is currently in progress.

### 4.3. 1,6- And 1,8-Disubstituted Pyrenes

**4.3.1. Linear Structures.** Oligopyrenes are expected to possess better fluorescent and electroluminescent properties than those of the pyrene monomer, because of their longer delocalized $\pi$-electron chain sequence. Electrochemical



Samsung Exhibit 1020, Page 40 of 55

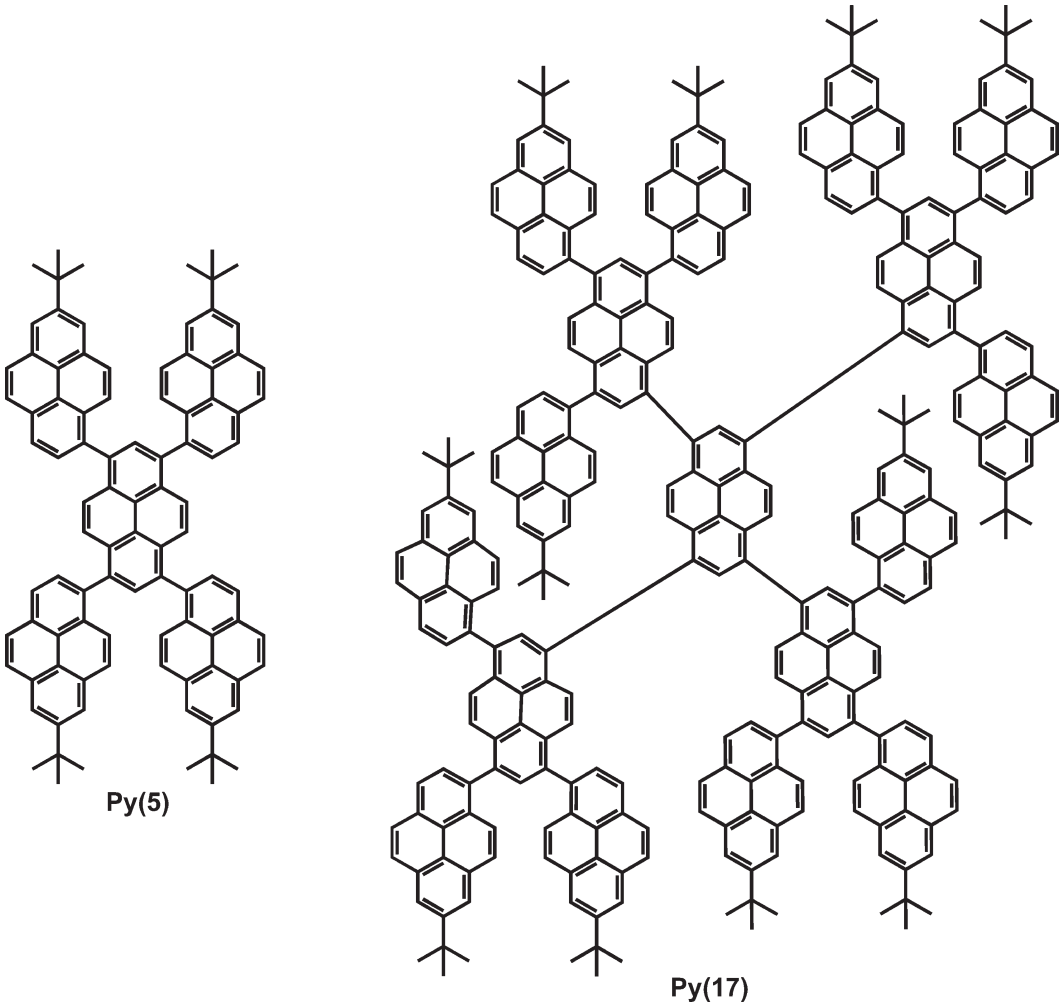


**Figure 85.** First and second generation of polypyrene, namely, **Py(5)** and **Py(17)**.

polymerization of unsubstituted pyrene[237−239] via a 1−1′ coupling was described to give insoluble and unprocessable films with high molecular weight or, alternatively, soluble materials with few repeat units. Thereby, the low degree of polymerization is presumed to be a consequence of the low solubility caused by the strong self-assembly of pyrene segments. Linear 1,6-oligopyrenes with a small number of pyrene units were obtained via electrochemical polymerization of pyrene and their properties were investigated.[240,241]

In the search for improved semiconducting materials, it is also common to attach other chromophores such as fluorene to the 1,6-positions of the pyrene ring.[242] Thus, a blue-light-emitting disubstituted pyrene **158** including fluorene units was synthesized via Suzuki coupling and used to fabricate OLED devices (Figure 86).

The nondoped device with configuration of ITO/PEDOT (30 nm)/NPB (15 nm)/TCTA (15 nm)/**158** (30 nm)/TPBI (30 nm)/Mg:Ag, exhibited a very stable electroluminescent spectrum at different applied voltages. The CIE coordinates ($x$ = 0.15, $y$ = 0.12) of the device are very close to the National Television Standards Committee's blue standard. A maximum $\eta_{ext}$ of 4.3% (current efficiency of 3.06 cd $A^{-1}$) was achieved at 19.8 mA $cm^{-2}$ with a luminance of 607 cd $m^{-2}$. The performance of the device is competitive with the best of the nondoped blue OLEDs, except for the luminance, which is still low.

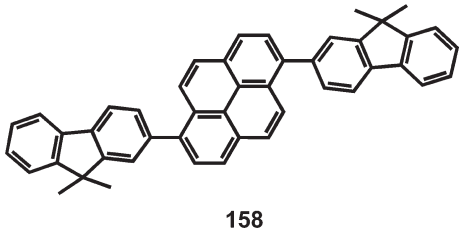


**Figure 86.** Structure of disubstituted pyrene **158**.

It was reported that the introduction of alkynyl groups into pyrene nuclei induces effective extension of the $\pi$-conjugation and a large increase of fluorescence intensities compared to unsubstituted pyrene, making these alkynylpyrenes improved biomolecular probes.[89] This fact inspired the same authors in the preparation of para- and meta-linked alkynylpyrene oligomers **159** and **160**, and they examined their photophysical properties for possible application in optical devices (Figure 87).[243] In this case, the preparation of the oligomers was achieved via Sonogashira coupling from a well-defined 1,6-disubstituted pyrene monomer, which allows the control of the oligomeric structure.

The resulting oligomers mainly consist of 2-mer to 6-mer based on MALDI-TOF mass spectra. From their absorption and



Samsung Exhibit 1020, Page 41 of 55

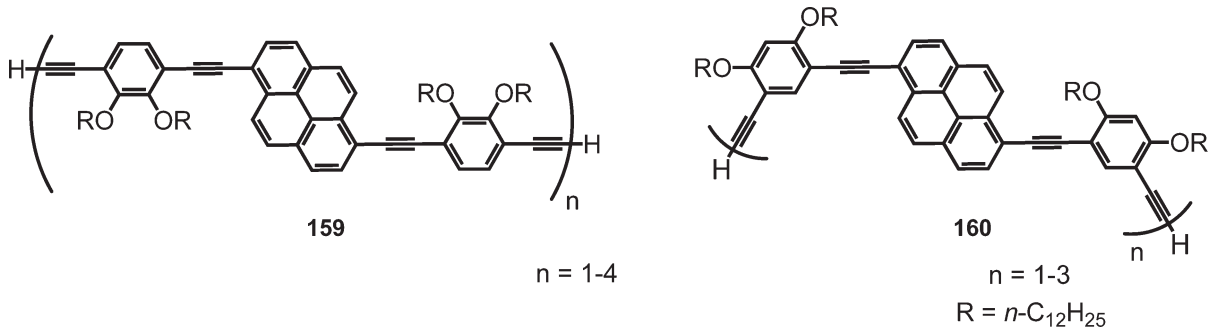


**Figure 87.** Chemical structure of para- and meta-linked alkynylpyrene oligomers **159** and **160**.

fluorescence spectra, the para-linked oligomers **159** were found to exhibit improved $\pi$-conjugation compared to the meta-linked **160**, and the fluorescence quantum yields decreased with increasing oligomer length ($\phi_{PL}$ = 0.79−0.55).

Two systems, **75** and **77**, bearing a carbazole unit as donor and pyrene as acceptor, were synthesized via Sonogashira coupling, as previously described in Figure 33, and their photoluminescence properties were investigated.[131] Both derivatives showed extremely high fluorescence quantum yields of nearly 100%. Compound **77** was selected for device fabrication due to its higher solubility relative to compound **75**. The blend of compound **77** with PVK resulted in an EL device with green emission at 500 nm, turn-on voltage of 11 V, maximum luminance of 1000 cd/m$^2$, external quantum efficiency of 0.85% at 15.5 V, and maximum power efficiency of 1.1 lm/W at 15.5 V. The high voltages and low efficiency translate into poor device performance for these green OLEDs.

Also using the Sonogashira coupling, a series of well-defined, monodisperse pyrene-modified ethynylene-linked oligocarbazoles was synthesized in order to study the influence of the pyrene units on the electroluminescent properties.[244] Ethynylene linkages at the 3- and 6-positions of carbazoles resulted in a zigzag shape of the molecular backbones (Figure 88), which defined the conjugation length of the molecules and suppressed red shifts in absorption and emission spectra of the oligomers in solution when the size of the oligomers increases. 1,8-Disubstituted pyrene was also used in the center as well as 1-substituted pyrene as the end groups.

Furthermore, the introduction of pyrene units improves significantly the fluorescence quantum efficiency and its insertion into different positions of the backbone effectively tunes the molecule's emission wavelength. OLED devices with different configurations revealed that the oligomers without pyrene could be used as hole-transporting materials only, while pyrene-modified oligomers exhibit both light-emitting properties and hole-transport abilities. It was demonstrated in this series of oligomers that bifunctional optoelectronic materials can be achieved with incorporation of pyrene units.

Only a limited number of polymers involve the use of pyrene along the polymeric backbone. For the preparation of these polymers, well-defined disubstituted pyrene monomers are required. For example, the poly(*p*-phenylenevinylene) (PPV) derivative containing pyrene segments (**78**) (Figure 89) was synthesized via Heck coupling of 1,6-dibromopyrene with dialkoxydivinylbenzene in high yield, as previously depicted in Figure 34.[132]

This polymer is readily soluble in organic solvents and shows a blue-green light emission in solution and green-yellow light emission in thin film. The emission's red-shift in the thin film relative to solution results from excimers/aggregates. This fact shows that the molecular architecture is not good enough to avoid the aggregation phenomena.

Also the synthesis, photophysics, and electroluminescence of alternating copolyfluorenevinylenes containing pyrene for optoelectronic applications were analyzed.[245] The idea was to combine the structural characteristics of PPVs and polyfluorenes with the highly emissive pyrene. The copolyfluorenevinylene containing pyrene **161** was synthesized via Heck coupling of 9,9-dihexyl-2,7-divinylfluorene with 1,6-dibromopyrene in 75% yield (Figure 90).

This polymer presented good solubility and was obtained with $M_n$ = 14 800 g/mol and $M_w/M_n$ = 2.3. Although the copolymer exhibited high efficiency, blue-greenish fluorescence in solution ($\phi_f$ = 59%), a significant decrease of PL efficiency was observed in thin films ($\phi_f$ = 6%), indicating the presence of concentration quenching in the solid state. The OLEDs showed EL with $\eta_{EL}$ = 0.31%, with red emission. This result supports the fact that this molecular design, with the double bond at the 1,6-disubstituted pyrene, is not the most appropriate to avoid aggregation, which results in the quenching of the fluorescence and red-shift of the emission band.

**4.3.2. Liquid Crystalline Structures.** Discotic liquid crystalline mesophases have been obtained using 1,6-disubstituted pyrene derivatives, taking advantage of the pyrene aromatic core decorated with dendritic groups. The stimuli-responsive luminescent liquid crystal **162** shows a shear-induced liquid crystalline phase transition associated with a change of the photoluminescent color.[246] Compound **162** was designed to exhibit both columnar and cubic phases, although it is difficult to intentionally induce a cubic phase. In compound **162**, the two dendritic groups are linked to a central pyrene moiety via Sonogashira coupling (Figure 91).

A variety of dendritic groups have been examined as LC molecular components, and the dendron having a methyl group at the focal point, which has a similar structure to that of the dendron introduced into **162**, has been reported to show a columnar phase.[247,248] It was also previously reported that dendritic H-bonded molecules with bulky substituents exhibit columnar−cubic phase transitions.[249,250] Compound **162** presents a shear-induced LC order−order transition from a micellar cubic to a columnar phase; this transition is accompanied by a change of the luminescent color. The micellar cubic phase exhibited by **162** is a metastable LC phase. This isothermal transition from metastable to stable phases may be useful for dynamically changing the properties of functional liquid crystals.



Samsung Exhibit 1020, Page 42 of 55

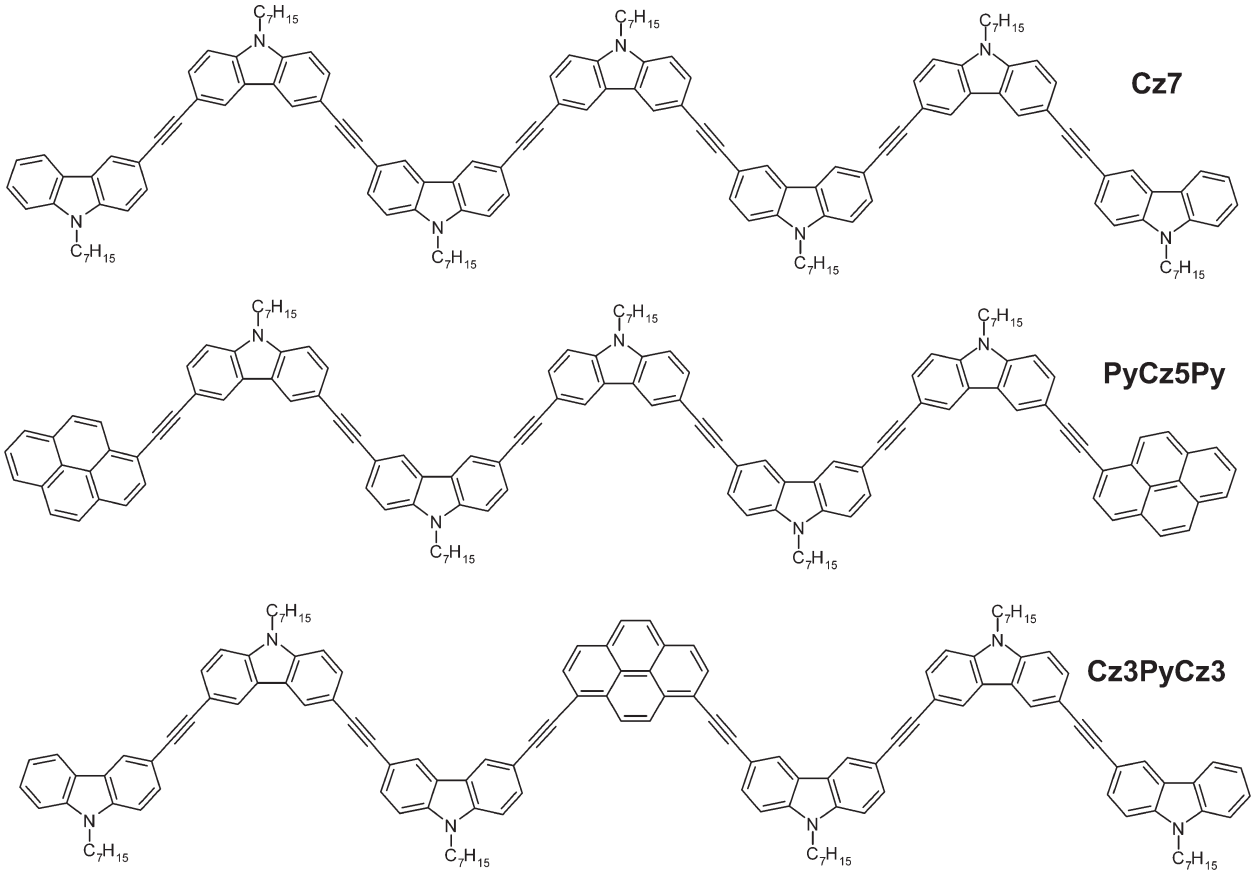


**Figure 88.** Chemical structure of pyrene-modified carbazole oligomers.

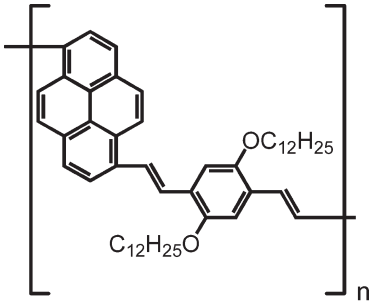


**78**

**Figure 89.** Chemical structure of poly(*p*-phenylenevinylene) (PPV) derivative containing pyrene (**78**).

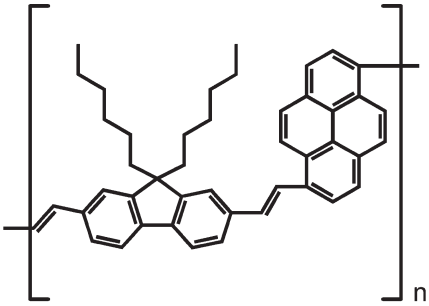


**161**

**Figure 90.** Chemical structure of copolyfluorenevinylene including pyrene **161**.

### 4.4. 1,3-Disubstituted Pyrenes

In the search for stable blue emitters, both in solution and in thin film, our group reported a novel nonaggregating polypyrene, which can be synthesized via a simple three-step chemical route from pyrene in good yields.[251] Poly-7-*tert*-butyl-1,3-pyrenylene (**163**) shows a high solid-state fluorescence quantum yield with blue emission, excellent solubility and stability, no aggregation in thin films, and good electro-optical performance in single-layer OLEDs. Poly-7-*tert*-butyl-1,3-pyrenylene (**163**) (Figure 92), with a defect-free structure, has the highest degree of polymerization reported up to now for polymers made up exclusively from pyrene units.

The use of *tert*-butyl groups was strategic in order to selectively obtain the 1,3-dibromo pyrene monomer. The polymerization of the monomer was carried out under Yamamoto conditions with a Ni(0) catalyst, followed by end-capping with bromobenzene. The resulting polymer **163** was obtained in 60% yield, and GPC (gel permeation chromatography) analysis (THF, PPP standards) revealed $M_n$ = 29 800 g/mol, $M_w$ = 51 500 g/mol, and PD = 1.7. This corresponds to a molecular structure of approximately 115 repeat units. In addition to the high molecular weight, we reported for the first time the suppression of aggregation in pyrene due to the highly twisted structure of the polymeric chain. In effect, through molecular structure design,



Samsung Exhibit 1020, Page 43 of 55

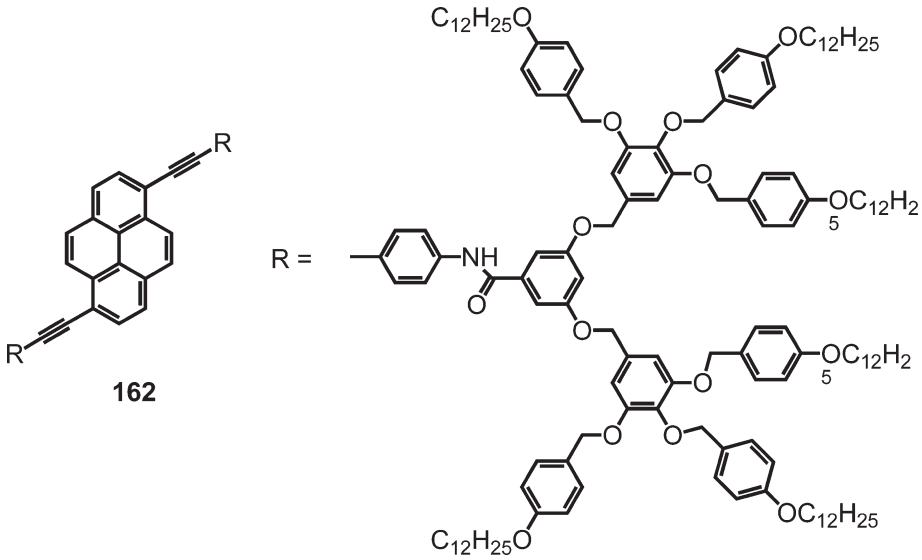


**Figure 91.** Chemical structure of liquid crystal **162**.

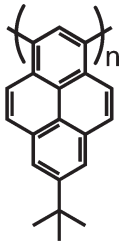


**Figure 92.** Chemical structure of poly-7-*tert*-butyl-1,3-pyrenylene (**163**).

the close packing/luminescence quenching effect in pyrene was controlled. The novel 1,3-substitution of the pyrene ring leads to important advantages, such as good solubility and a high fluorescence quantum yield in THF of $\Phi_{PL}$ = 0.88. OLED devices with the ITO/PEDOT:PSS/**163**/CsF/Al configuration showed bright blue−turquoise electroluminescence with a maximum at 465 nm and a profile very similar to the photoluminescence in the solid state. Luminance values of 300 cd/m$^2$ were measured at a bias voltage of 8 V with favorable blue color coordinates of $x$ = 0.15 and $y$ = 0.32. The OLEDs display a detectable onset of electroluminescence at approximately 3.5 V and maximum efficiencies of ca. 0.3 cd/A. In conclusion, this remarkable poly-7-*tert*-butyl-1,3-pyrenylene presents the benefit of very stable blue emission, which is a consequence of the new 1,3-substitution, resulting in a large dihedral angle between pyrene units that strongly suppresses aggregation and excimer emission.

Macrocycles with rigid, unsaturated hydrocarbon backbones have attracted great interest in the past few years, owing to their unique properties and their role as building blocks of three-dimensional nanostructures, discotic liquid crystals, extended tubular channels, guest−host complexes, and porous organic solids.[252−255] These molecules consist of a shape-persistent scaffold in a planar or nearly planar conformation, with minimal ring strain and a large diameter-to-thickness ratio.[256] The cyclic, stiff backbone of these macrocycles is typically decorated with solubilizing aliphatic side chains, which can contain various functionalities. The aliphatic substituents are most often attached at the periphery, but in some cases, the side chains have been reported to fill the internal void of the macrocycle.[257,258] Due to $\pi$-stacking interactions, some of these building blocks self-assemble into discotic columnar superstructures.[259] The nanophase separation of the aliphatic part, which fills the columnar periphery, from the rather rigid aromatic cores further promotes thermotropic mesophase formation.[259−261] The variation of the molecular architecture allows the control of these thermotropic properties, but requires appropriate synthetic methods for an efficient preparation of macrocycles.[262−264] Studies of the supramolecular organization of these macrocycles have provided a better understanding of the noncovalent driving force responsible for their self-assembly.[265−268]

Inspired by the ability of macrocycles to self-assemble in supramolecular arrangements and by the optoelectronic properties of pyrene, our group became interested in the design of pyrene-based macrocycles. Macrocycles constituted exclusively of pyrene units are extremely interesting structures from the optical, electronic, and synthetic point of view. The pyrene-based macrocycle **164** is depicted in Figure 93.[269]

The synthesis begins with the conversion of 2-*tert*-1,3-dibromopyrene to 2-*tert*-1,3-diiodopyrene as well as to 2-*tert*-1-bromo-3-boronic ester pyrene. The desymmetrization of 2-*tert*-1,3-dibromopyrene was the key step to obtain the desired pyrene-based macrocycle. A Suzuki coupling reaction between these two building blocks afforded the trimer bearing two bromide functions. Yamamoto coupling using Ni(0) catalyst under diluted conditions afforded the desired macrocycle in low yield (10%). The photophysical properties of this new macrocycle were also investigated in solution and compared to a linear pyrene hexamer. The maximum absorption was measured at 360 nm with fluorescent emission at 439 nm. These values are red-shifted compared to the linear hexamer. This fact suggests additional intermolecular interactions in the case of the macrocycle. This structure further serves as a precursor for the planarized macrocycle via cyclodehydrogenation reaction for possible self-assembly into ordered columnar structures.



Samsung Exhibit 1020, Page 44 of 55

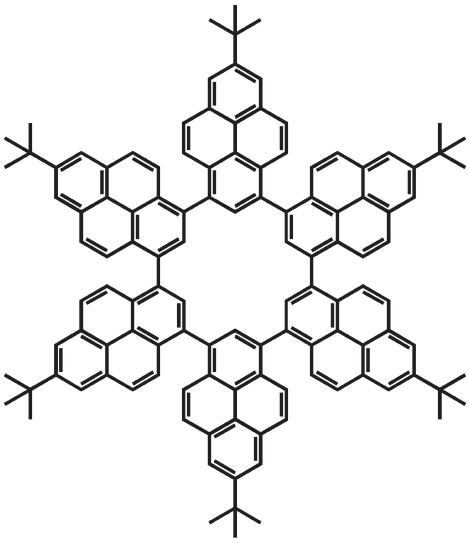

164

Figure 93. Chemical structure of pyrene macrocycle **164**.

### 4.5. 2,7-Disubstituted Pyrenes

Recently, our group reported the first 2,7-linked conjugated polypyrenylene, **165** (Figure 94), tethering four aryl groups.[270] We have previously demonstrated that oligopyrenes linked at their 2,7-positions, to a first approximation, possess electronically decoupled pyrene subunits due to the nodal properties of their frontier orbitals.[271] This insight strongly encouraged us to construct 2,7-linked polypyrenylenes, since such polymers should act both as blue light emitters and as probes for local polarity.

Poly(2,7-pyrenylene) (**165**) exhibits an intriguing blue and solvent-dependent fluorescence in solution and strong red-shifted emission in films. A high molecular weight of $M_n$ = 21 800 g/mol and PD = 1.7, which corresponds to approximately 20 repeat units, was obtained via Yamamoto coupling reaction utilizing microwave heating. Polymer **165** displays a blue fluorescence in solution, with an emission maximum at $\lambda$ = 429 nm, thus fulfilling well the requirements for a blue-emitting polymer. However, the fluorescence spectra of **165** reveal a remarkable long-wavelength tailing as well as additional emission bands with maxima at $\lambda$ = 493 and 530 nm. A fluorescence concentration dependence study was performed in order to find a possible explanation for the green emission bands in the blue conjugated polymer.

The fluorescence spectral shape of **165** did not change, even under very high dilutions such as 10−8 M per monomer unit, indicating that the polymers do not form interchain aggregates in solution. The intensity ratio between the localized emission maxima in the fluorescence spectra of the thin film samples was drastically changed when going to the solid state. The polymer presents a blue fluorescence in solution with an emission band maximum at $\lambda$ = 429 nm, fulfilling the requirements for a blue-emitting organic semiconductor. The red-shifted broad emission bands observed in the polymer fluorescence in solution are not caused by aggregation but by intramolecular energy redistribution between the vibrational manifold of the single polymer chain. The additional red-shifted emission of the polymer in the solid state could be strongly reduced by blending with

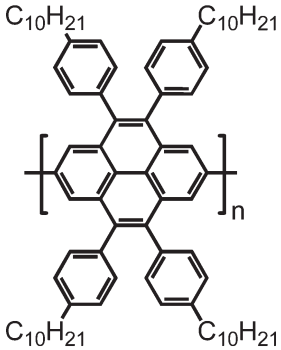


165

Figure 94. Chemical structure of poly(2,7-pyrenylene) (**165**).

a nonconjugated polymer such as the polystyrene. Finally, in solution, the polymer possesses fluorescence with solvent-dependent features and could be used for probing local solvent polarity.

Highly symmetrical, star-shaped molecules such as hexaarylbenzenes have attracted interest in materials science in recent years, for applications as light-emitting and charge-transport layers in OLEDs and as precursors for photoconductive polycyclic aromatic hydrocarbons and discotic liquid crystals. For this reason, hexapyrenylbenzene **166** (Figure 95) was prepared, and its spectroscopic properties were analyzed.[272]

In this structure, pyrenyl subchromophores were chosen because of the rich and well-known photochemistry of pyrene. To design this structure it was fundamental that pyrene is bound at the 2-position to the central benzene ring, because this minimizes direct orbital overlap with the benzene core because of the pyrene HOMO and LUMO having nodes through the 2- and 7-positions. To achieve the 2,7-positions, an indirect approach was established, as previously described in Figure 40 for the synthesis of the precursor **90**, which was then involved in a Sonogashira coupling to afford the pyrene alkyne derivative, with the last step being the cyclotrimerization reaction using a cobalt catalyst. The emission spectrum is independent of the concentration such that excimer formation between two molecules of **166** could be excluded. This pyrene derivative exhibits strong and red-shifted fluorescence both from locally excited pyrene states and from the excitonic states of the aggregate.

### 4.6. 4,5,9,10-Substituted Pyrenes

In the search for new semiconducting materials for molecular electronics, the 4,5,9,10-positions of the pyrene ring appear as a very attractive alternative to prepare extended aromatic systems. More precisely, the pyrene-4,5,9,10-tetraone or it is derivatives allows by simple condensation reactions a simple method to extend conjugation for elaboration of large polycyclic aromatic hydrocarbons (PAHs).

To fabricate memory and electronic circuits, it is important to develop both p- and n-type semiconductor organic materials; however, the vast majority of organic materials developed so far corresponds to p-type organic molecules. A new class of n-type semiconductor materials using pyrene between pyrazine units in a one-dimensional multipyrazine-containing acene-type conjugated molecules with different molecular lengths was reported (Figure 96).[273]

Heterocyclic aromatic compounds containing imine nitrogen atoms generally have a less negative reduction potential



Samsung Exhibit 1020, Page 45 of 55

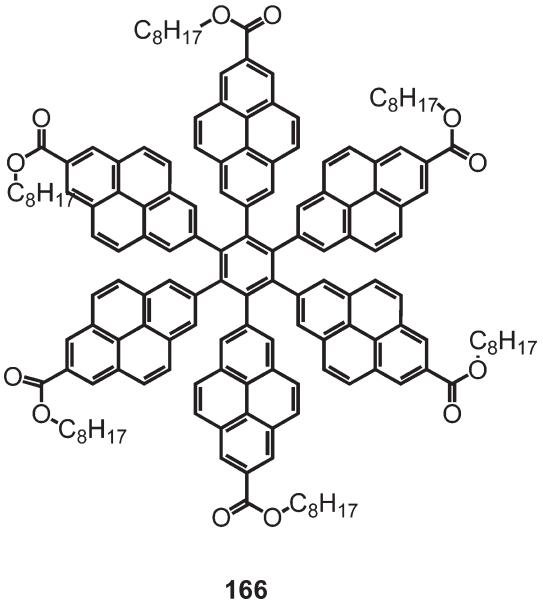


**Figure 95.** Chemical structure of hexapyrenylbenzene **166**.

compared to hydrocarbon analogues and heterocyclics containing oxygen or sulfur atoms. In addition to the strongly enhanced electron affinity, the successive replacement of CH moieties by nitrogen atoms in PAH offers opportunities to manipulate the intermolecular interactions and molecular arrangements in the solid state and therefore to tune electronic properties. Under optimized condensation conditions, the acene-type compounds (**1**−**5**) containing two to six pyrazine units and up to 16 rectilinearly arranged fused aromatic rings were synthesized from a pyrene-4,5,9,10-tetraone derivative containing *tert*-butyl groups or alkoxy chains at the 2,7-positions. Compound **5**, with 16 planar arranged fused aromatic rings, has a long length of about 5 nm. Absorption measurements reveal that the energy gaps of the molecules decrease with an increase in molecular length. All of these molecules tend to aggregate in solution, which can be greatly suppressed by introducing bulky *tert*-butyl groups. The n-type semiconducting nature of these acene-type compounds has been verified by the electrochemical data. With the increasing number of pyrazine rings and the increasing length of the molecules, the electron affinity of these compounds is significantly enhanced. As a result, the LUMO energy levels decrease from −3.24 to −3.78 eV, comparable to a well-known n-type material, PCBM. High electron affinity, high environmental stability, and ease of structural modification make these compounds excellent n-type semiconductors.

The synthesis and properties of a novel class of pyrene discotic materials for electronic applications were presented.[274] 6,7,15,16-Tetrakis(alkylthio)quinoxalino[2′,3′:9,10]phenanthro[4,5-*abc*]-phenazine (**167**) was synthesized by condensation reaction of pyrene-4,5,9,10-tetraone (Figure 97).

All OFET devices of **167a** displayed p-channel characteristics. The average saturation hole mobility was around $10^{-3}$ $cm^2 V^{-1} s^{-1}$. The average threshold voltage was −43.7 ± 5.8 V. These values are typical for thin-film OFETs with discotic liquid crystal materials.

A similar pyrene discotic, but this time bearing a bis-crown ether, was synthesized and the binding properties analyzed. Compound

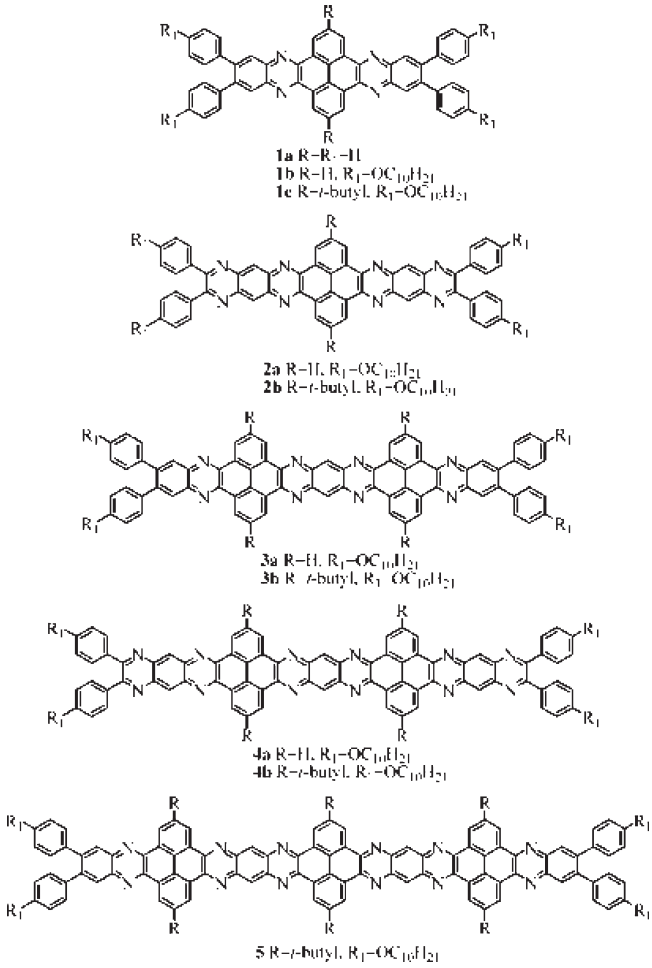


**Figure 96.** Chemical structure of pyrene-modified multipyrazine derivatives.

**168** composed of an quinoxalino[2′,3′:9,10]phenanthro[4,5-*abc*]-phenazine core bearing two 18-crown-6 moieties is represented in Figure 98.[275]

In order to identify the factors that control the thin film crystallization processes, the thin film microstructure of a related material was investigated.[276] The organic semiconductor (6,7,15,16-tetrakis(dodecylthio)quinoxalino-[2′,3′:9,10]phenanthro[4,5-*abc*]phenazine was developed as a potential charge-transport material for organic electronic applications. The characterization strategy proved effective in determining a nearly complete crystal packing model. Notable features of the packing are the arrangement in segregated vertical layers; the highly tilted core long axes and side chains; within the layers, the absence of alkane interdigitation between layers; and the cofacial packing of tilted planes.

Recently, we reported new electron-deficient *N*-heteroaromatic linkers for the elaboration of large and soluble polycyclic aromatic hydrocarbons (PAHs).[277] The synthesis of these extended PAHs of different sizes and shapes relies on a synthetic approach starting from the 2,7-di-*tert*-butylpyrene-4,5-dione to achieve the soluble oligophenylene precursor **169** with a well-defined structure, which was then planarized via cyclodehydrogenation (Figure 99). The selective oxidation of the perimeter of a 6-fold *tert*-butylated tetrabenzo[*bc,ef,hi,uv*]ovalene, led to the formation of the α-diketone **169**. This versatile building block



Samsung Exhibit 1020, Page 46 of 55

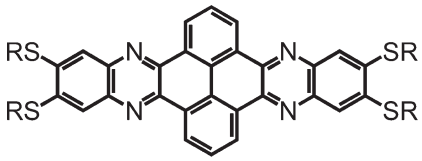


**167a**, R = $C_{12}H_{25}$
**167b**, R = $C_{10}H_{21}$
**167c**, R = $C_8H_{17}$
**167d**, R = $C_6H_{13}$

**Figure 97.** Chemical structure of 6,7,15,16-tetrakis(alkylthio)-quinoxalino[2′,3′:9,10]phenanthro[4,5-*abc*]phenazine (**167**).

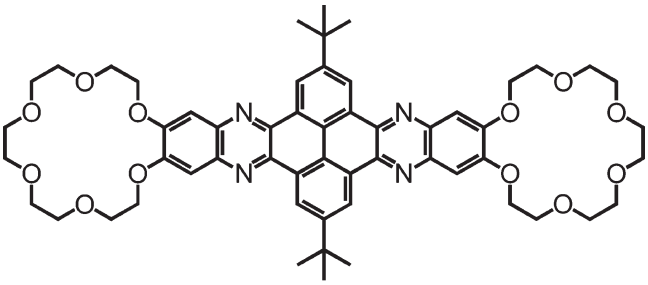

**168**

**Figure 98.** Chemical structure of quinoxalino[2′,3′:9,10]phenanthro-[4,5-*abc*]phenazine derivative **168**.

took part in quinoxaline condensations to afford several giant heteroatom-containing PAHs, such the ones depicted in Figure 99.

The distortion from planarity of the aromatic frameworks of **169** by the bulky *tert*-butyl groups brought extraordinarily high solubilities, presumably through the suppression of aggregation of the aromatic $\pi$-systems.[278] According to CV, the introduction of quinoxaline or tetraazaanthracene bridges into the large aromatic moiety significantly reduces the LUMO level, thus rendering them strongly electron-accepting systems. The novel nanographene **172**, with 98 atoms in the aromatic core, is so far the largest known PAH with a well-resolved $^1$H NMR spectrum and exhibits strong fluorescence solvatochromism. The emission of **172** shifts with the polarity of the solvent, suggesting that this system can function as a $\pi$-electron-accepting unit only in the excited state.

The quinoxaline condensation using the precursor **169** could also be used in the synthesis of very large heterocycles capable of complexation to a metal center, as shown in Figure 100.

The largest known ligand to be complexed to a metal center has also been synthesized. Ligand **173**, which is composed of 60 skeletal atoms (56 carbon and 4 nitrogen), was used to form a ruthenium complex, **174**. Using this approach, we also constructed a range of large metal complexes by varying the metal as well as the number and nature of the giant ligands. Copper phthalocyanine **176** is the largest known phthalocyanine derivative. It has an absorption maximum at 865 nm (Q-band) and excellent chemical stability (stable up to ca. 450 °C). This makes it an attractive system for use in long-term archival storage devices, such as write-once, read-many-times disks. Metallophthalocyanines have been demonstrated to possess remarkable semiconducting properties with n-type properties. The copper phthalocyanine **176** presents a small HOMO−LUMO gap (1.34 eV), which can be used for the fabrication of n-type OFETs.

A similar precursor, this time prepared from the 2,7-di-*tert*-butylpyrene-4,5,9,10-tetraone, allowed the preparation of a series of five well-defined monodisperse polyphenylene ribbons (**177**) with increasing length, containing up to six dibenzo[*e,l*]pyrene units in a three-dimensional backbone (Figure 101).[279]

In spite of the apparent backbone flexibility due to the linkage of the dibenzo[*e,l*]pyrene units by "zigzag"-bonded biphenyl bridges, the polyphenylene ribbons are expected to have a quasirigid linear structure because of the steric hindrance between the neighboring stiff and bulky dibenzo[*e,l*]pyrene units. These polyphenylene ribbons were designed to serve as precursor molecules toward large PAH ribbons via a cyclodehydrogenation reaction, which was demonstrated for the lowest homologue containing 132 carbon atoms in the aromatic core. These graphitic nanoribbons with two-dimensional, essentially planar conformations result in high delocalization of electrons along the backbone and, consequently, high charge carrier mobilities.

The heptacene derivative frequently called "twistacene" (**98**) shows high distortion from planarity, mostly due to the presence of the phenyl substitutents (Figure 44).[280] The synthesis of this electroluminescent pyrene derivative **98** started from the pyrene-4,5-dione **95**, as depicted in Figure 44. The terminal pyrene moieties were designed to serve two functions: (1) to stabilize the inherently unstable heptacene and (2) to enable the oligoacene to be a strongly fluorescent molecule. The material's photoluminescence (PL) spectrum spans from 520 to 700 nm. The band gap value is 2.5 eV, based on CV experiments, which places the band gap of twistacene between those of tetracene (2.6 eV) and pentacene (2.1 eV). The solid-state structure further reveals that this molecule is so strongly twisted out of planarity that the terminal pyrene units end up in the same plane. This nonplanarity prevents the molecules from closely approaching each other in the solid state. Therefore, the self-quenching effect could be reduced. To achieve white-light emission, the twistacene was doped into a blue fluorene-based polymer. Very bright and efficient white emission PLEDs, with a maximum luminance exceeding 20 000 cd/m$^2$ based on blue polyfluorene doped with 1 wt % TBH, were fabricated.[281] The maximum luminous efficiency was 3.55 cd/A at 4228 cd/m$^2$, while the maximum power efficiency was 1.6 lm/W at 310 cd/m$^2$. The white color was achieved by incomplete energy transfer from the blue polyfluorene to TBH. The luminous efficiency of this PLED device is comparable to that of the doped phosphorescence devices reported recently.[282] Moreover, compared to these previously reported phosphorescence LEDs, the device based on the twistacene has higher power efficiency due to the lower turn-on and operating voltages. Another advantage of this device is that the device CIE coordinates vary little as a function of current density.

A new series of pyrene-based, pure-blue, fluorescent, stable monomers, namely, the 2,7-di-*tert*-butyl-4,5,9,10-tetrakis(*p*-*R*-phenylethynyl)pyrenes (**178**) (Figure 102), have been synthesized by Pd/Cu-catalyzed Sonogashira coupling of the precursor 4,5,9,10-tetrabromo-2,7-di-*tert*-butylpyrene (**100**) formerly described in Figure 45, using the *tert*-butyl groups as positional protective groups.[283]



Samsung Exhibit 1020, Page 47 of 55

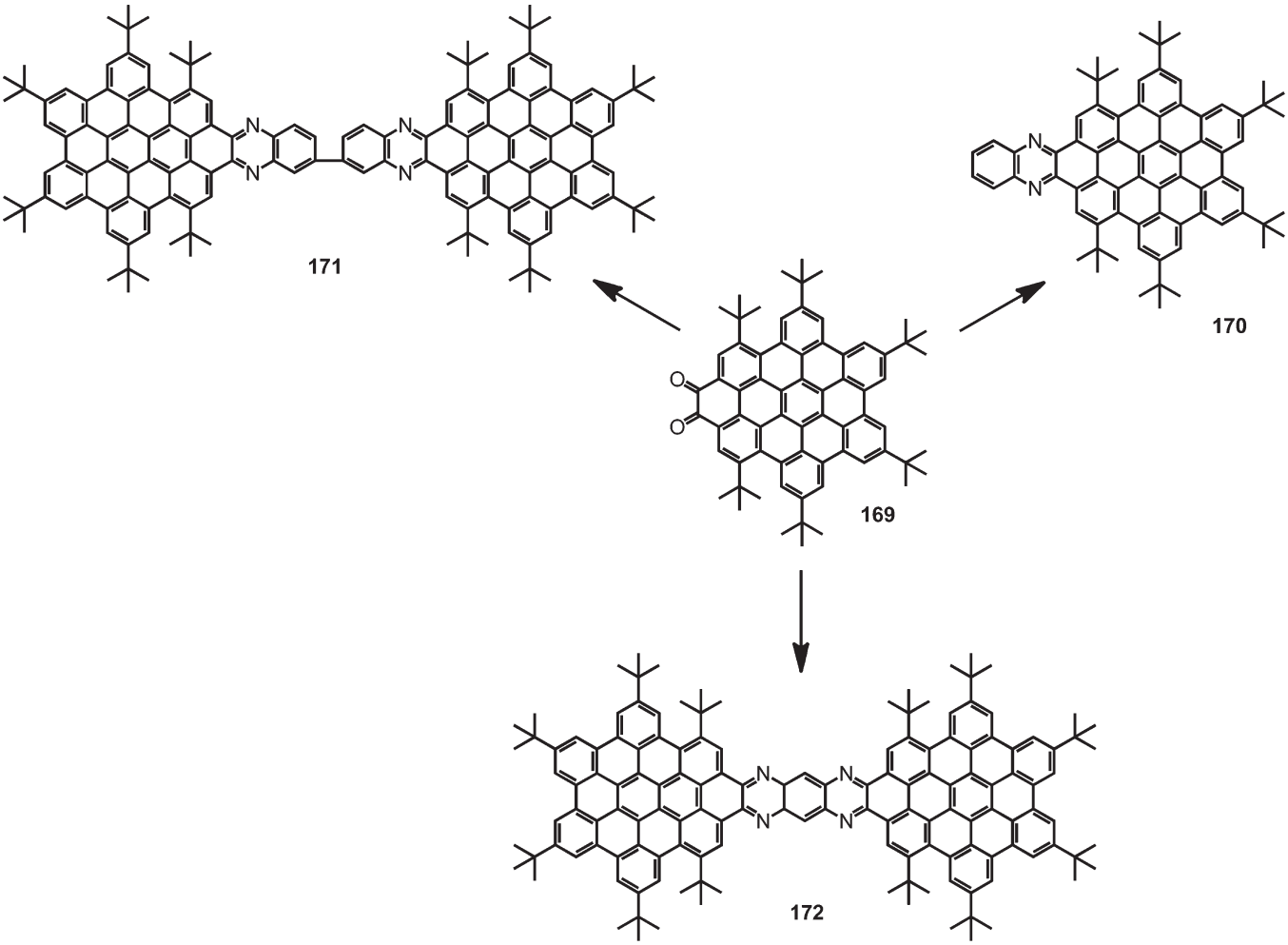


**Figure 99.** Heteroatom-containing nanographenes from precursor **169**.

As revealed from single-crystal X-ray analysis, there is a herringbone pattern between stacked columns, but the $\pi-\pi$ stacking distance of adjacent pyrene units was not especially short at about 5.82 Å, due to the introduction of the two bulky *tert*-butyl groups in the pyrene rings at the 2- and 7-positions. Photophysical characterization showed that the extension of $\pi$-conjugation in these pyrene chromophores through phenylacetylenic substituents serves to shift the wavelength of absorption and fluorescence emission into the pure blue visible region, for possible application as blue-emitting materials in OLEDs.

In the continuous search for innovative perylene bisimide derivatives for photovoltaic devices, Mikroyannidis et al. reported the symmetrical pyrene−perylene dyad **180** (Figure 103).[284,285]

Concerning bulk heterojunction solar cells, the state-of-the-art is currently represent by photovoltaic devices with a power conversion efficiency close to 8% based on composites of acceptor-type fullerenes derivatives, such as PCBM with donor polymers or small molecules. These composites have the advantage of good charge carrier mobility but suffer from a relatively large band gap and low absorption coefficients. PCBM is considered the ideal acceptor in organic solar cells; however, it suffers the disadvantage of poor absorption in the visible spectrum. For further improvement of the power conversion efficiency, it is important to develop new-donor-type organic/polymer semiconductors with higher carrier mobility and low band gap, and simultaneously, an electron acceptor material that absorbs photons in the visible region.

Bulk heterojunction solar cells were fabricated using the small molecule **179**, which contains a central *p*-phenylenevinylene unit, intermediate thiophene moieties, and terminal cyanovinylene 4-nitrophenyls and possesses the donor−acceptor architecture. Specifically, the central dialkoxyphenylene and intermediate thiophene behaved as electron-donating segments, while the terminal cyanovinylene 4-nitrophenyls acted as electron acceptors. Thus, an intramolecular charge transfer took place in this compound, which reduced its optical band gap. Compound **179** was used as donor and the perylene−pyrene bisimide **180** as acceptor to design the BHJ layer. The conversion efficiency of the photovoltaic device with the donor:acceptor ratio 1:3.5 is about 1.87%, which is relatively good. This is attributed to the improved light harvesting by the bulk heterojunction thin film layer. When a ZnO layer was inserted in between the BHJ layer and the top Al electrode, the efficiency was enhanced to 2.47%, which is attributed to a further improved light absorption by the active layer due to the optical interference between the incident light and the reflected light and the improved electron transport in the device. The power conversion efficiency is further improved to



Samsung Exhibit 1020, Page 48 of 55

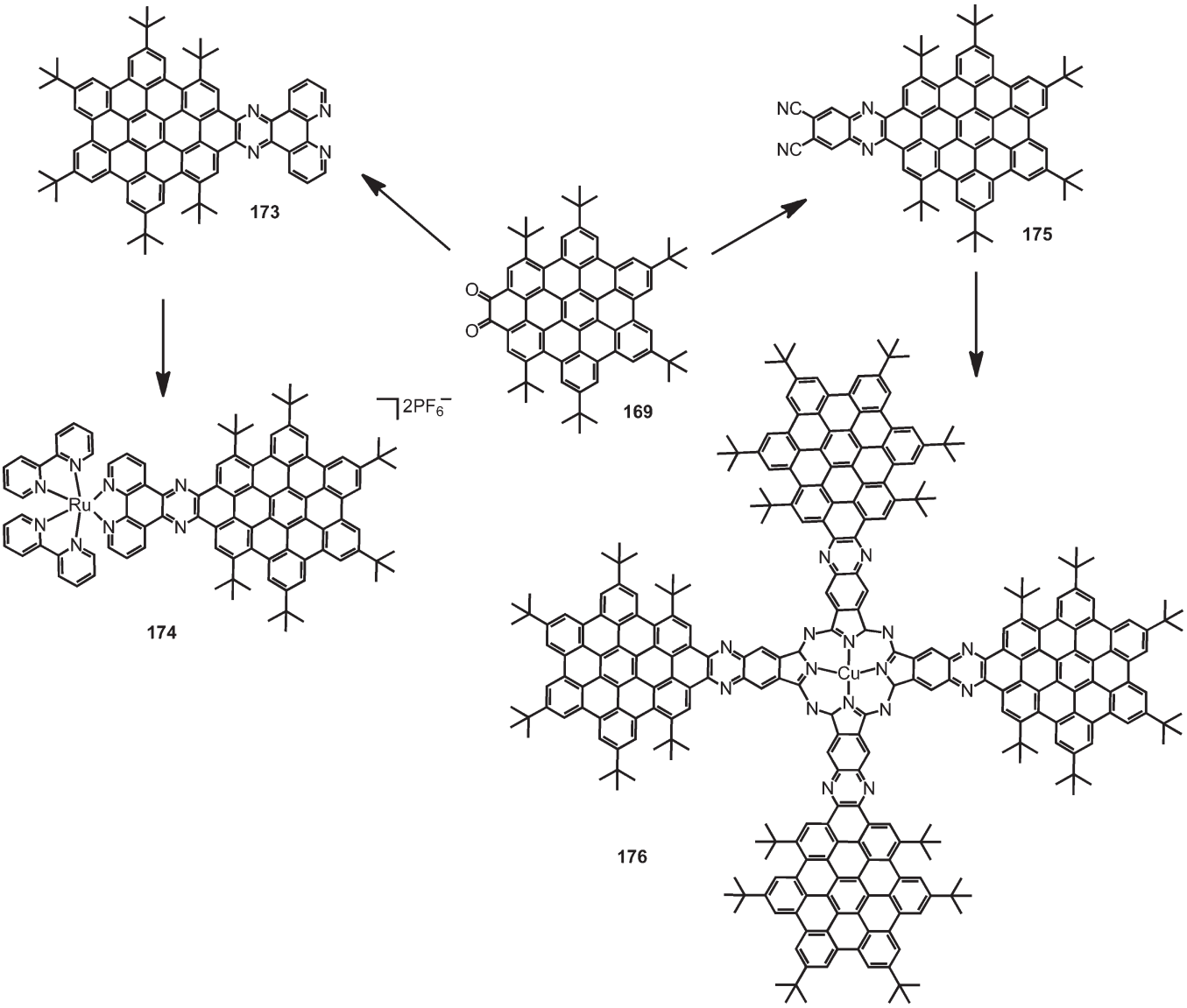


**Figure 100.** Metal-containing nanographenes from precursor **169**.

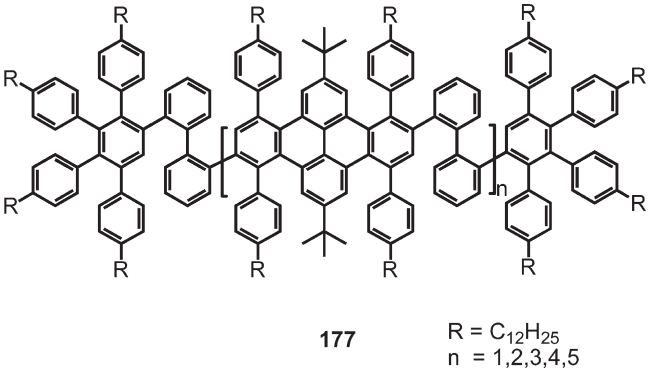


**177**

**Figure 101.** Graphitic nanoribbons **177**.

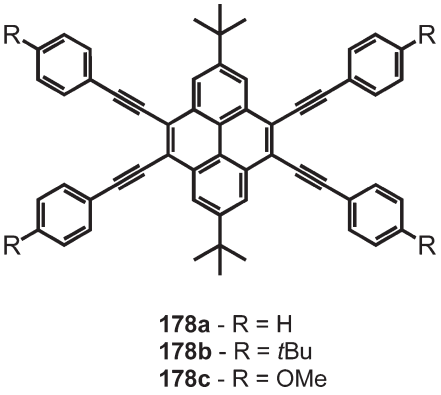


**Figure 102.** Chemical structure of phenylethynylpyrenes **178**.

3.17% when the device is annealed at a temperature of 100 °C for 5 min, which is attributed to the increased crystalline nature of active layer leading to further improvement in charge transport.

These values correspond to the highest values reported so far for bulk heterojunction solar cells based on a perylene derivative



Samsung Exhibit 1020, Page 49 of 55

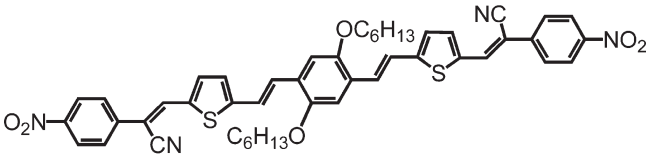


179

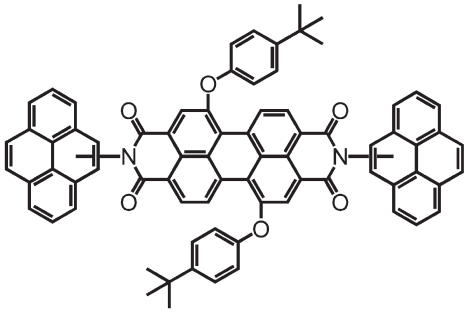


180

**Figure 103.** Pyrene−perylene dyad **180** and small molecule donor **179**.

as an acceptor material. The pyrene unit in this case should contribute to an enhancement of the absorption in the visible region, as well as photoinduced processes such as energy and/or electron transfer, in addition to a favorable morphology due to the twisted structure between pyrene and perylene, which results in an improvement of exciton diffusion.

## 5. CONCLUSION

In the current paper, we have presented an overview of the use of pyrene in organic electronics. We have started with the design of the compounds, which is directly related to chemical issues, passing over to the photophysical characterization and investigation of the different processes, such as energy and electron transfer, and ending with the fabrication of the final devices.

It cannot be stressed enough that materials research starts with synthesis. Providing the right material for electronic and optoelectronic application is, foremost, a molecular issue. How can we control the properties of a conjugated $\pi$-system, such as pyrene, by chemical functionalization and derivatization?

The shape of pyrene, four fused aromatic rings, leads to very particular reactivities; more precisely, the pyrene ring presents three different reactivities in the same molecule. These different reactivities lead to many selectivity problems as well as mixtures of isomers that are very difficult to separate, making pyrene a very challenging chemical system. Because electrophilic substitution occurs preferentially at the 1,3,6,8-positions, the mono- and tetrasubstituted pyrenes can be easily obtained. On the other hand, the preparation of disubstituted pyrenes is much more demanding but at the same time highly necessary for the preparation of well-defined linear or cyclic oligomers and polymers. The 1,6- and 1,8-disubstituted pyrenes can only be isolated via tedious purification based on slightly differing solubilities. The 1,3-disubstituted pyrenes were not accessible for many decades, due to the preferred formation of 1,6- and 1,8-disubstituted derivatives; however, very recently, we could overcome that problem. The 2,7-disubstituted pyrenes must be prepared through indirect routes consisting of multistep and low-yielding reactions. The 4,5,9,10-substituted pyrenes appear as very interesting building blocks for the preparation of extended conjugated systems as large polycyclic aromatic hydrocarbons. During the past decades, these difficulties in accessing some positions of the pyrene ring have partially limited the use of such building blocks.

Simultaneously, thanks to its very special optical and electronic properties, pyrene has attracted much attention as an important organic semiconductor for application in OLEDs, OFETs, OLEFETs and, recently, also photovoltaic devices, such as BHJs and DSCs. To this purpose, efforts have been made in order to enhance the electronic and optical properties of pyrene derivatives by modifying its molecular structure. The electro-optical properties can be fine-tuned by introducing specific electron-donating or -accepting groups or, alternatively, by simply modifying the molecular architecture via substitution at the pyrene ring. Fluorescent blue OLEDs, based on pyrene derivatives, have shown excellent performance, achieving among the highest reported values. Fabrication of light-emitting field effect transistors using pyrene derivatives has been also very successful. Recently, bulk heterojunction solar cells, using a pyrene−perylene acceptor, have shown the highest reported values of power conversion efficiency for BHJ solar cells with perylene as the acceptor material.

Certainly, the development of new and simple synthetic methods to circumvent the synthetic difficulties, such as the simple preparation of 1,3-disubstituted pyrenes using a *tert*-butyl as a positional protecting group or the accessibility to 2,7-disubstituted pyrenes via two simple steps, opens many further possibilities in terms of new pyrene-based semiconductors with enhanced opto-electronic properties. The key to new pyrene-based semiconductors is the development of new synthetic methods necessary to reach the desirable substitutions, allowing the use of pyrene in organic electronics. This will successfully lead to a new era in terms of pyrene chemistry and promote the expansion of pyrene as a building block for organic electronics.

As far as chemical functionalization is concerned, the chemistry of pyrenes proceeds in solution. The function of organic devices, however, relates to thin solid films and thus to the solid-state packing. The first concern, thereby, is sufficient solubility in organic solvents for film deposition. The other is to establish the right morphology. In an OLED, for example, amorphous films are preferred in order to avoid light scattering at microcrystallites. In an OFET, high charge carry mobility is desired for which certain packing modes and high supramolecular order are crucial. Finally, in a bulk heterojunction solar cell, an important prerequisite for the formation of separate percolation pathways of holes and electrons is the formation of nanophase separated regimes. All of these features are quite sensitive toward processing from solution, which includes nucleation, phase formation, wetting−dewetting phenomena, and the templating effect of substrate surfaces.

Another concern, however, is to achieve these morphological properties via molecular design, e.g., by substitution with different alkyl chains and introduction of polar and/or unpolar functions, which assist the formation of the desired supramolecular structures. In that sense the synthesis of pyrene molecules is only the first step in a whole chain of events, since not only the appropriate molecular but also the supramolecular architecture must be established en route to the best structural hierarchies including the interfacing with substrates and electrodes. This is, above all, a chemical challenge, and while much has been learned about the correlation of molecular structures and $\pi$-electron



Samsung Exhibit 1020, Page 50 of 55

properties, there is still much to be gained from more reliable correlations between device function and supramolecular structures.

The final question to be addressed, when attempting to proceed from organic and polymer synthesis to optimized performance in electronic and optoelectronic devices, is whether it makes sense to single out particular $\pi$-systems such as pyrene. One could suggest that the study of organic semiconductors is partly a matter of fashion and of availability of a sample. Thus, perylenetetracarboxydiimides have played a key role in the search for suitable organic semiconductors, not only because they are so unique and important but because they are commercially available. Pentacene, the fruitfly of the study of organic semiconductors in the field effect transistors, seems to play a special role in justifying all the many physical and theoretical approaches which it has attracted. But, here again, a key driving force in this development has been the chemical functionalization of pentacenes, e.g., by going toward thia derivatives or by synthesizing ethynyl derivatives. Highlighting pyrene and its possible functions as an organic semiconductor does not necessarily imply its role as a front runner in this field, but many excellent cases can be made from this review, how new synthetic methods stimulate new fundamental and theoretical concepts and lead to unprecedented device function. It is hoped that, vice versa, theory and physics can identify new targets for pyrene synthesis.

## AUTHOR INFORMATION

### Corresponding Author

*E-mail: muellen@mpip-mainz.mpg.de.

## BIOGRAPHIES

Dr. Teresa Marina Figueira-Duarte was born in Sintra, Portugal, in 1978. She received her Ph.D. in 2007 from the Université Louis Pasteur, Strasbourg, on the topic of fullerene derivatives for material science applications under the advisement of Prof. Jean-Francois Nierengarten. Between 2007 and 2010 she performed postdoctoral research at the Max Planck Institute for Polymer Research in Mainz, Germany, in the group of Prof. Klaus Müllen on the subject of innovative pyrene-based systems for organic electronics. In 2010 she joined BASF SE in Ludwigshafen, Germany, where her current focus is on the further development of organic light-emitting diodes toward market implementation.

Klaus Müllen is one of the directors at the Max Planck Institute for Polymer Research in Mainz, Germany, a post he has held since 1989. His research interests range from new polymer-forming reactions, including methods of organometallic chemistry, multidimensional polymers with complex shape-persistent architectures, and molecular materials with liquid crystalline properties for electronic and optoelectronic devices, to the chemistry and physics of single molecules, nanocomposites, and biosynthetic hybrids. He is Past President of the German Chemical Society and serves as a member of many editorial advisory boards and as an associate editor of the Journal of the American Chemical Society. His work has led to the publication of over 1300 papers, and he is one of the most cited authors in his field. He holds numerous honorary degrees and has received, among many others, the Max-Planck-Research-Prize, the Philip-Morris-Research-Prize, the Elhuyar Goldschmidt Award of the Spanish Chemical Society, the International Award of the Society of Polymer Science Japan, and the American Chemical Society Award in Polymer Chemistry.

## REFERENCES

(1) Laurent, A. *Ann. Chim. Phys.* **1837**, *66*, 136.
(2) Graebe, C. *Liebigs Ann.* **1871**, *158*, 285.
(3) Meyer, R. *Chem. Ber* **1912**, *45*, 1609.
(4) Freund, M. *Chem. Ber.* **1897**, *30*, 1383.
(5) Steiner, H. *J. Inst. Pet.* **1947**, *33*, 410.
(6) Weitzenbock, R. *Mh. Chem.* **1913**, *34*, 193.
(7) Chatterjee, N. N.; Bose, A.; Roy, H. B. *J. Indian Chem. Soc.* **1947**, *24*, 169.
(8) Freund, M.; Fleischer, K. *Liebigs Ann.* **1914**, *402*, 77.
(9) Fleischer, K.; Retze, E. *Chem. Ber.* **1922**, *55*, 3280.
(10) von Braun, J; Rath, E *Chem. Ber.* **1928**, *61*, 956.
(11) Cook, J. W. *J. Chem. Soc.* **1934**, 366.
(12) Baker, W.; Mcomie, J. F. W.; Norman, J. M. *Chem. Ind.* **1950**, 77.
(13) Baker, W.; Mcomie, J. F. W.; Norman, J. M. *J. Chem. Soc.* **1951**, 1114.
(14) Baker, W.; Mcomie, J. F. W.; Warburton, W. K. *J. Chem. Soc.* **1952**, 2991.
(15) Pelchowicz, Z.; Bergmann, E. D. *Bull. Res. Council Israel* **1953**, *3*, 91.
(16) Bacon, R. G. R.; Lindsay, W. S. *J. Chem. Soc.* **1958**, 1375.
(17) Welham, R. D. *J. Soc. Dyers Color* **1963**, *79*, 98.
(18) Förster, T.; Kasper, K. *Z. Elektrochem.* **1955**, *59*, 976.
(19) Birks, J. B. *Photophysics of Aromatic Molecules*; Wiley-Interscience: London, 1970.
(20) Kalyanasundaram, K.; Thomas, J. K. *J. Am. Chem. Soc.* **1977**, *99*, 2039.



Samsung Exhibit 1020, Page 51 of 55

(21) Winnik, M. A.; Winnik, F. M. *Adv. Chem. Ser.* **1993**, 485.
(22) Winnik, F. M. *Chem. Rev.* **1993**, *93*, 587.
(23) Goedeweeck, R.; Vanderauweraer, M.; Deschryver, F. C. *J. Am. Chem. Soc.* **1985**, *107*, 2334.
(24) Hammarstrom, P.; Kalman, B.; Jonsson, B. H.; Carlsson, U. *FEBS Lett.* **1997**, *420*, 63.
(25) Sahoo, D.; Weers, P. M. M.; Ryan, R. O.; Narayanaswami, V. *J. Mol. Biol.* **2002**, *321*, 201.
(26) Sahoo, D.; Narayanaswami, V.; Kay, C. M.; Ryan, R. O. *Biochemistry* **2000**, *39*, 6594.
(27) Paris, P. L.; Langenhan, J. M.; Kool, E. T. *Nucleic Acids Res.* **1998**, *26*, 3789.
(28) Lewis, F. D.; Zhang, Y. F.; Letsinger, R. L. *J. Am. Chem. Soc.* **1997**, *119*, 5451.
(29) Yamana, K.; Iwai, T.; Ohtani, Y.; Sato, S.; Nakamura, M.; Nakano, H. *Bioconjugate Chem.* **2002**, *13*, 1266.
(30) Yamana, K.; Takei, M.; Nakano, H. *Tetrahedron Lett.* **1997**, *38*, 6051.
(31) Tong, G.; Lawlor, J. M.; Tregear, G. W.; Haralambidis, J. *J. Am. Chem. Soc.* **1995**, *117*, 12151.
(32) Ollmann, M.; Schwarzmann, G.; Sandhoff, K.; Galla, H. J. *Biochemistry* **1987**, *26*, 5943.
(33) Pap, E. H. W.; Hanicak, A.; Vanhoek, A.; Wirtz, K. W. A.; Visser, A. J. W. G. *Biochemistry* **1995**, *34*, 9118.
(34) Kurzchalia, T. V.; Parton, R. G. *Curr. Opin. Cell Biol.* **1999**, *11*, 424.
(35) Song, X. D.; Swanson, B. I. *Langmuir* **1999**, *15*, 4710.
(36) Smit, J. M.; Bittman, R.; Wilschut, J. *J. Virol.* **1999**, *73*, 8476.
(37) Irurzun, A.; Nieva, J. L.; Carrasco, L. *Virology* **1997**, *227*, 488.
(38) Pillot, T.; Goethals, M.; Vanloo, B.; Talussot, C.; Brasseur, R.; Vandekerckhove, J.; Rosseneu, M.; Lins, L. *J. Biol. Chem.* **1996**, *271*, 28757.
(39) Somerharju, P. *Chem. Phys. Lipids* **2002**, *116*, 57.
(40) Birks, J. B.; Munro, I. H.; Lumb, M. D. *Proc. R. Soc. London A: Math. Phys. Sci.* **1964**, *280*, 289.
(41) Templer, R. H.; Castle, S. J.; Curran, A. R.; Rumbles, G.; Klug, D. R. *Faraday Discuss.* **1998**, 41.
(42) Pokhrel, M. R.; Bossmann, S. H. *J. Phys. Chem.B* **2000**, *104*, 2215.
(43) Fujiwara, Y.; Amao, Y. *Sens. Actuators B: Chem.* **2003**, *89*, 58.
(44) Lee, E. D.; Werner, T. C.; Seitz, W. R. *Anal. Chem.* **1987**, *59*, 279.
(45) Nagel, C. C.; Bentsen, J. G.; Yafuso, M; et al. US Patent 5,498,549, 1996.
(46) Nagel, C. C.; Bentsen, J. G.; Dektar, J. L.; et al. US Patent 5,409,666, 1995.
(47) Ikeda, H.; Nakamura, M.; Ise, N.; Oguma, N.; Nakamura, A.; Ikeda, T.; Toda, F.; Ueno, A. *J. Am. Chem. Soc.* **1996**, *118*, 10980.
(48) Aoyagi, T.; Ikeda, H.; Ueno, A. *Bull. Chem. Soc. Jpn.* **2001**, *74*, 157.
(49) Ueno, A.; Suzuki, I.; Osa, T. *Anal. Chem.* **1990**, *62*, 2461.
(50) Valeur, B.; Leray, I. *Coord. Chem. Rev.* **2000**, *205*, 3.
(51) Yang, R. H.; Chan, W. H.; Lee, A. W. M.; Xia, P. F.; Zhang, H. K.; Li, K. A. *J. Am. Chem. Soc.* **2003**, *125*, 2884.
(52) Strauss, J.; Daub, J. *Org. Lett.* **2002**, *4*, 683.
(53) Bodenant, B.; Fages, F.; Delville, M. H. *J. Am. Chem. Soc.* **1998**, *120*, 7511.
(54) Yang, J. S.; Lin, C. S.; Hwang, C. Y. *Org. Lett.* **2001**, *3*, 889.
(55) Ludwig, R.; Dzung, N. T. K. *Sensors* **2002**, *2*, 397.
(56) Bodenant, B.; Weil, T.; Businelli-Pourcel, M.; Fages, F.; Barbe, B.; Pianet, I.; Laguerre, M. *J. Org. Chem.* **1999**, *64*, 7034.
(57) Suzuki, Y.; Morozumi, T.; Nakamura, H.; Shimomura, M.; Hayashita, T.; Bartsh, R. A. *J. Phys. Chem. B* **1998**, *102*, 7910.
(58) Monahan, C.; Bien, J. T.; Smith, B. D. *Chem. Commun.* **1998**, 431.
(59) Anthony, J. E. *Angew. Chem. Int. Ed.* **2008**, *47*, 452.
(60) Shirota, Y.; Kageyama, H. *Chem. Rev.* **2007**, *107*, 953.
(61) Wu, J. S.; Pisula, W.; Müllen, K. *Chem. Rev.* **2007**, *107*, 718.
(62) Tang, C. W.; Vanslyke, S. A. *Appl. Phys. Lett.* **1987**, *51*, 913.
(63) Burroughes, J. H.; Bradley, D. D. C.; Brown, A. R.; Marks, R. N.; Mackay, K.; Friend, R. H.; Burns, P. L.; Holmes, A. B. *Nature* **1990**, *347*, 539.
(64) Moliton, A. *Molecular and Polymer Optoelectronics: From Concepts to Devices*; Springer: New York: 2005.
(65) Jiang, J. X.; Xu, Y. H.; Yang, W.; Guan, R.; Liu, Z. Q.; Zhen, H. Y.; Cao, Y. *Adv. Mater.* **2006**, *18*, 1769.
(66) Liu, J.; Zhou, Q. G.; Cheng, Y. X.; Geng, Y. H.; Wang, L. X.; Ma, D. G.; Jing, X. B.; Wang, F. S. *Adv. Mater.* **2005**, *17*, 2974.
(67) Gong, X.; Wang, S.; Moses, D.; Bazan, G. C.; Heeger, A. J. *Adv. Mater.* **2005**, *17*, 2053.
(68) Qiu, Y.; Wei, P.; Zhang, D. Q.; Qiao, J.; Duan, L.; Li, Y. K.; Gao, Y. D.; Wang, L. D. *Adv. Mater.* **2006**, *18*, 1607.
(69) Xu, Q. F.; Duong, H. M.; Wudl, F.; Yang, Y. *Appl. Phys. Lett.* **2004**, *85*, 3357.
(70) Shao, Y.; Yang, Y. *Appl. Phys. Lett.* **2005**, *86*, 073510.
(71) Carlson, B.; Phelan, G. D.; Kaminsky, W.; Dalton, L.; Jiang, X. Z.; Liu, S.; Jen, A. K. Y. *J. Am. Chem. Soc.* **2002**, *124*, 14162.
(72) Geffroy, B.; Le Roy, P.; Prat, C. *Polym. Int.* **2006**, *55*, 572.
(73) Bevilacqua, P. C.; Kierzek, R.; Johnson, K. A.; Turner, D. H. *Science* **1992**, *258*, 1355.
(74) Jia, W. L.; McCormick, T.; Liu, Q. D.; Fukutani, H.; Motala, M.; Wang, R. Y.; Tao, Y.; Wang, S. N. *J. Mater. Chem.* **2004**, *14*, 3344.
(75) Chabinyc, M. L.; Salleo, A. *Chem. Mater.* **2004**, *16*, 4509.
(76) Veres, J.; Ogier, S.; Lloyd, G.; de Leeuw, D. *Chem. Mater.* **2004**, *16*, 4543.
(77) Mcculloch, I.; Heeney, M.; Bailey, C.; Genevicius, K.; Macdonald, I.; Shkunov, M.; Sparrowe, D.; Tierney, S.; Wagner, R.; Zhang, W. M.; Chabinyc, M. L.; Kline, R. J.; Mcgehee, M. D.; Toney, M. F. *Nat. Mater.* **2006**, *5*, 328.
(78) Sundar, V. C.; Zaumseil, J.; Podzorov, V.; Menard, E.; Willett, R. L.; Someya, T.; Gershenson, M. E.; Rogers, J. A. *Science* **2004**, *303*, 1644.
(79) Allard, S.; Förster, M.; Souharce, B.; Thiem, H.; Scherf, U. *Angew. Chem. Int. Ed.* **2008**, *47*, 4070.
(80) Gao, P.; Beckmann, D.; Tsao, H. N.; Feng, X. L.; Enkelmann, V.; Baumgarten, M.; Pisula, W.; Müllen, K. *Adv. Mater.* **2009**, *21*, 213.
(81) Tsao, H. N.; Müllen, K. *Chem. Soc. Rev.* **2010**, *39*, 2372.
(82) Tang, C. W. *Appl. Phys. Lett.* **1986**, *48*, 183.
(83) Oregan, B.; Gratzel, M. *Nature* **1991**, *353*, 737.
(84) Vollmann, H.; Becker, H.; Corell, M.; Streeck, H. *Liebigs Ann.* **1937**, *531*, 1.
(85) Altschuler., L; Berliner, E. *J. Am. Chem. Soc.* **1966**, *88*, 5837.
(86) Dewar, M. J. S.; Dennington, R. D. *J. Am. Chem. Soc.* **1989**, *111*, 3804.
(87) Hites, R. A. *Calculated Molecular Properties of Polycyclic Aromatic Hydrocarbons*; Elsevier: New York, 1987.
(88) Miyazawa, A.; Yamato, T.; Tashiro, M. *Chem. Express* **1990**, *5*, 381.
(89) Maeda, H.; Maeda, T.; Mizuno, K.; Fujimoto, K.; Shimizu, H.; Inouye, M. *Chem.—Eur. J.* **2006**, *12*, 824.
(90) Yang, C. H.; Guo, T. F.; Sun, I. W. *J. Luminesc.* **2007**, *124*, 93.
(91) Amann, N.; Pandurski, E.; Fiebig, T.; Wagenknecht, H. A. *Angew. Chem. Int. Ed.* **2002**, *41*, 2978.
(92) Amann, N.; Pandurski, E.; Fiebig, T.; Wagenknecht, H. A. *Chem.—Eur. J.* **2002**, *8*, 4877.
(93) Suzuki, K.; Seno, A.; Tanabe, H.; Ueno, K. *Synth. Met.* **2004**, *143*, 89.
(94) Wu, K. C.; Ku, P. J.; Lin, C. S.; Shih, H. T.; Wu, F. I.; Huang, M. J.; Lin, J. J.; Chen, I. C.; Cheng, C. H. *Adv. Funct. Mater.* **2008**, *18*, 67.
(95) Mikroyannidis, J. A.; Fenenko, L.; Adachi, C. *J. Phys. Chem.B* **2006**, *110*, 20317.
(96) Okamoto, H.; Arai, T.; Sakuragi, H.; Tokumaru, K. *Bull. Chem. Soc. Jpn.* **1990**, *63*, 2881.
(97) Moggia, F.; Videlot-Ackermann, C.; Ackermann, J.; Raynal, P.; Brisset, H.; Fages, F. *J. Mater. Chem.* **2006**, *16*, 2380.
(98) Liu, F.; Tang, C.; Chen, Q. Q.; Li, S. Z.; Wu, H. B.; Xie, L. H.; Peng, B.; Wei, W.; Cao, Y.; Huang, W. *Org. Electron.* **2009**, *10*, 256.



Samsung Exhibit 1020, Page 52 of 55

(99) Benniston, A. C.; Harriman, A.; Lawrie, D. J.; Rostron, S. A. *Eur. J. Org. Chem.* **2004**, 2272.
(100) Suzuki, H.; Kondo, A.; Inouye, M.; Ogawa, T. *Synthesis* **1986**, 121.
(101) Radner, F. *Acta Chem. Scand.* **1989**, *43*, 481.
(102) Goldschmiedt, G. *Mh. Chem.* **1881**, *2*, 580.
(103) Babu, P.; Sangeetha, N. M.; Vijaykumar, P.; Maitra, U.; Rissanen, K.; Raju, A. R. *Chem.—Eur. J.* **2003**, *9*, 1922.
(104) Pu, Y. J.; Higashidate, M.; Nakayama, K.; Kido, J. *J. Mater. Chem.* **2008**, *18*, 4183.
(105) Caruso, F.; Mohwald, H. *J. Am. Chem. Soc.* **1999**, *121*, 6039.
(106) Thomas, K. R. J.; Lin, J. T.; Tao, Y. T.; Ko, C. W. *Adv. Mater.* **2000**, *12*, 1949.
(107) Dyker, G.; Kadzimirsz, D. *Eur. J. Org. Chem.* **2003**, 3167.
(108) Hahma, A.; Bhat, S.; Leivo, K.; Linnanto, J.; Lahtinen, M.; Rissanen, K. *New J. Chem.* **2008**, *32*, 1438.
(109) Granzhan, A.; Teulade-Fichou, M. P. *Tetrahedron* **2009**, *65*, 1349.
(110) Barfield, M.; Collins, M. J.; Gready, J. E.; Sternhell, S.; Tansey, C. W. *J. Am. Chem. Soc.* **1989**, *111*, 4285.
(111) MIller, D. W.; Evans, F. E.; Fu, P. P.; Yang, D. T. C. *J. Chem. Res., Synop.* **1984**, *12*, 418.
(112) Chen, J. J.; Wang, I. J. *Dyes Pigm.* **1995**, *29*, 305.
(113) Malashikhin, S.; Finney, N. S. *J. Am. Chem. Soc.* **2008**, *130*, 12846.
(114) Ji, H. M. T.; Ebitani, K.; Kaneda, K. *Tetrahedron Lett.* **2002**, *43*, 7179.
(115) Goswami, S.; Jana, S.; Dey, S.; Adak, A. K. *Chem. Lett.* **2005**, *34*, 194.
(116) Drefahl, G.; Keil, E. *J. Prakt. Chem.* **1958**, *6*, 80.
(117) Bair, K. W.; Tuttle, R. L.; Knick, V. C.; Cory, M.; Mckee, D. D. *J. Med. Chem.* **1990**, *33*, 2385.
(118) Sessler, J. L.; Kubo, Y.; Harriman, A. *J. Phys. Org. Chem.* **1992**, *5*, 644.
(119) Yoshioka, N.; Andoh, C.; Kubo, K.; Igarashi, T.; Sakurai, T. *J. Chem. Soc. Perkin Trans. 2* **2001**, 1927.
(120) LEE, H. M.; Luna, E.; Hinz, M.; Stezowski, J. J.; Kiselyov, A. S.; Harvey, R. G. *J. Org. Chem.* **1995**, *60*, 5604.
(121) Lampkins, A. J.; O'Neil, E. J.; Smith, B. D. *J. Org. Chem.* **2008**, *73*, 6053.
(122) Cicchi, S.; Fabbrizzi, P.; Ghini, G.; Brandi, A.; Foggi, P.; Marcelli, A.; Righini, R.; Botta, C. *Chem.—Eur. J.* **2009**, *15*, 754.
(123) Bernhardt, S.; Kastler, M.; Enkelmann, V.; Baumgarten, M.; Müllen, K. *Chem.—Eur. J.* **2006**, *12*, 6117.
(124) Sotoyama, W.; Sato, H.; Kinoshita, M.; Takahashi, T. *SID 03 Dig.* **2003**, 1294.
(125) Hayer, A.; de Halleux, V.; Kohler, A.; El-Garoughy, A.; Meijer, E. W.; Barbera, J.; Tant, J.; Levin, J.; Lehmann, M.; Gierschner, J.; Cornil, J.; Geerts, Y. H. *J. Phys. Chem. B* **2006**, *110*, 7653.
(126) Hayer, A.; de Halleux, V.; Kohler, A.; El-Garoughy, A.; Meijer, E. W.; Barbera, J.; Tant, J.; Levin, J.; Lehmann, M.; Gierschner, J.; Cornil, J.; Geerts, Y. H. *J. Phys. Chem. B* **2006**, *110*, 7653.
(127) Gingras, M.; Placide, V.; Raimundo, J. M.; Bergamini, G.; Ceroni, P.; Balzani, V. *Chem.—Eur. J.* **2008**, *14*, 10357.
(128) Hassheider, T.; Benning, S. A.; Kitzerow, H. S.; Achard, M. F.; Bock, H. *Angew. Chem. Int. Ed.* **2001**, *40*, 2060.
(129) Grimshaw, J.; Trocha-Grimshaw, J. *J. Chem. Soc. Perkin Trans. 1* **1972**, 1622.
(130) Oh, H. Y.; Lee, C.; Lee, S. *Org. Electron.* **2009**, *10*, 163.
(131) Xing, Y. J.; Xu, X. J.; Zhang, P.; Tian, W. J.; Yu, G.; Lu, P.; Liu, Y. Q.; Zhu, D. B. *Chem. Phys. Let.* **2005**, *408*, 169.
(132) Mikroyannidis, J. A. *Synth. Met.* **2005**, *155*, 125.
(133) Figueira-Duarte, T. M.; Simon, S. C.; Wagner, M.; Drtezhinin, S. I.; Zachariasse, K. A.; Müllen, K. *Angew. Chem. Int. Ed.* **2008**, *47*, 10175.
(134) Coventry, D. N.; Batsanov, A. S.; Goeta, A. E.; Howard, J. A. K.; Marder, T. B.; Perutz, R. N. *Chem. Commun.* **2005**, 2172.
(135) Oberender, F. G.; Dixon, J. A. *J. Org. Chem.* **1959**, *24*, 1226.
(136) Stille, J. K.; Mainen, E. L. *Macromolecules* **1968**, *1*, 36.
(137) Young, E. R. R.; Funk, R. L. *J. Org. Chem.* **1998**, *63*, 9995.
(138) CHO, H.; Harvey, R. G. *Tetrahedron Lett.* **1974**, 1491.
(139) Hu, J.; Zhang, D.; Harris, F. W. *J. Org. Chem.* **2005**, *70*, 707.
(140) Mateo-Alonso, A.; Kulisic, N.; Valenti, G.; Marcaccio, M.; Paolucci, F.; Prato, M. *Chem. Asian J.* **2010**, *5*, 482.
(141) Yamato, T.; Fujimoto, M.; Miyazawa, A.; Matsuo, K. *J. Chem. Soc. Perkin Trans. 1* **1997**, 1201.
(142) Oseki, Y.; Fujitsuka, M.; Sakamoto, M.; Majima, T. *J. Phys. Chem. A* **2007**, *111*, 9781.
(143) Guldi, D. M.; Spanig, F.; Kreher, D.; Perepichka, I. F.; van der Pol, C.; Bryce, M. R.; Ohkubo, K.; Fukuzumi, S. *Chem.—Eur. J.* **2008**, *14*, 250.
(144) Pevenage, D.; Van der Auweraer, M.; De Schryver, F. C. *Chem. Phys. Lett.* **2000**, *319*, 512.
(145) Techert, S.; Schmatz, S.; Wiessner, A.; Staerk, H. *J. Phys. Chem. A* **2000**, *104*, 5700.
(146) Fiebig, T.; Kuhnle, W.; Staerk, H. *Chem. Phys. Lett.* **1998**, *282*, 7.
(147) Schneider, S.; Kurzawa, J.; Stockmann, A.; Engl, R.; Daub, J.; Matousek, P.; Towrie, M. *Chem. Phys. Lett.* **2001**, *348*, 277.
(148) Daub, J.; Engl, R.; Kurzawa, J.; Miller, S. E.; Schneider, S.; Stockmann, A.; Wasielewski, M. R. *J. Phys. Chem. A* **2001**, *105*, 5655.
(149) Yang, S. W.; Elangovan, A.; Hwang, K. C.; Ho, T. I. *J. Phys. Chem. B* **2005**, *109*, 16628.
(150) Sessler, J. L.; Karnas, E.; Kim, S. K.; Ou, Z. P.; Zhang, M.; Kadish, K. M.; Ohkubo, K.; Fukuzumi, S. *J. Am. Chem. Soc.* **2008**, *130*, 15256.
(151) Ammerer, L.; Zinke, A. *Mh. Chem.* **1953**, *84*, 25.
(152) Fatiadi, A. J. *J. Org. Chem.* **1967**, *32*, 2903.
(153) Baumgarten, M.; Gherghel, L.; Friedrich, J.; Jurczok, M.; Rettig, W. *J. Phys. Chem. A* **2000**, *104*, 1130.
(154) Nefedov, V. A. *Russ. J. Org. Chem.* **2007**, *43*, 1163.
(155) Suzuki, K.; Seno, A.; Tanabe, H.; Ueno, K. *Synth. Met.* **2004**, *143*, 89.
(156) Tao, S. L.; Peng, Z. K.; Zhang, X. H.; Wang, P. F.; Lee, C. S.; Lee, S. T. *Adv. Funct. Mater.* **2005**, *15*, 1716.
(157) Zhao, Z. J.; Xu, X. J.; Jiang, Z. T.; Lu, P.; Yu, G.; Liu, Y. Q. *J. Org. Chem.* **2007**, *72*, 8345.
(158) Jiao, S. B.; Liao, Y.; Xu, X. J.; Wang, L. P.; Yu, G.; Wang, L. M.; Su, Z. M.; Ye, S. H.; Liu, Y. Q. *Adv. Funct. Mater.* **2008**, *18*, 2335.
(159) Tang, C.; Liu, F.; Xia, Y. J.; Lin, J.; Xie, L. H.; Zhong, G. Y.; Fan, Q. L.; Huang, W. *Org. Electron.* **2006**, *7*, 155.
(160) Tang, C.; Liu, F.; Xia, Y. J.; Xie, L. H.; Wei, A.; Li, S. B.; Fan, Q. L.; Huang, W. *J. Mater. Chem.* **2006**, *16*, 4074.
(161) Liu, F.; Tang, C.; Chen, Q. Q.; Shi, F. F.; Wu, H. B.; Xie, L. H.; Peng, B.; Wei, W.; Cao, Y.; Huang, W. *J. Phys. Chem. C* **2009**, *113*, 4641.
(162) Thomas, K. R. J.; Velusamy, M.; Lin, J. T.; Tao, Y. T.; Cheun, C. H. *Adv. Funct. Mater.* **2004**, *14*, 387.
(163) Zhao, Z. J.; Xu, X. J.; Wang, F.; Yu, G.; Lu, P.; Liu, Y. Q.; Zhu, D. B. *Synth. Met.* **2006**, *156*, 209.
(164) Thomas, K. R. J.; Velusamy, M.; Lin, J. T.; Chuen, C. H.; Tao, Y. T. *Chem. Mater.* **2005**, *17*, 1860.
(165) Ko, C. W.; Tao, Y. T. *Synth. Met.* **2002**, *126*, 37.
(166) He, C.; He, Q. G.; Chen, Q.; Shi, L.; Cao, H. M.; Cheng, J. G.; Deng, C. M.; Lin, T. *Tetrahedron Lett.* **2010**, *51*, 1317.
(167) Kelnhofer, K.; Knorr, A.; Tak, Y. H.; Bassler, H.; Daub, J. *Acta Polym.* **1997**, *48*, 188.
(168) Aso, Y.; Okai, T.; Kawaguchi, Y.; Otsubo, T. *Chem. Lett.* **2001**, 420.
(169) Otsubo, T.; Aso, Y.; Takimiya, K. *J. Mater. Chem.* **2002**, *12*, 2565.
(170) Wang, Y.; Wang, H. M.; Liu, Y. Q.; Di, C. A.; Sun, Y. M.; Wu, W. P.; Yu, G.; Zhang, D. Q.; Zhu, D. B. *J. Am. Chem. Soc.* **2006**, *128*, 13058.
(171) Wang, H. M.; Zhang, D. Q.; Guo, X. F.; Zhu, L. Y.; Shuai, Z. G.; Zhu, D. B. *Chem.Commun.* **2004**, 670.
(172) Anthony, J. E.; Brooks, J. S.; Eaton, D. L.; Parkin, S. R. *J. Am. Chem. Soc.* **2001**, *123*, 9482.



Samsung Exhibit 1020, Page 53 of 55

(173) Anthony, J. E.; Eaton, D. L.; Parkin, S. R. *Org. Lett.* **2002**, *4*, 15.
(174) Lehnherr, D.; Murray, A. H.; McDonald, R.; Ferguson, M. J.; Tykwinski, R. R. *Chem.—Eur. J.* **2009**, *15*, 12580.
(175) Pujari, S. R.; Kambale, M. D.; Bhosale, P. N.; Rao, P. M. R.; Patil, S. R. *Mater. Res. Bull.* **2002**, *37*, 1641.
(176) Rivera, E.; Belletete, M.; Zhu, X. X.; Durocher, G.; Giasson, R. *Polymer* **2002**, *43*, 5059.
(177) Nomura, R.; Yamada, K.; Masuda, T. *Chem. Commun.* **2002**, 478.
(178) Zhao, H. C.; Sanda, F.; Masuda, T. *Macromolecules* **2004**, *37*, 8893.
(179) Zhao, H. C.; Sanda, F.; Masuda, T. *Polymer* **2006**, *47*, 1584.
(180) Liaw, D. J.; Wang, K. L.; Chang, F. C. *Macromolecules* **2007**, *40*, 3568.
(181) Mikroyannidis, J. A.; Persephonis, P. G.; Giannetas, V. G. *Synth. Met.* **2005**, *148*, 293.
(182) Vyprachticky, D.; Cimrova, V. *Macromolecules* **2002**, *35*, 3463.
(183) Cimrova, V.; Vyprachticky, D. *Appl. Phys. Lett.* **2003**, *82*, 642.
(184) Cornil, J.; Lemaur, V.; Calbert, J. P.; Brédas, J. L. *Adv. Mater.* **2002**, *14*, 726.
(185) Deibel, C.; Janssen, D.; Heremans, P.; De Cupere, V.; Geerts, Y.; Benkhedir, M. L.; Adriaenssens, G. J. *Org. Electron.* **2006**, *7*, 495.
(186) Simpson, C. D.; Wu, J. S.; Watson, M. D.; Müllen, K. *J. Mater. Chem.* **2004**, *14*, 494.
(187) Kim, Y. H.; Yoon, D. K.; Lee, E. H.; Ko, Y. K.; Jung, H. T. *J. Phys. Chem. B* **2006**, *110*, 20836.
(188) Watson, M. D.; Fechtenkotter, A.; Müllen, K. *Chem. Rev.* **2001**, *101*, 1267.
(189) Clar, E. *The Aromatic Sextet*; John Wiley: London, 1972.
(190) Clar, E. *Polycyclic Hydrocarbons*; Academic Press Inc.: London and New York, 1964.
(191) Diederich, F.; Rubin, Y. *Angew. Chem. Int. Ed.* **1992**, *31*, 1101.
(192) Tchebotareva, N.; Yin, X. M.; Watson, M. D.; Samori, P.; Rabe, J. P.; Müllen, K. *J. Am. Chem. Soc.* **2003**, *125*, 9734.
(193) Jackel, F.; Yin, X.; Samori, P.; Tchebotareva, N.; Watson, M. D.; Venturini, A.; Müllen, K.; Rabe, J. P. *Synth. Met.* **2004**, *147*, 5.
(194) Baker, L. A.; Crooks, R. M. *Macromolecules* **2000**, *33*, 9034.
(195) Wilken, R.; Adams, J. *Macromol. Rapid Commun.* **1997**, *18*, 659.
(196) Brauge, L.; Veriot, G.; Franc, G.; Deloncle, R.; Caminade, A. M.; Majoral, J. P. *Tetrahedron* **2006**, *62*, 11891.
(197) Severac, M.; Leclaire, J.; Sutra, P.; Caminade, A. M.; Majoral, J. P. *Tetrahedron Lett.* **2004**, *45*, 3019.
(198) Yuan, W. Z.; Yuan, J. Y.; Zhou, M.; Pan, C. Y. *J. Polym. Sci. Part A: Polym. Chem.* **2008**, *46*, 2788.
(199) Killops, K. L.; Campos, L. M.; Hawker, C. J. *J. Am. Chem. Soc.* **2008**, *130*, 5062.
(200) Bolink, H. J.; Barea, E.; Costa, R. D.; Coronado, E.; Sudhakar, S.; Zhen, C.; Sellinger, A. *Org. Electron.* **2008**, *9*, 155.
(201) Giovanella, U.; Mroz, W.; Foggi, P.; Fabbrizzi, P.; Cicchi, S.; Botta, C. *ChemPhysChem* **2010**, *11*, 683.
(202) Stewart, G. M.; Fox, M. A. *J. Am. Chem. Soc.* **1996**, *118*, 4354.
(203) Thomas, K. R. J.; Velusamy, M.; Lin, J. T.; Chuen, C. H.; Tao, Y. T. *J. Mater. Chem.* **2005**, *15*, 4453.
(204) Sautter, A.; Kaletas, B. K.; Schmid, D. G.; Dobrawa, R.; Zimine, M.; Jung, G.; van Stokkum, I. H. M.; De Cola, L.; Williams, R. M.; Wurthner, F. *J. Am. Chem. Soc.* **2005**, *127*, 6719.
(205) Dincalp, H.; Kizilok, S.; Icli, S. *Dyes Pigm.* **2010**, *86*, 32.
(206) Lo, M. Y.; Zhen, C. G.; Lauters, M.; Jabbour, G. E.; Sellinger, A. *J. Am. Chem. Soc.* **2007**, *129*, 5808.
(207) Zhou, Y.; Kim, J. W.; Kim, M. J.; Son, W. J.; Han, S. J.; Kim, H. N.; Han, S.; Kim, Y.; Lee, C.; Kim, S. J.; Kim, D. H.; Kim, J. J.; Yoon, J. *Org. Lett.* **2010**, *12*, 1272.
(208) Oyamada, T.; Uchiuzou, H.; Akiyama, S.; Oku, Y.; Shimoji, N.; Matsushige, K.; Sasabe, H.; Adachi, C. *J. Appl. Phys.* **2005**, *98*, 074506-7.
(209) Oyamada, T.; Sasabe, H.; Oku, Y.; Shimoji, N.; Adachi, C. *Appl. Phys. Lett.* **2006**, *88*, 093514-3.
(210) Bisri, S. Z.; Takahashi, T.; Takenobu, T.; Yahiro, M.; Adachi, C.; Iwasa, Y. *Front. Mater. Res.* **2008**, *10*, 103.
(211) Bisri, S. Z.; Takahashi, T.; Takenobu, T.; Yahir, M.; Adachi, C.; Iwasa, Y. *Jap. J. Appl. Phys. Part 2* **2007**, *46*, L596.
(212) Qin, D. S.; Tao, Y. *Appl. Phys. Lett.* **2005**, *86*, 113507.
(213) Moorthy, J. N.; Natarajan, P.; Venkatakrishnan, P.; Huang, D. F.; Chow, T. J. *Org. Lett.* **2007**, *9*, 5215.
(214) Kim, Y. H.; Shin, D. C.; Kim, S. H.; Ko, C. H.; Yu, H. S.; Chae, Y. S.; Kwon, S. K. *Adv. Mater.* **2001**, *13*, 1690.
(215) Kim, Y. H.; Jeong, H. C.; Kim, S. H.; Yang, K. Y.; Kwon, S. K. *Adv. Funct. Mater.* **2005**, *15*, 1799.
(216) Tao, S. L.; Hong, Z. R.; Peng, Z. K.; Ju, W. G.; Zhang, X. H.; Wang, P. F.; Wu, S. K.; Lee, S. T. *Chem. Phys. Lett.* **2004**, *397*, 1.
(217) Xie, W.; Hou, J.; Liu, S. *Semicond. Sci. Technol.* **2003**, *18*, L42.
(218) Shih, H. T.; Lin, C. H.; Shih, H. H.; Cheng, C. H. *Adv. Mater.* **2002**, *14*, 1409.
(219) Oh, J. W.; Lee, Y. O.; Kim, T. H.; Ko, K. C.; Lee, J. Y.; Kim, H.; Kim, J. S. *Angew. Chem. Int. Ed.* **2009**, *48*, 2522.
(220) Kim, H. M.; Lee, Y. O.; Lim, C. S.; Kim, J. S.; Cho, B. R. *J. Org. Chem.* **2008**, *73*, 5127.
(221) Zhao, Z. J.; Chen, S. M.; Lam, J. W. Y.; Lu, P.; Zhong, Y. C.; Wong, K. S.; Kwok, H. S.; Tang, B. Z. *Chem. Commun.* **2010**, *46*, 2221.
(222) Benning, S. A.; Hassneider, T.; Keuker-Baumann, S.; Bock, H.; Della Sala, F.; Frauenheim, T.; Kitzerow, H. S. *Liq. Cryst.* **2001**, *28*, 1105.
(223) Hassheider, T.; Benning, S. A.; Lauhof, M. W.; Oesterhaus, R.; Alibert-Fouet, S.; Bock, H.; Goodby, J. W.; Watson, M.; Müllen, K.; Kitzerow, H. S. *Liq. Cryst. Mater. Dev. Appl.* **2003**, *5003*, 167.
(224) de Halleux, V.; Calbert, J. P.; Brocorens, P.; Cornil, J.; Declercq, J. P.; Brédas, J. L.; Geerts, Y. *Adv. Funct. Mater.* **2004**, *14*, 649.
(225) Sienkowska, M. J.; Monobe, H.; Kaszynski, P.; Shimizu, Y. *J. Mater. Chem.* **2007**, *17*, 1392.
(226) Chaiken, R. F.; Kearns, D. R. *J. Chem. Phys.* **1968**, *49*, 2846.
(227) Tierney, M.; Lubman, D. *Appl. Spectrosc.* **1987**, *41*, 880.
(228) Holroyd, R. A.; Preses, J. M.; Bottcher, E. H.; Schmidt, W. F. *J. Phys. Chem.* **1984**, *88*, 744.
(229) Hirose, T.; Kawakami, O.; Yasutake, M. *Mol. Cryst. Liq. Cryst.* **2006**, *451*, 65.
(230) Yasutake, M.; Fujihara, T.; Nagasawa, A.; Moriya, K.; Hirose, T. *Eur. J. Org. Chem.* **2008**, 4120.
(231) Qin, T. S.; Zhou, G.; Scheiber, H.; Bauer, R. E.; Baumgarten, M.; Anson, C. E.; List, E. J. W.; Müllen, K. *Angew. Chem. Int. Ed.* **2008**, *47*, 8292.
(232) Qin, T.; Wiedemair, W.; Nau, S.; Trattnig, R.; Sax, S.; Winkler, S.; Vollmer, A.; Koch, N.; Baumgarten, M.; List, E. J. W.; Müllen, K. *J. Am. Chem. Soc.* **2011**, *133*, 1301.
(233) Liu, F.; Lai, W. Y.; Tang, C.; Wu, H. B.; Chen, Q. Q.; Peng, B.; Wei, W.; Huang, W.; Cao, Y. *Macromol. Rapid Commun.* **2008**, *29*, 659.
(234) Zhao, Z. J.; Li, J. H.; Chen, X. P.; Wang, X. M.; Lu, P.; Yang, Y. *J. Org. Chem.* **2009**, *74*, 383.
(235) Zhao, Z. J.; Li, J. H.; Chen, X. P.; Lu, P.; Yang, Y. *Org. Lett.* **2008**, *10*, 3041.
(236) Modrakowski, C.; Flores, S. C.; Beinhoff, M.; Schluter, A. D. *Synthesis* **2001**, 2143.
(237) Bargon, J.; Mohmand, S.; Waltman, R. J. *IBM J. Res. Dev.* **1983**, *27*, 330.
(238) Hino, S.; Iwasaki, K.; Matsumoto, K. *Synth. Met.* **1994**, *64*, 259.
(239) Lu, G.; Shi, G. *J. Electroanal. Chem.* **2006**, *586*, 154.
(240) Qu, L.; Shi, G. *Chem. Commun.* **2004**, 2800.
(241) Tamura, S.; Sakamoto, Y.; et al. US patent 7,244,516, *B1* 2007.
(242) Wang, Z.; Xu, C.; Wang, W.; Fu, W.; Niu, L.; Ji, B. *Solid-State Electron.* **2010**, *54*, 524.
(243) Shimizu, H.; Fujimoto, K.; Furusyo, M.; Maeda, H.; Nanai, Y.; Mizuno, K.; Inouye, M. *J. Org. Chem.* **2007**, *72*, 1530.
(244) Zhao, Z. J.; Xu, X. J.; Wang, H. B.; Lu, P.; Yu, G.; Liu, Y. Q. *J. Org. Chem.* **2008**, *73*, 594.
(245) Mikroyannidis, J. A.; Fenenko, L.; Yahiro, M.; Adachi, C. *J. Polym. Sci. Part A: Polym. Chem.* **2007**, *45*, 4661.



Samsung Exhibit 1020, Page 54 of 55

(246) Sagara, Y.; Kato, T. *Angew. Chem. Int. Ed.* **2008**, *47*, 5175.
(247) Percec, V.; Cho, W. D.; Ungar, G.; Yeardley, D. J. P. *J. Am. Chem. Soc.* **2001**, *123*, 1302.
(248) Percec, V.; Aqad, E.; Peterca, M.; Imam, M. R.; Glodde, M.; Bera, T. K.; Miura, Y.; Balagurusamy, V. S. K.; Ewbank, P. C.; Wurthner, F.; Heiney, P. A. *Chem.—Eur. J.* **2007**, *13*, 3330.
(249) Kato, T.; Matsuoka, T.; Nishii, M.; Kamikawa, Y.; Kanie, K.; Nishimura, T.; Yashima, E.; Ujiie, S. *Angew. Chem. Int. Ed.* **2004**, *43*, 1969.
(250) Kamikawa, Y.; Nishii, M.; Kato, T. *Chem.—Eur. J.* **2004**, *10*, 5942.
(251) Figueira-Duarte, T. M.; Del Rosso, P. G.; Trattnig, R.; Sax, S.; List, E. J. W.; Müllen, K. *Adv. Mater.* **2010**, *22*, 990.
(252) Faust, R. *Angew. Chem. Int. Ed.* **1998**, *37*, 2825.
(253) Bunz, U. H. F.; Rubin, Y.; Tobe, Y. *Chem. Soc. Rev.* **1999**, *28*, 107.
(254) Haley, M. M.; Pak, J. J.; Brand, S. C. *Top. Curr. Chem.* **1999**, *201*, 81.
(255) Höger, S. *J. Polym. Sci. Part A: Polym. Chem.* **1999**, *37*, 2685.
(256) Höger, S. *Chem.—Eur. J.* **2004**, *10*, 1320.
(257) Höger, S.; Cheng, X. H.; Ramminger, A. D.; Enkelmann, V.; Rapp, A.; Mondeshki, M.; Schnell, I. *Angew. Chem. Int. Ed.* **2005**, *44*, 2801.
(258) Jung, S. H.; Pisula, W.; Rouhanipour, A.; Räder, H. J.; Jacob, J.; Müllen, K. *Angew. Chem. Int. Ed.* **2006**, *45*, 4685.
(259) Mindyuk, O. Y.; Stetzer, M. R.; Heiney, P. A.; Nelson, J. C.; Moore, J. S. *Adv. Mater.* **1998**, *10*, 1363.
(260) Lehn, J. M.; Malthete, J.; Levelut, A. M. *Chem. Commun.* **1985**, 1794.
(261) Fischer, M.; Lieser, G.; Rapp, A.; Schnell, I.; Mamdouh, W.; De Feyter, S.; De Schryver, F. C.; Höger, S. *J. Am. Chem. Soc.* **2004**, *126*, 214.
(262) Bunz, U. H. F. *Acc. Chem. Res.* **2001**, *34*, 998.
(263) Moore, J. S. *Acc. Chem. Res.* **1997**, *30*, 402.
(264) Moore, J. S.; Zhang, J. S. *Angew. Chem. Int. Ed.* **1992**, *31*, 922.
(265) Shetty, A. S.; Zhang, J. S.; Moore, J. S. *J. Am. Chem. Soc.* **1996**, *118*, 1019.
(266) Venkataraman, D.; Lee, S.; Zhang, J. S.; Moore, J. S. *Nature* **1994**, *371*, 591.
(267) Zhang, J. S.; Pesak, D. J.; Ludwick, J. L.; Moore, J. S. *J. Am. Chem. Soc.* **1994**, *116*, 4227.
(268) Staab, H. A.; Neunhoef., K. *Synthesis* **1974**, 424.
(269) Figueira-Duarte, T. M.; Lorbach D.; Müllen, K. Submitted, 2011.
(270) Kawano, S. I.; Yang, C.; Ribas, M.; Baluschev, S.; Baumgarten, M.; Müllen, K. *Macromolecules* **2008**, *41*, 7933.
(271) Kreyenschmidt, M.; Baumgarten, M.; Tyutyulkov, N.; Müllen, K. *Angew. Chem. Int. Ed.* **1994**, *33*, 1957.
(272) Rausch, D.; Lambert, C. *Org. Lett.* **2006**, *8*, 5037.
(273) Gao, B. X.; Wang, M.; Cheng, Y. X.; Wang, L. X.; Jing, X. B.; Wang, F. S. *J. Am. Chem. Soc.* **2008**, *130*, 8297.
(274) Kaafarani, B. R.; Lucas, L. A.; Wex, B.; Jabbour, G. E. *Tetrahedron Lett.* **2007**, *48*, 5995.
(275) Jradi, F. M.; Ai-Sayah, M. H.; Kaafarani, B. R. *Tetrahedron Lett.* **2008**, *49*, 238.
(276) Lucas, L. A.; DeLongchamp, D. M.; Richter, L. J.; Kline, R. J.; Fischer, D. A.; Kaafarani, B. R.; Jabbour, G. E. *Chem. Mater.* **2008**, *20*, 5743.
(277) Fogel, Y.; Kastler, M.; Wang, Z. H.; Andrienko, D.; Bodwell, G. J.; Müllen, K. *J. Am. Chem. Soc.* **2007**, *129*, 11743.
(278) Wasserfallen, D.; Kastler, M.; Pisula, W.; Hofer, W. A.; Fogel, Y.; Wang, Z. H.; Müllen, K. *J. Am. Chem. Soc.* **2006**, *128*, 1334.
(279) Fogel, Y.; Zhi, L. J.; Rouhanipour, A.; Andrienko, D.; Rader, H. J.; Müllen, K. *Macromolecules* **2009**, *42*, 6878.
(280) Duong, H. M.; Bendikov, M.; Steiger, D.; Zhang, Q. C.; Sonmez, G.; Yamada, J.; Wudl, F. *Org. Lett.* **2003**, *5*, 4433.
(281) Xu, Q. F.; Duong, H. M.; Wudl, F.; Yang, Y. *Appl. Phys. Lett.* **2004**, *85*, 3357.
(282) Gong, X.; Ma, W. L.; Ostrowski, J. C.; Bazan, G. C.; Moses, D.; Heeger, A. J. *Adv. Mater.* **2004**, *16*, 615.
(283) Hu, J. Y.; Era, M.; Elsegood, M. R. J.; Yamato, T. *Eur. J. Org. Chem.* **2010**, 72.
(284) Sharma, G. D.; Suresh, P.; Mikroyannidis, J. A.; Stylianakis, M. M. *J. Mater. Chem.* **2010**, *20*, 561.
(285) Mikroyannidis, J. A.; Stylianakis, M. M.; Roy, M. S.; Suresh, P.; Sharma, G. D. *J. Power Sources* **2009**, *194*, 1171.



Samsung Exhibit 1020, Page 55 of 55